



Semeone Mesfin, B.Sc.

**Driveability analysis of offshore large diameter steel pile
foundations using PDI GRLWEAP**

MASTER'S THESIS

Submitted in fulfilment of the requirements for the degree of

Diplom-Ingenieur

Master's degree programme: Geotechnical and Hydraulic Engineering

at

Graz University of Technology

Supervisor

Univ.-Prof. Dipl.-Ing. Dr.techn. Roman Marte

Institute of Soil Mechanics and Foundation Engineering

Graz University of Technology

and

Bauer Spezialtiefbau GmbH

Industry Supervisors

Dipl.-Ing. Joachim Gaus (Bauer Spezialtiefbau GmbH)

Dipl.-Ing. Ulli Wiedenmann (Bauer Spezialtiefbau GmbH)

Graz, April 2018

Confidentiality Clause

This master's thesis contains confidential data of Bauer Spezialtiefbau GmbH. This work may only be made available to the first and second reviewers and authorized members of the board of examiners. Any publication and duplication of this master's thesis - even in part – is prohibited. An inspection of this work by third parties requires the expressed permission of the author and the company Bauer Spezialtiefbau GmbH.

Semeone Mesfin

April, 2018

Zusammenfassung

Die Offshore-Pfahlrammung bezieht sich auf die Herstellung von Pfahlfundamenten mittels Rammhämmern tief auf dem Meeresgrund. Dies erfordert hohe Investitionen und Erfahrung. Beim Rammen von hohlen Pfahlteilen mit großen Durchmessern ist es möglich, auf eine nicht durchörterbare harte Schicht zu stoßen, was dazu führt, dass die gewünschte Tiefe nicht erreicht wird. Dieses Problem wird durch Hilfsbohrungen gelöst. Hilfsbohrungen verringern die innere Reibung im bereits hergestellten Abschnitt, was in weiterer Folge zu einem geringeren Rammwiderstand führt. Für diesen Vorgang wird ein separates Bohrgerät benötigt, das jederzeit mit voller Mannschaft und Ausstattung für den Einsatz zur Verfügung steht. Dies führt zu einem hohen Angebotspreis und hohen Kosten während der Bauphase.

Eine Studie zur Rammpbarkeit wird mit der Software PDI GRLWEAP, einer Software zur Pfahlrammanalyse, durchgeführt. Die Analyse erlaubt eine Abschätzung, ob Hilfsbohrungen wahrscheinlich sind oder nicht. Die verschiedenen Eingabemethoden zur statischen Widerstandsanalyse der Software werden mit einem externen Verbrennungs-Hammer miteinander verglichen. Die BAUER Spezialtiefbau GmbH hat das Offshore-Windparkprojekt Beatrice als Fallbeispiel verwendet.

Diese Forschungsarbeit wird in Zukunft von den Planern der BAUER Spezialtiefbau GmbH genutzt werden, um bei Entscheidung über die Notwendigkeit eines zusätzlichen Bohrgerätes für Hilfsbohrungen ein besseres technisches Urteilsvermögen zu haben und bzw. oder um während der Ausschreibungsphase Alternativen aufzuzeigen.

Abstract

Offshore pile driving refers to the installation of pile foundations deep on the sea/ocean bed level using pile driving hammers. It requires high investment and experience. When driving hollow large diameter pile sections, it is possible to come across a hard stratum, causing refusal prior to reaching a desired depth. This issue is resolved by relief drilling. Relief drilling reduces internal friction of the driven section resulting in reduced resistance to driving. For this operation a separate drilling machine is required which stands by with full crew and equipment in the event it might be needed. This results in a high cost consideration during tendering and monetary expenditure during the construction phase.

A driveability analysis is to be carried out using the software PDI GRLWEAP, which is a pile driving analysis software. The analysis was used to predict if relief drilling is probable or not. The different static resistance analysis input methods of the software are compared using an External Combustion Hammer. BAUER Spezialtiefbau GmbH has used the Beatrice offshore wind farm project as a case study.

This research will be used in the future, to enable Bauer designers to have a better engineering judgment when making a decision on the necessity of a drilling machine for relief drilling and/or consideration of alternative options during tendering phase.

Acknowledgments

First and foremost, I would like to thank God Almighty for giving me the strength, knowledge, ability and opportunity to undertake this master's study and to persevere and complete it satisfactorily. Without his blessings, this achievement would not have been possible.

Secondly, I would like to thank Bauer Spezialtiefbau GmbH for providing me with the opportunity to do my master's thesis. In particular, I would like to thank my supervisor Dipl.-Ing. Joachim Gaus. Since the commencement of my thesis in Schrobenhausen, Mr. Gaus has been very supportive and encouraging. He has made a great deal of effort in helping me acquire all the necessary data and made time whenever I needed to discuss any topic regarding my thesis. He consistently allowed this paper to be my own work, but steered me in the right direction whenever he thought I needed it. Mr. Gaus has also given a very thorough revision and critical commenting on this thesis. Without him, this thesis would not have been completed.

I would also like to express my gratitude to my university supervisor Prof. Roman Marte. He has been very supportive during my thesis since the beginning, by personally contacting Bauer and securing this master's thesis opportunity. Prof. Marte has also been an inspiration during his lectures, and has always supported me when I have approached him with questions and ideas. As my supervisor he has also made final remarks of this thesis and gave invaluable remarks. I could not have imagined having a better mentor for my master's study.

I would like to thank my girlfriend, Aline Telzerow, MSc., for her invaluable time and extensive effort to go through pages and pages of meaningless text, while giving critical comments and suggestions on this thesis. I would also like to thank my brother Fitsum Samuel, MSc., for his tremendous effort to read through this thesis multiple times and make invaluable comments. They have given me constructive criticisms for my thesis as well as helped me in proofreading.

A special thank you to Mr. Erwin Girsch, Dipl.-Ing. Martin Heinrich and Dipl.-Ing. Ulli Wiedenmann for making my master's thesis stay with Bauer Spezialtiefbau GmbH possible. I am enormously grateful for the opportunity. I would also like to thank Florian Mann, MSc., Dipl.-Ing. Marina Andrade-Silva and Dipl.-Ing. Kamgang Elvis for their tremendous help and assistance in acquiring the necessary data for this thesis.

Finally, I must express my very profound gratitude to my mothers, Ms. Kidest Gedlu and Ms. Elisabeth Ayele, for providing me with unfailing support and continuous encouragement throughout my years of study. This accomplishment would not have been possible without them. I would also like to thank my brothers, for their continuous support in all my endeavors.

Dedication

This thesis is dedicated to my mother **Ms. Kidest Gedlu Teklemariam**, because of who, I am who I am today. እናቱ : አሞሰግናለሁ

Semeone Mesfin
Graz University of Technology
April 2018

Table of Contents

AFFIDAVIT	ii
Confidentiality Clause	iii
Zusammenfassung	iv
Abstract	v
Acknowledgments	vi
Dedication	vii
List of Figures	x
List of Tables	xii
List of Abbreviations and Acronyms	xiii
1. Introduction	1
2. Driven Piles	4
2.1 General Overview.....	4
2.2 Types and Selection Criteria of Driven Piles	4
2.2.1 Material Classification	4
2.2.2 Load Transfer Method and Performance of Classification.....	7
2.2.3 Section-type Classification.....	9
2.2.4 Classification Based on Soil and Environmental Conditions.....	11
2.3 Types of Offshore Foundations and Recent Developments	16
2.4 Pile Driving Installation Methods	19
2.4.1 Machineries	19
2.4.2 Hammers	22
2.5 Environmental Impact of Offshore Pile Driving.....	26
3. Driveability Analysis with PDI GRLWEAP	31
3.1 Pile Driving Analysis Background	31
3.2 WEAP Analysis Model and PDI GRLWEAP	33
3.2.1 Introduction.....	33
3.2.2 External Combustion Hammers (ECH) Model.....	37
3.2.2.1 The Ram and Assembly of EC Hammers.....	37
3.2.2.2 Hammer Losses of Double Acting and ECH Hammers	39
3.2.3 Driving System Model.....	40
3.2.4 Pile Model.....	41
3.2.5 Soil Model.....	42
3.2.5.1 Static Resistance Model.....	42
3.2.5.2 Dynamic (damping) Resistance Model.....	44
3.2.6 Numerical Procedures and Integration.....	45

3.2.7	Blow Count Computation	48
3.2.8	Static Geotechnical Analysis.....	49
3.2.8.1	Soil Type Based Method (ST)	50
3.2.8.2	SPT N-value Based Method (SA).....	51
3.2.8.3	The Cone Penetration Test (CPT) Method in GRLWEAP	53
3.2.8.4	The API Method in GRLWEAP	54
3.3	Driveability Analysis.....	60
3.3.1	Analysis Description	60
3.3.2	Soil Setup and Gain/Loss Factors.....	60
3.4	Refusal	63
4.	Driveability Analysis of BOWL.....	65
4.1	Project Overview	65
4.2	Input Data Summary.....	74
4.2.1	Overview.....	74
4.2.2	Static Geotechnical Analysis.....	79
4.3	Driveability Analysis Results and Discussion	82
4.3.1	Analysis Type-1 (T1-Lower_bound_unplugged (coring)).....	83
4.3.2	Analysis Type-2 (T2-Upper_bound_unplugged (coring)).....	86
5.	Conclusions	90
	Bibliography.....	92
	Appendices	95
Appendix A	Driveability Analysis Input and Results.....	96
Appendix B	Calculation Steps for Resistance Output.....	100
Appendix C	Reference Tables and Formats	107
Appendix D	Raw and Correlation Data	110

List of Figures

Figure 2.1 Timber piles. Source: (Hannigan et al. 2016)	5
Figure 2.2 Square pre-stressed concrete piles. Source: (Hannigan et al. 2016).....	5
Figure 2.3 Large diameter open-ended steel pile. Source: (BOWL 2011).....	6
Figure 2.4 Point bearing pile. Source: (FinnRA 2000)	8
Figure 2.5 Friction pile. Source: (FinnRA 2000).....	8
Figure 2.6 Cohesion pile. Source: (FinnRA 2000)	9
Figure 2.7 Winged piles. Source: (Tomlinson et al. 2008)	11
Figure 2.8 Types of closed-ended piles. Source: (FinnRA 2000, Tomlinson et al. 2008).....	12
Figure 2.9 Open-ended plugged pile.	13
Figure 2.10 Cast in-situ driven piles. Source: (Hannigan et al. 2016)	13
Figure 2.11 Mandrel driven cast in-situ piles. Source: (Buza 1999).....	14
Figure 2.12 Common foundations for offshore wind turbine structures with descriptions. Source: (Scottish Power Renewables 2012).....	16
Figure 2.13 Current developments of foundations for offshore wind turbine installations. Source: (EWEA 2013)	18
Figure 2.14 Types of piling rigs for pile driving. Source: (RTG Rammtechnik GmbH 2016, Bauer-Pileco Inc. 2016).....	19
Figure 2.15 Types of crane-supported leaders for pile driving. Source: (BAUER Maschinen GmbH 2017, The Constructor 2017).....	20
Figure 2.16 Pile driving guides. Sources: (Tomlinson et al. 2008, Martijn van Delft 2016)...	21
Figure 2.17 Pile hammer classification. Source: (Hannigan et al. 2006).....	22
Figure 2.18 Diesel hammer operation schematic (left to right). Source: (Bauer-Pileco Inc. 2016).....	23
Figure 2.19 P-23 Vibro Hammer. Source: (BAUER-Pileco Inc. 2015).....	24
Figure 2.20 Schematics of single and double acting hydraulic hammers. Source: (Hannigan et al. 2006)	25
Figure 2.21 Noise shroud for IHC hydrohammer. Source: (Hannigan et al. 2006)	25
Figure 2.22 Acoustic mitigation devices (AMD). Source: (OSC 2018)	29
Figure 2.23 Bubble curtains used for noise mitigation. Source: (Rumes et al. 2016).....	29
Figure 3.1 Wave propagation in a pile. Source: (Hannigan et al. 2006).....	35
Figure 3.2 Energy balance in the Hammer-Pile-Soil system. Source: (Pile Dynamics 2010)37	
Figure 3.3 Scheme and model of a typical ECH hammer, pile and soil. Source: (Pile Dynamics 2010).....	38
Figure 3.4 ECH ram and assembly Model. Source: (Pile Dynamics 2010)	38
Figure 3.5 Force deformation curve for slack model. Source: (Pile Dynamics 2010)	39

Figure 3.6 Driving system model. Source: (Pile Dynamics 2010)	41
Figure 3.7 Pile-Soil model. Source: (Pile Dynamics 2010)	42
Figure 3.8 Soil Model. Source: (Rausche 2009).....	43
Figure 3.9 Static shaft and toe quake resistance. Source: (Rausche 2009).....	43
Figure 3.10 Schematic of model of segment i (left) and free-body diagram (right) (Source: Goble and Rausche 1986).....	46
Figure 3.11: Block diagram of predictor-corrector analysis. Source: (Pile Dynamics 2010) .	48
Figure 3.12: GRLWEAP's ST analysis method input window. Source: (Pile Dynamics 2010)	51
Figure 3.13: GRLWEAP's SA analysis method input window. Source: (Pile Dynamics 2010)	52
Figure 3.14: GRLWEAP's CPT analysis method input window. Source: (Pile Dynamics 2010)	54
Figure 3.15: GRLWEAP's API analysis method input window. Source: (Pile Dynamics 2010)	55
Figure 4.1 BAUER Dive Drill C40. Source: (BAUER Renewables Ltd. 2018)	65
Figure 4.2 Beatrice Offshore Wind farm Ltd. installation layout. Source: (BOWL 2017))	66
Figure 4.3 The vessel with PIF, Hammer and BAUER DD C40. Source: (BOWL 2017)	67
Figure 4.4 Pile Installation Frame (PIF). Source: (BOWL 2017)	68
Figure 4.5 Internal Lifting Tool (ILT). Source: (BOWL 2017).....	68
Figure 4.6 Stabbed piles ready for hammering. Source: (Journal John O'Groat 2017).....	69
Figure 4.7 IHC S-2500 Hydrohammer and section detail. Source: (SHL 2017)	71
Figure 4.8 Cluster - 3 steel pipe detail partially. Source: (BOWL-project documents).....	72
Figure 4.9 Steel pile production and storage. Source: (BOWL 2011)	73
Figure 4.10 Pile and Driving Equipment data for BE-L9. Source: (BOWL-project documents)	75
Figure 4.11 Manufacturer's recommended driving system	76
Figure 4.12 Steel pile production and storage	78
Figure 4.13 Summary of the soil investigation bore log report for BHI-69	80
Figure 4.14 Shaft and toe resistance distributions for ST (left), SA (center) and API method in GRLWEAP (right).....	81
Figure 4.15 Type 1-driveability prediction of BE-L9 with G/L-0.833/1.000	84
Figure 4.16 Type 1-driveability prediction of BE-L9 with G/L-1.000/1.000	85
Figure 4.17 Type 2-driveability prediction of BE-L9 with G/L-0.833/1.000	88
Figure 4.18 Type 2-driveability prediction of BE-L9 with G/L-1.000/1.000	89

List of Tables

Table 3.1 GRLWEAP recommendations of shaft and toe quakes. Source: (Pile Dynamics 2010).....	44
Table 3.2 Recommended damping factors after Smith. Source: (Pile Dynamics 2010)	45
Table 3.3 Soil parameters input possibility for SA analysis.....	52
Table 3.4 Soil parameters input possibility for API - GRLWEAP analysis	55
Table 3.5 Soil parameters input possibility for SA analysis.....	56
Table 3.6 Recommended analysis for non-plugging pile with partial internal friction	58
Table 3.7 Lower bound analysis of large diameter open-ended piles with partial plugging ..	58
Table 3.8 Upper bound analysis of large diameter open ended piles with full plugging	58
Table 3.9 Recommended analysis for small diameter open-ended piles with full plugging ..	59
Table 3.10 Recommended analysis for SRD after Stevens et al. (Stevens et al. 1982).....	59
Table 4.1 IHC S-2500 Specification. Source: (SHL 2017)	70
Table 4.2 BOWL pile specification.....	71
Table 4.3 General input parameters used	77
Table 4.4 Brief summary of major soil types.....	82
Table 4.5 Analysis type-1, lower bound, coring (unplugged)	83
Table 4.6 Analysis type-2, upper bound, coring (unplugged).....	86

List of Abbreviations and Acronyms

API	American Petroleum Institute
BG	Bearing Graph
BOWL	Beatrice Offshore Wind farm Limited
CAPWAP	Case Pile Wave Analysis Program
CPT	Cone Penetration Test
D-table	Depth Driving Modification Form
EIA	Environmental Impact Assessment
ECH	External Combustion Hammers
IC	Inspector's Chart
ICH	Internal Combustion Hammers
ILT	Internal Lifting Tool
LAT	Least Astronomical Tide
LTSR	Long Term Static Resistance
NDT	Non-destructive testing
SA	SPT N-value based method
SEA	Strategic Environmental Assessment
SRD	Static Resistance to Driving
ST	Simple soil type method
S1	Soil Property Input for Driveability Analysis
PD	Post Driving
PDA	Pile Driving Analyzer
PDI GRLWEAP	<u>P</u> ile <u>D</u> ynamic <u>I</u> nstitute - <u>G</u> obble, <u>R</u> ausche and <u>L</u> inks - <u>W</u> ave <u>E</u> quation <u>A</u> nalysis of <u>P</u> ile <u>D</u> riving

1. Introduction

In a world that is getting more cautious of climate change and its dire effects, renewable clean energy is being adopted by many developed countries as the way forward. In Europe, the total installed energy generation is trending to renewable sources such as wind, solar and others. Common power generation trends like coal and oil and nuclear are slowly being decommissioned and put out of use (Wind Europe 2016). From these renewables, wind energy has shown a higher growth rate. According to Wind Europe (Wind Europe 2016), the wind energy sector has shown a constant growth in Europe. In 2016, it has taken coal's place as the second highest form of energy generation. Onshore wind energy generation in Europe is the popular trend. But in recent years, offshore wind farms are getting more investments. Wind Europe (Wind Europe 2016) reported that in 2016 offshore wind projects alone were responsible for more than half of the investment activity in the renewable energy sector of Europe. The United Kingdom has the most operating offshore wind energy in Europe, with 2000 wind turbines spread out in 69 wind farms (EWEA 2014). Energy supplying firms are investing more on offshore wind energy because of vast amount of available wind power, closeness to populated coastal areas, saving of land resource, mobility ease and preservation of nature (Malhotra 2011). The European Wind Energy Association (EWEA 2013) estimates that at the end of 2020 the offshore wind energy operated in Europe will be between 20 and 40 Gigawatt.

For these offshore wind farm projects piles are commonly chosen as a foundation solution. Piles are cylindrically shaped elements that are used for transmitting loads to a competitive sub base (Tomlinson 1994). In the earlier days the use of piles as a foundation solution was limited by economics, which was due to the installation technologies, and method of analysis to predict the long term performance of the piles. Increased adoption of piling works in the present day are a direct result of development of advanced analysis methods for design, NDT (Non-destructive testing) methods for load and integrity, and simpler and more advanced machineries produced for installation pile. For offshore projects, the bearing stratum for the piles is found at the bottom of the sea/ocean bed. This fact makes installation capabilities a governing factor for the choice of a foundation system. From the different pile foundations, steel tubes are usually adopted and are driven down by a hammer. They are chosen because they are light and easier to handle, hence can easily be floated into position. In addition, driving of piles can be done from a vessel, which makes installations in such a difficult environment simpler. Common types of offshore wind turbines are monopiles. They are large diameter open ended piles. For deeper water levels, usually above 30 m, jackets are adopted. They are 3-leg or 4-leg lattice structures which are pinned on each leg to the sea bed by piles.

In any pile driving operation unprecedented challenges may occur. They might be due to unexpected resistance from the soil, driving system breakdown and others problems. Compared to onshore sites, problems arising on an offshore site may take some time to solve. Not to mention that the financial loss is also relatively higher. Soil resistance that is higher than the applied energy is said to cause refusal. This means the pile cannot be driven down without causing damage to the pile or hammer. In this case measures to mitigate the problem of refusal can be adopted. Jetting and relief drilling are some of the common methods applied. Through jetting or drilling, the material on the inner or outer part removed to reduce the frictional resistance on the pile lateral surface from the soil. If it is not possible to predict the scenario of refusal, an additional machinery and crew has to be on standby in the event that refusal might occur. But it is possible to run pile driveability analysis beforehand to predict if the driving is possible with a specified hammer and pile makeup.

Driveability analysis consists of appropriate hammer selection, pile detail configuration and analysis of soil type to attain the target penetration depth or attain the desired resistance that matches a blow count that does not damage the pile (Anusic et al. 2016). The wave equation has been used to evaluate dynamic pile driving problems. The computer program GRLWEAP (Pile Dynamics 2010) developed by Goble, Rausche and Likens (GRL), is the software that is widely used in the industry to perform pile driveability (Malhotra 2011). A good driveability analysis will give good prediction results. This result can make a very big difference in the initial stages of the project, especially when tendering. When accompanied by good geotechnical investigation data and experience, a driveability analysis will enable the designer to make a very good prediction and make a reasonable tender offer.

When dealing with offshore pile driving, an important and often big part of the overall construction is the environment. According to Bailey et al. (Bailey et al. 2014), the main environmental issues as a direct and indirect result of offshore wind developments are noise pollution, risk of collisions, changes to benthic and pelagic habitats, alterations to food webs, and water pollution caused by vessel traffic or contaminants released from seabed sediments. In Europe, before an offshore wind farm project is approved, two major environmental studies are carried out to account for these environmental concerns. They are Environmental Impact Assessment (EIA) and Strategic Environmental Assessment (SEA) (Mockler et al. 2015). Environmental repercussions of offshore wind projects are assessed before approval using the EIA. Evaluation of environmental effects during the preparation of policies, plans, programs and legislations (including executive regulations) is done in the SEA (Mockler et al. 2015). And hence, the impact assessment studies for offshore wind farm projects undertake extensive environmental studies before being the go ahead. Aside from the previously

mentioned impacts, these studies also address concerns such as gas emission due to vessel transits and helicopter journeys, dismantling of structures onshore/nearshore, disposal/recycling of materials post dismantling, protection of marine archaeology and other site specific issues.

Bauer Renewables Ltd is a construction company that works in the offshore construction sector for wind and tidal energy developments (BAUER Renewables Ltd. 2018). In recent years, BAUER Renewables Ltd. was involved in the foundation work of an offshore wind farm project, to provide relief drilling services with an underwater drilling rig (Dive Drill C40) (BauerNews 2017). The primary aim of this research is to determine if it is possible to use the software PDI GRLWEAP to perform driveability analysis and also predict refusal. The study will be done on the mega wind farm project Beatrice Offshore Wind farm Limited (BOWL). Finally, a driveability prediction will be compared with the post driving data to make the conclusion.

2. Driven Piles

2.1 General Overview

In a spreading and growing construction world, using more efficient and economical methods is the only way forward. Driven piles made of timber, and installed using drop hammers, go back to 800 BC. Other pile types go back as early as 200 BC. However, driven piles with reinforced concrete material have a history of over a century. Around the same time, driven piles made of steel frames of different sections started being used. Octagonal and square, precast, prestressed concrete piles as well as 36 inch (91.5 cm) and 54 inch (137 cm) diameter post-tensioned concrete cylinder piles were developed in the 1950's (Hannigan et al. 2016).

Driven piles are foundation elements that are hammered or vibrated into a stratum. Once installed, they can be used to transfer loads (vertical or horizontal) to the lower level of soil. Load transfer can be through frictional resistance of the shaft or end bearing of the pile toe, or a combination of the two. Different types of driven piles exist. They vary in their functionality, load transfer mechanism, strength, site condition and other deciding factors. The following sections describe the different types of driven piles.

2.2 Types and Selection Criteria of Driven Piles

2.2.1 Material Classification

In terms of material, Bowles (Bowles 1997) classifies piles into timber piles, concrete piles, and steel piles. They are also combined to form composite piles.

Timber piles: are made of tree trunks with the branches carefully trimmed off, usually treated with a preservative, and driven with the small end as a point. Occasionally the large end is driven for special purposes as in very soft soil where the soil will flow back against the shaft and with the butt resting on a firm stratum for increased bearing. The tip may be provided with a metal driving shoe when the pile has to penetrate hard or gravelly soils; otherwise it may be cut either square or with some point (Bowles 1997). Timber piles are best serving when placed fully under water. Unless treated with chemicals, fluctuation of wetting and drying considerably limits their lifetime. Additionally, in a dry condition, they are prone to attacks from termite and boring birds (Bowles 1997).



Figure 2.1 Timber piles. Source: (Hannigan et al. 2016)

Concrete piles: are of both precast and cast in place types. The prestressed concrete piles are precast elements made from concrete and reinforcement. They are usually manufactured in a fabrication yard and then transported to the construction site. There are different shapes of concrete ranging from rectangular to circular and from solid to hollow. Fabrication may be done using ordinary reinforcement or using pre-stressing elements. Precast piles that are normally reinforced are used to resist bending during mobilizing and lateral loading, and resistance against axial loads during driving (Bowles 1997). Pre-stressed concrete piles are made from pre-stressed tendons which are encased in concrete. The tendons will give the concrete tensile resistance which may be required during installation. Prestressed concrete piles vary from the most common solid square section to a hollow round section e.g. prestressed hollow concrete (PHS) (Hannigan et al. 2016). Cast-in place driven piles are piles that involve driving followed by concrete filling operation. Pipes, tapered piles, and monotube piles are common cast-in-place piles. More description about cast-in-place piles is written in section 2.2.4.



Figure 2.2 Square pre-stressed concrete piles. Source: (Hannigan et al. 2016)

In general, concrete can be damaged from acidic substances, which are produced by some soil types (e.g. organic). Unless special measures are taken, saltwater can also form undesired bond with the concrete. Furthermore, concrete pile located offshore may wear due to wave movement and dredges in the water. Ice formation and melting may also cause damage to the concrete (Bowles 1997).

Steel piles: are usually rolled into pipe or forged H-section shapes. The flange and web of H-section piles have equal thickness. Their cross-sectional area is also not very large which creates a small-volume displacement. Pipe piles are either welded or seamless steel pipes, which may be driven either open-end or closed-end (Bowles 1997). The pipe piles may also have different variations.

In general, due to their robustness, steel piles have a very good capability of being driven to higher depths. During pile driving the pile is subjected to a high level of stress. Compared to other material types steel has a higher capacity of carrying high compressive loads and it is also very light to handle. Additionally, their resistance to buckling and bending forces combined with their high resilience capacity makes their application versatile. But they are relatively more expensive than other materials that make up a pile. Their cost per meter is high compared with precast concrete piles. Another issue with steel piles is corrosion, which can be treated by applying anti-corrosion coatings to the water exposed sections (Tomlinson et al. 2008).



Figure 2.3 Large diameter open-ended steel pile. Source: (BOWL 2011)

Composite piles: are made up of two or more sections of different materials or different pile types. Various composite sections may be used, based on the properties of the underlying stratum. The lower section may be compiled of timber, pipe or an H-section steel section. Whereas the top part maybe composed of prestressed concrete, steel or corrugated shell (Hannigan et al. 2016).

2.2.2 Load Transfer Method and Performance of Classification

The British Standard Code of Practice for Foundations (BS 8004 1986) places driven piles in three categories: large displacement piles, small displacement piles and replacement piles (Tomlinson et al. 2008). The classification summarizes and groups commonly used types of piles as described below.

Large displacement piles: are piles which can be either solid or open section, but having a closed bottom. They can be installed by impact driving to overcome the soil resistance (Figure 2.4). Driven type of large displacement piles can be classified as timber, steel tubes and boxes, precast and prestressed concrete, and fluted or tapered steel tubes (Tomlinson et al. 2008). Driven and cast-in-place piles are also further classified. They are steel tube driven and withdrawn after placing concrete, steel tube driven with closed end, left in place and filled with reinforced concrete, precast concrete shell filled with concrete, thin-walled steel shell driven by withdrawable mandrel and then filled with concrete, rotary displacement auger and screw piles, and expander body (Tomlinson et al. 2008).

Small-displacement piles: are piles which have a lower cross-sectional area and are installed by impact driving (Figure 2.5a). They may be of rolled steel H or I-sections types as a full section, or may be open ended with a pipe or rectangular section. The latter small displacement piles, depending on the soil type, may core through the soil or plug (Tomlinson et al. 2008). When these pile types plug with soil during driving they become large displacement piles (Figure 2.5b). BS (BS 8004 1986) classifies small-displacement piles as; precast and prestressed concrete piles (both as open-ended pipes), steel H-sections, steel tube section (open-ended with possible soil plug removal), and steel box section (open-ended with possible soil plug removal) (Tomlinson et al. 2008).

Replacement piles: are pile which are installed by removing the soil material prior to being installed. Concrete pouring may be done into a cased or uncased hole, or the casing may be removed after concrete pouring (BS 8004 1986). It is also possible to place timber or steel in these pre-drilled holes. Typical types are: concrete placed in a hole which is drilled by rotary auger, baling, grabbing, airlift or reverse circulation methods (bored and cast-in-place), tubes placed in a hole drilled and filled with concrete, precast concrete units placed in a drilled hole, cement mortar or concrete injected into a drilled hole, steel sections placed in a drilled hole, and steel tube drilled down (Tomlinson et al. 2008).

These pile types are also combined in various forms with each other to form composite piles, either from the same category or with the others. Aside from the mentioned methods of classification, piles can also be categorized based on their performance. According to Finnish

National Road Administration (FinnRA 2000), piles can also be point bearing, friction and cohesion piles.

Point bearing piles: have a system where the majority of the pile load is transferred to a rock or hard base layer. This is also known as an end bearing pile, where the remaining part of the load is carried by the shaft friction. As the diameter of the pile increases, the end bearing resistance can be greatly enhanced and can be made to carry larger loads.

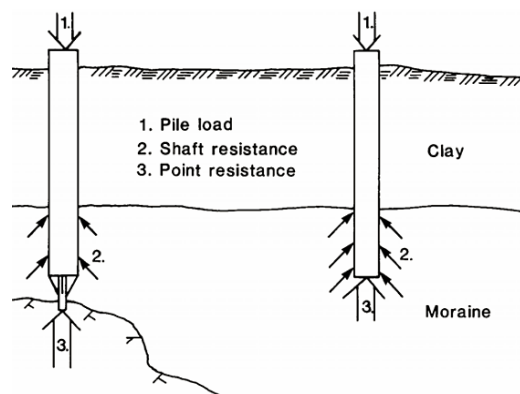


Figure 2.4 Point bearing pile. Source: (FinnRA 2000)

Friction piles: have a system where the majority of the pile load is carried by the surrounding soil layer through shaft frictional resistance. The remaining part of the load is carried by the end bearing resistance. For the end bearing resistance, an open-ended section can have two load transfer mechanisms. The first type Figure 2.5a, is for a pile with an external and internal friction, where the end bearing acts on the sectional area of the pile bottom. For this case, a non-displacement open-ended pile is a good example. The second type Figure 2.5b, transfers part of the load to the surrounding soil through external shaft resistance and part of the load is carried by an internal frictional resistance between the soil plug which is forced into the pile. This is known as a plugged pile. During an analysis the plug effect can be considered by applying a full toe area for the end bearing resistance.

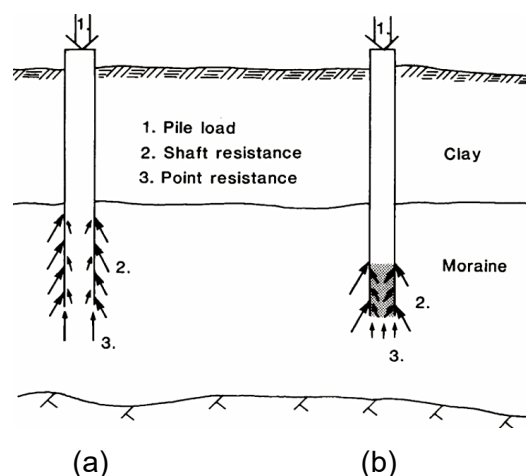


Figure 2.5 Friction pile. Source: (FinnRA 2000)

Cohesion piles: these types of piles use friction as a medium of load transfer, but mainly through adhesion developed on the shaft surface. A structure founded on such piles is subject to settlement because they are acting on compressible soil. Hence, the allowable settlements criteria usually govern the applicability of such piles. They are also known as floating piles.

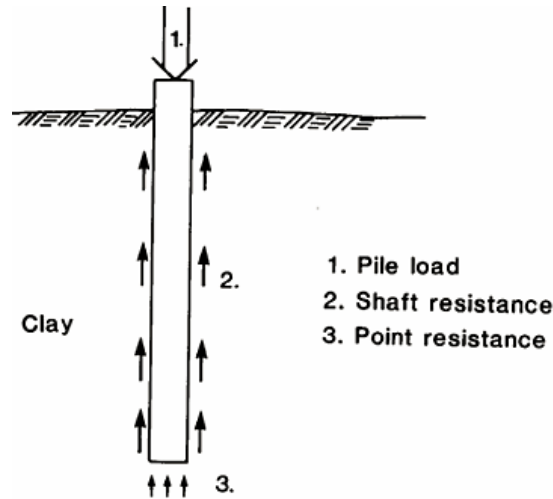


Figure 2.6 Cohesion pile. Source: (FinnRA 2000)

Aside from the above classifications, piles also behave differently with size. Large compression and tension can be carried by steel pipes having larger diameters. They can be applied to different areas and structures with: high bending loads, offshore structures and touch soil conditions. They are mostly adopted when dealing with bridges, coastal structures and susceptible structures (FinnRA 2000).

2.2.3 Section-type Classification

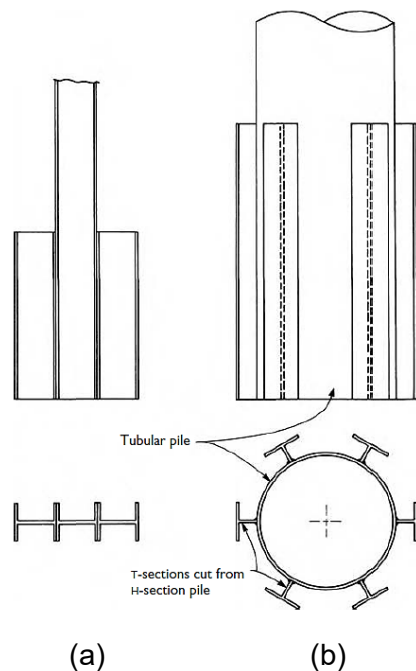
Steel piles can have different sections, and maybe modified to fit a certain requirement for driving. They mainly include boxes built up from sheet piles, box-sections, H-sections, plain tubes and fluted and tapered tubes. For the open-ended sections, concrete filling may be subjective. For example, offshore foundation applications have a requirement of resilience than rigidity and hence are preferred to be left un-concreted. When it is desired to concrete open-ended sections, removal of material from the inner side is carried out with grabbing, augers and by water-circulation drilling or by airlift (in case of non-cohesive soil). When soil has to be cleaned out for subsequent placement of concrete steel tubular piles are the preferred shape. This is because it avoids corners where it may be difficult to remove the soil material. Furthermore, circular shape is advantageous in minimizing drag and oscillation from waves and currents (Tomlinson et al. 2008). They are chosen for marine structures, where they can be fabricated and driven in large diameters to resist the lateral forces in deep-water structures. Open-ended pipe piles are normally used, because they can carry high compressive loads. Alternatively, their bottom section may be closed to give the piles a higher

end bearing resistance. Another case may be, a stiffened bulkhead closure with a perforation for water pressure dissipation, may be placed in the intermediate height of the pile for the purpose of driving to a deep penetration (Tomlinson et al. 2008).

Welding is usually the way to connect different sections of steel pipes forming the pile. However, they may be subjected to change depending on the location of application. Steel tubes can be welded in sections: either spirally or longitudinally. Depending on the section, they may also be seamless, or a combination with welding. Spiral welding is carried out by machines and hence can be made to longer sections but sections may be limited with machine capacity. In this case, there is a risk of the bottom welding cracking open during hard driving, also known as unzipping. Longitudinal welding is done on sections that are formed by rolling a steel plate. Different attachments and variations can be applied to the steel sections, based on the design capacities and economic considerations.

For on-site welding operations, steel pipe piles are extended either by arc welding or gas arc welding. Arc welding is the most basic type of welding. It uses an electric current, transferred through a welding stick, to form an electric arc between the stick and the metals to be joined. A gas arc welding, also known as metal inert gas (MIG) welding, is a welding process in which an electric arc process forms between a consumable wire electrode and the metals, which melts and joins the metals (Volume and American Welding Society 2004). For on-site welding procedures, since gas arc welding is sensitive to disruption from wind, arc welding is usually preferred (FinnRA 2000). However, for offshore applications, first class welding may not be possible, due to the stability of the vessel or an influence from the swaying pile due to water current waves. Here, first-class welding refers to the quality of the weld and the welder (first-class welder). First class welders usually work with steel or alloy that is under high pressure. Structures like boiler pipes, gas tanks and other structures that require extreme accuracy and require first class welder certification (Volume and American Welding Society 2004). Unsupported welded sections (above the sea bed) of an offshore pile, are exposed to high lateral forces and corrosive influences, which will result in cracking of the welds. Nevertheless, the soil supported steel section of the pile may be able to carry compressive loads even after suffering cracking. Usually the steel sections for an offshore pipe pile are prefabricated in a separate location and welded thoroughly in a horizontal position. Since such a welding is not performed underwater, the steel piles are fabricated with the maximum predicted length plus any surplus cut-off length.

Previously mentioned in section 2.2.1, one of the popular steel section for pile driving are H-sections. They are preferred for situations where ground heave is not allowed. They have a penetrating ability in stiff clay and dense sand layers, and also have a high compressive load carrying capacity. When using H-piles, driving through loose and medium dense sands layers, soil tightening is relatively avoided. This is because of their relatively small cross-



sectional area. Which also implies that H-piles cannot develop a high end-bearing resistance. In addition, the weaker axis of an H-pile may fail under high bending stress resistance when terminated in soils or in weak or broken rocks. In Germany and Russia, it frequently is the practice to weld short H-sections on to the flanges of the piles near their toes to form 'winged piles' (Figure 2.7a) (Tomlinson et al. 2008). This increases the toe area and improves the end bearing resistance. It also doesn't affect the feature of its penetrability. The same can be done for tubular sections, where a T-section is welded along the circumference, (Figure 2.7b).

Figure 2.7 Winged piles. Source: (Tomlinson et al. 2008)

Furthermore, there are several pile steel sections that have been developed over the years. One of the types are monotube piles, which possess a combination of uniform top and tapered lower section. Another type is a 'Soilex' system with an expandable body forming an enlarged bulb to displace and compact soil. Similarly, tubular steel pile sections can be equipped with additional add-on sections, called 'shoes'. They are used when open-ended piles are applied in strata resistant to driving or used in weak rock. The ring-like shoe is welded either in the inner or the outer section of the pile. Inner shoe is applied when a full frictional capacity of the pile is developed, whereas an outer shoe is applied for reduction of friction enabling deeper penetration of end bearing piles. Further stiffening can be done by cruciform steel plates, which are plate-bracings forming a cross (Tomlinson et al. 2008).

2.2.4 Classification Based on Soil and Environmental Conditions

Embedding soil layers along with other geotechnical and geological conditions are considered when choosing and designing steel piles. The presence of thick layers of soft soils and ground water for instance, demands the consideration of the high buckling potential, which results in large diameter piles. On another case, when driving through a dense soil layer, the governing

factor becomes penetrability. Types of foundation systems for driven open-ended pipes based on soil types can be broadly classified as follows.

Close-ended piles: may be used either when piles are driven through a hard stratum or bouldery moraine or when the total toe area is needed to mobilize bearing resistance. If there is a sloping rock surface or the pile tip rests on a rock layer, then a rock shoe (Figure 2.8a) may be used. For bearing resistance development of a tubular pile section may be used a bottom plate may be used (Figure 2.8b). Another type is a Franki pile, Figure 2.8c, which uses a drop hammer to drive a concrete or gravel plug along with an encasing drive tube. It achieves the bearing capacity mostly from the bulb that is formed during the driving process. Since this is basically achieved through densification; a non-cohesive soil would be appropriate to apply a Franki pile on. Application to cohesive soils will not give a good result, as their compaction ability is relatively low (Tomlinson et al. 2008).

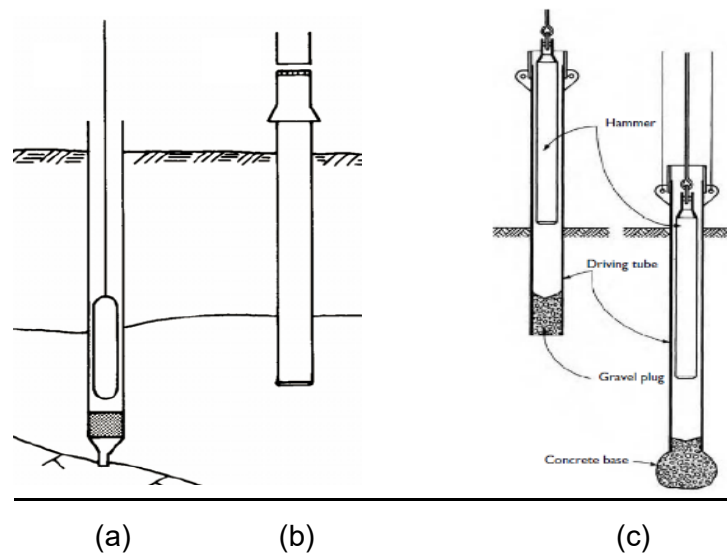


Figure 2.8 Types of closed-ended piles. Source: (FinnRA 2000, Tomlinson et al. 2008)

Open ended piles: are used where sensitive structures are present with a relatively small soil mass being driven through, they do not cause much displacement and disturbance. Generally, there should be enough thickness of coarse grained soil or bearing layer superseding a rock layer to develop enough bearing resistance. They can be of two main types; plugged and unplugged (Tomlinson et al. 2008).

The plugging pile, Figure 2.9, exists when a soil plug develops inside the pile due to the influence of friction. If the ratio of the soil plug to the diameter of the pile is comparable or more than one, then plugging may occur. This holds true, when the soil is dense, well graded and there is very small silt content. Sounding techniques can confirm the formation of plugging,

otherwise an unplugged pile should be assumed and redesigned with a longer pile section (FinnRA 2000). In this case, the internal shaft friction will not be activated, rather the end bearing resist will act on the full bottom area. An unplugged open-ended pile, Figure 2.5a, occurs when only external shaft frictional resistance is developed and plugging is not confirmed. Depending on the soil type and uniformity of the pipe pile, considerations of the internal friction may be made. For analysis purposes different approaches may be taken, which consider different possibilities of internal friction development along the shaft of the open-ended pile.

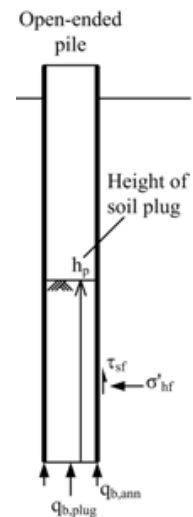


Figure 2.9 Open-ended plugged pile.

Source: (FinnRA 2000, Tomlinson et al. 2008)

Cast-in-situ driven piles: are piles which are used in granular soils to acquire a higher shaft resistance. A steel section is first driven and then concreted with reinforcement. The steel section may be driven with or without a mandrel. A mandrel is usually a heavy tubular steel section inserted into the pile that greatly improves pile driveability. If a mandrel is not present, the driven section is usually driven from the top. At the end of driving a concreting and reinforcement Pipe piles, Monotube piles and tapered piles are typical examples. They develop higher resistance of compression loading due to their tapering (Hannigan et al. 2016).



(a)



(b)

Figure 2.10 Cast in-situ driven piles. Source: (Hannigan et al. 2016)

The mandrel driven piles are usually closed ended piles and are driven from the bottom (Figure 2.11). A water tight bottom plate is used at the bottom, which will be lost. After driving, the mandrel is removed and concrete is placed. Based on the type and site condition, the steel section may or may not be removed after concreting.

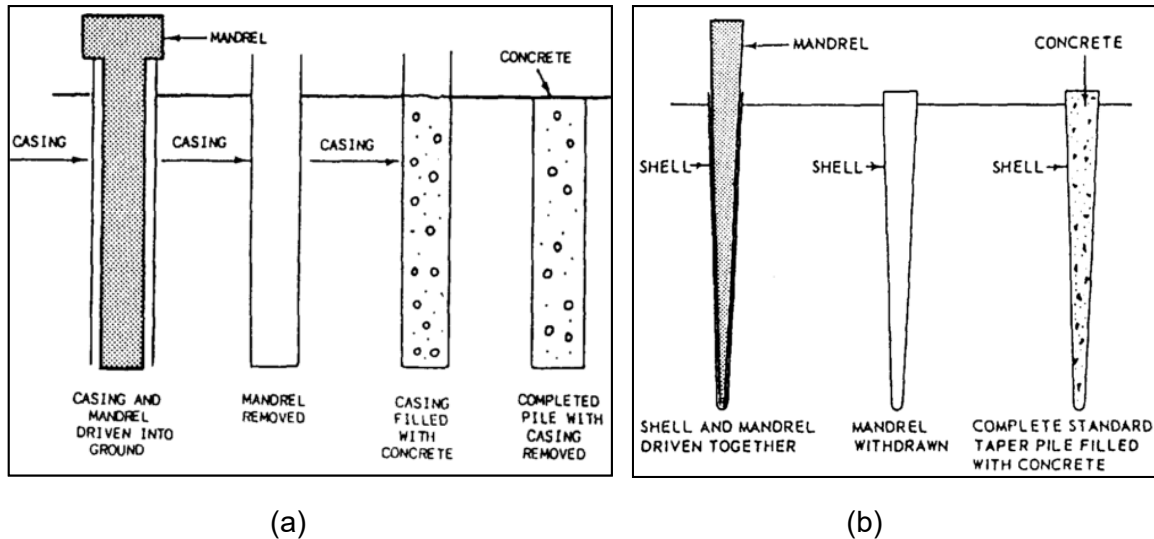


Figure 2.11 Mandrel driven cast-in-situ piles. Source: (Buza 1999)

Another main reason for using permanently cased piles is caving in of the encasing soil materials. This may occur when installing long bored piles with in different layers. The European norm (EN 1997-2 2007) for drilled piles asks for a permanent casing in soils where undrained shear strength (C_u) is less than 15 KPa (FinnRA 2000). In case an artesian pressure is encountered, the casing is usually not removed. This can be done with tremie method, which is a concrete placement method used to pour concrete using a tubular pile below water level. The driving procedure may involve hammers, vibrator, presses or oscillators. A casing may be made from a steel section with a small thickness and less quality (FinnRA 2000).

Consequences resulting from driving operations might also be a governing factor for the choice of a pile type. During driving settlements, soil disturbance, pore pressure rise, vibration and noise may occur. Different standards and codes, govern constructions to be in the allowable range to prevent this problems from occurring. According to EN:1997 (2004), a ground in which piles are located may be subject to displacement caused by consolidation, swelling, adjacent loads, creeping soil, landslides or earthquakes. These phenomena have to be considered as they can affect the piles by causing downdrag (negative skin friction) heave, stretching, transverse loading and displacement. Open ended piles may be applied for sites where structures with soil displacement sensitivity are present. This limits their end-bearing capacity. Close-ended piles, however have a lower soil displacement capacity than their concrete pile counterparts.

Settlement is an important environmental consideration. It may occur when driving through loose coarse grained soils. The densification is desirable, nevertheless it results in ground subsidence and may cause settlements in nearby structures. On the contrary, heaving and

horizontal displacement may occur when dealing with fine-grained soils. Since clay and silt layers are not suitable for compaction, the surrounding layers may be subject to heaving and the volume of heave most likely matches the heave volume. In all cases, it is advised that risky locations which are prone to such defects should be given priority for driving. Leveling techniques may be used to control the extent of settlements around these buildings with constant monitoring (FinnRA 2000).

Disturbance of soil layers is another major issue that makes the design and prediction of post driving behaviour of steel piles difficult. Dynamic effects initiated from the driving process result in the loss of strength of the surrounding soil. This is typical for fine grained soils. Rising of pore water pressure in fine grained soils can happen in the presence of water. This rise will cause the reduction of effective stresses. This can be controlled by removing fine grained soils, using open-ended piles, installing vertical drains and by driving slowly (or in periods) in order to give time for the water molecules to escape. Therefore, the pile does not possess the predicted design resistance immediately after it has been driven. From the time of driving, depending on the soil type, it takes three to five months to restore some of its initial strength (Tomlinson et al. 2008). This regaining of strength may be subjective to the consolidation history of the soil, meaning that an over consolidated soil will most likely regain its strength partially. This effect occurs in fine grained soils and it is called 'setup'. The reverse might occur in coarse grained soils and is referred to as relaxation. This is due to the compaction of the coarse grained soils during driving (FinnRA 2000).

Vibration and noise regulations on pile driving procedures also govern the pile selection procedure. Recording the maximum velocity of oscillation can be done to inspect the damages on nearby structures due to vibration. If needed acceleration and frequency may also be monitored (FinnRA 2000). One should note that vibrations are transmitted in higher magnitudes in soft clay and silt. This is also true for soils with a higher water concentration. The opposite is true for gravel and moraine, since they contain and reduce the vibration frequencies faster. To further monitor vibrations, gypsum strips, tapes or glass might be placed in sensitive places. Excessive vibration can be prevented when the driving is executed with a rig that is in a good condition. Furthermore, avoiding in-eccentric hammer blows, pre-drilling a dense layer and avoiding usage of hammers in cohesive soils may help prevent vibration. In extension, noise level requirements have to be kept within limits while driving. Where applicable, the source can be isolated or hammer and pile cushioning can be used as a solution to the noise problems (FinnRA 2000).

2.3 Types of Offshore Foundations and Recent Developments

The application of offshore foundations is dependent on the location of the structure and the corresponding depth of the seabed. From the offshore developments mentioned in chapter 1 wind farms may be taken as an example. Wind farms can be located anywhere in the sea. The depth of the foundation type used may be subjective in accordance with the corresponding depth of the construction. Concrete foundations (gravity based) and monopiles are the common foundations methods employed so far. As wind farm developments are stretching out to the deeper waters, the use of jacket structures is getting more popular.

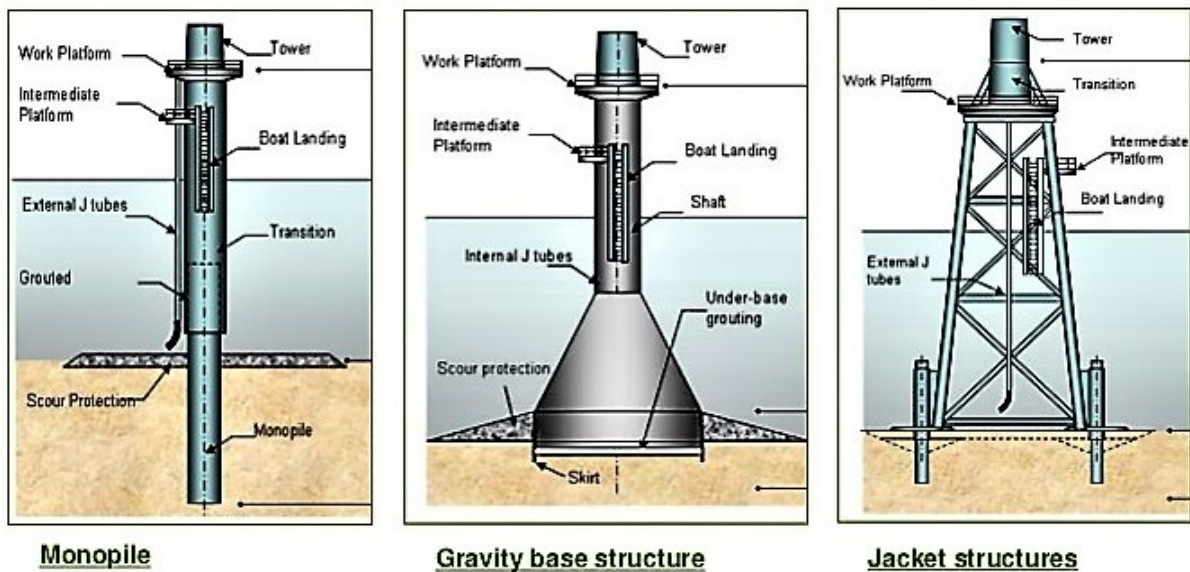


Figure 2.12 Common foundations for offshore wind turbine structures with descriptions.
Source: (Scottish Power Renewables 2012)

Gravity base structures: are foundation systems that resist the overturning loads and achieve stability solely by means of their own gravity (Figure 2.12 (center)). They are mostly applied on sites located in shallow waters. They are also applied in offshore sites where piles cannot be installed due to tough seabed soil condition. Typical types are gravity caissons. One type of gravity structures are gravity caissons. When the loads from the surrounding water movement is low, they are relatively cheap to produce (Malhotra 2011).

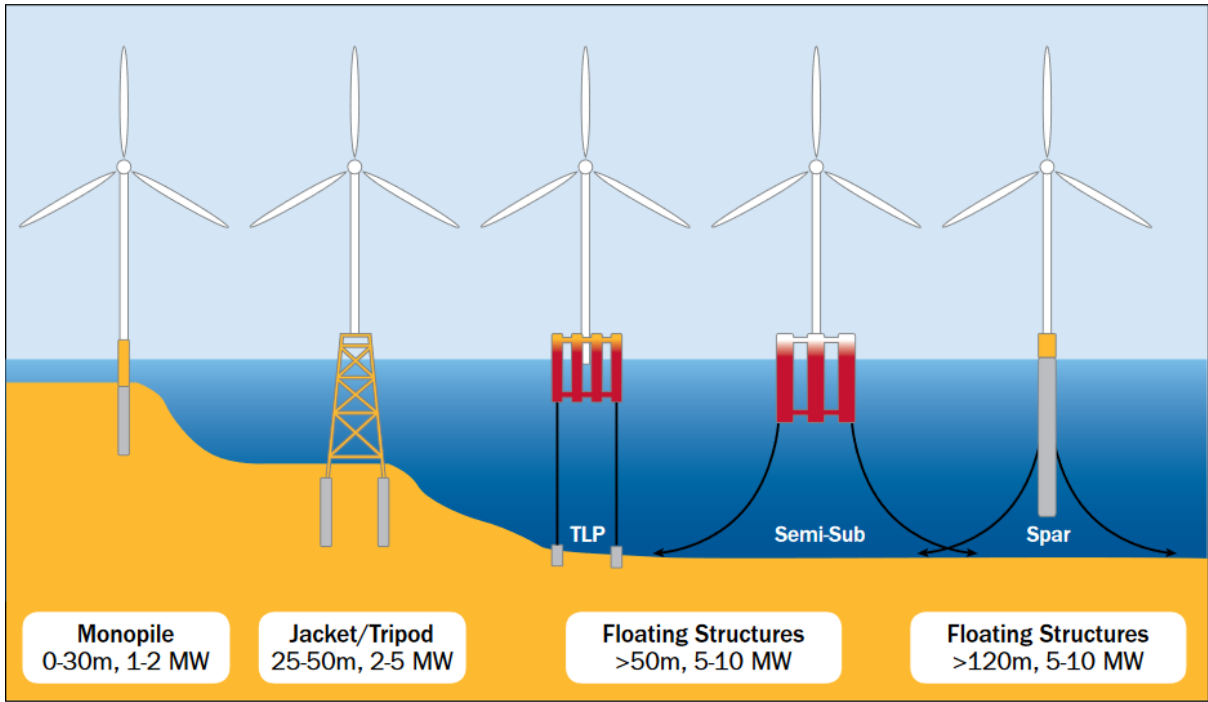
Monopiles: consist of a simple design which support the wind turbine connected with a transition piece. This transition piece is made up of steel. A monopile (Figure 2.12 (left) and Figure 2.13a) is usually an open-ended large diameter steel pipe. Its diameter can be as high as 6 m and a thickness of 150 mm. Based on the soil stratum, it can be installed with impact driving using a hammer, a vibrator or it can be grouted into sockets that are predrilled into a rock. The environmental impact of monopiles is less than gravity base structures. They are

the most common foundations solutions that are employed by the offshore wind energy development sector (Malhotra 2011).

Jacket structures: are 3-leg or 4-leg structural frames consisting of prefabricated steel pipe members (pin piles) connecting each corner (Figure 2.12 (right) and Figure 2.13b). They are employed in deeper waters to limit the deflection of the tower coming from current, wave and wind loads. Structurally, a jacket is interconnected with bracings to provide the required stiffness. A jacket leg is installed at each corner which is diagonally and horizontally braced to a transition piece in the center. Manufacturing of the frame and the piles is done onshore and is then transported by barge to installation location. Another merit of jacket structures is that they do not require extensive clearing of the seabed in preparation for the installation of the piles (Malhotra 2011).

In general, the criteria for the selection of pile types are mainly the location and type of structure, ground conditions and durability. Precast and prestressed concrete pile become heavier to handle as the water levels get higher. For this reason, tubular sections of either steel or concrete are applied (Tomlinson et al. 2008). Aside from the previously mentioned foundation types, the wind farm development sector has also adopted different foundation methods from other industries. According to a report by the European Wind Energy Association (EWEA 2013), adopted from the oil and gas industry, the offshore wind development sector uses mainly three types of foundation systems for offshore wind farm applications.

1. Tension Leg Platform (TLP): is a system where a floating structure that is partially submerged is anchored to the sea bed (Figure 2.13c). The anchoring is done by tensioned cables attached to the buoyant structure to attain equilibrium (EWEA 2013).
2. Semi-submersible Foundation: is a system that uses a partially submerged addition to attain equilibrium (Figure 2.13d). It is moored with a cable but is basically floating. Wind Float, which is a foundation system for offshore wind turbines, uses this technology (EWEA 2013).
3. Spar Buoy: using a ballast to attain equilibrium (Figure 2.13e). This ballast is part of a cylindrical floating structure. The cylinder is usually hollow on the top, and hence there will be enough buoyancy to float the cylinder and also enough ballast weight that counters it. Which means that the centre of buoyancy will be higher and centre of gravity will be lower. One example of this system is the Hywind (EWEA 2013).



Source: Principle Power

- (a) (b) (c) (d) (e)

Figure 2.13 Current developments of foundations for offshore wind turbine installations.
Source: (EWEA 2013)

2.4 Pile Driving Installation Methods

2.4.1 Machineries

There was a world-wide increase in the construction of heavy foundations in the period from 1950 to the 1970s as a result of developments in high office buildings, heavy industrial plants and shipyard facilities. The same period also brought the major developments of offshore oilfields. A high proportion of the heavy structures required for all such developments involved piled foundations, which brought about a great acceleration in the evolution of piling equipment (Tomlinson et al. 2008). Piles can be installed by boring, driving or jetting. Some of the governing factors are; soil type, equipment, the bearing capacity required and experience on the particular site. Depending on the types and function, the techniques used are evolving and reaching new boundaries. In this regard, the offshore development sector is a concrete example. Different methods of driven pile installations, according to Tomlinson (Tomlinson et al. 2008), are described as follows:

Piling rigs: mounted with a base carrier; the frames carry the hammer and guide the pile to maintain the correct alignment throughout the driving process. The essential parts of a piling frame are the leaders or leads. These are stiff members of solid, channel, box or tubular sections held by a lattice or tubular mast. The lattice or mast is in turn supported at the base by a movable carriage and at the upper level by back stays (Tomlinson et al. 2008). Their main purpose is to align the hammer and pile and also carry them (The Constructor 2017).

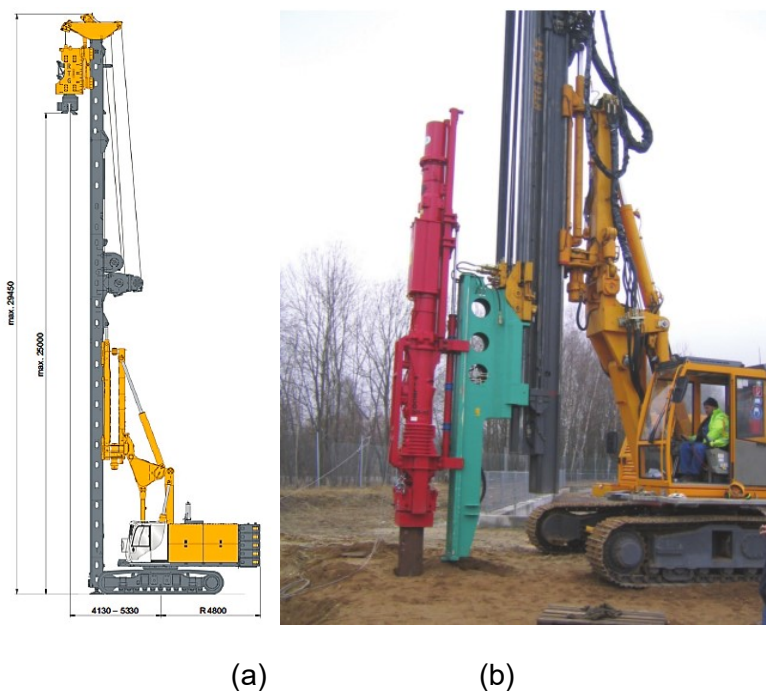


Figure 2.14 Types of piling rigs for pile driving. Source: (RTG Rammtechnik GmbH 2016, Bauer-Pileco Inc. 2016)

The leader can be extended vertically and adjusted at angle to maintain alignment (Figure 2.14a). The base of the equipment has a hydraulic adjustment which allows to tilt the leader backwards or to the front. This enables rotating of the base machine at any angle and tilting the leader, to drive different piles while remaining in the same position (The Constructor 2017). These machineries can be equipped with a fixed leader or telescopic mast (Figure 2.14b) (Tomlinson et al. 2008).

Crane-supported leaders: is a system where a crane hoists a fixed leader from the top by a swivel, and from the bottom by a hydraulically controlled bracing called spotter (Figure 2.15a). The spotter controls the verticality as well as the side movement of the leader. A variation of this type of pile driving machine are the 'hanging and swinging' leaders (Figure 2.15b). They are suspended from the top of the crane jib with a head block which allows free movement to fit over a stabbed pile where guides are provided (Tomlinson et al. 2008). When working with a stabbed pile they facilitate free movement, allowing fitting on a desired location and orientation. The leaders can also be used to mount different driving equipment such as vibrators and sheet pile presses (Tomlinson et al. 2008).



Figure 2.15 Types of crane-supported leaders for pile driving. Source: (BAUER Maschinen GmbH 2017, The Constructor 2017)

Guides: use a system of pile driving guided by a movable trestle. First, a crane is used to set up on each pile to be driven. Then the pile is centralized and held in position by two points known as ‘gates’. Depending on its design, the hammer is only supported by the pile and is held in alignment with it by leg guides on the hammer which may extend over the upper part of the pile shaft (Tomlinson et al. 2008). A decade ago pile a driving guide system, shown in Figure 2.16 (left), was developed in Germany. They are typically applied for offshore operations and also in barges with an opening (‘moon-pool’). A movable gantry (guide) is cantilevered from the vessel or is fixed between the barge opening. Movement of the guide and final adjustments are controlled by an electric motor and hydraulic rams, respectively (Tomlinson et al. 2008). Different types of guides with the same working principle are also applies in current practice of offshore pile driving, Figure 2.16 (right).

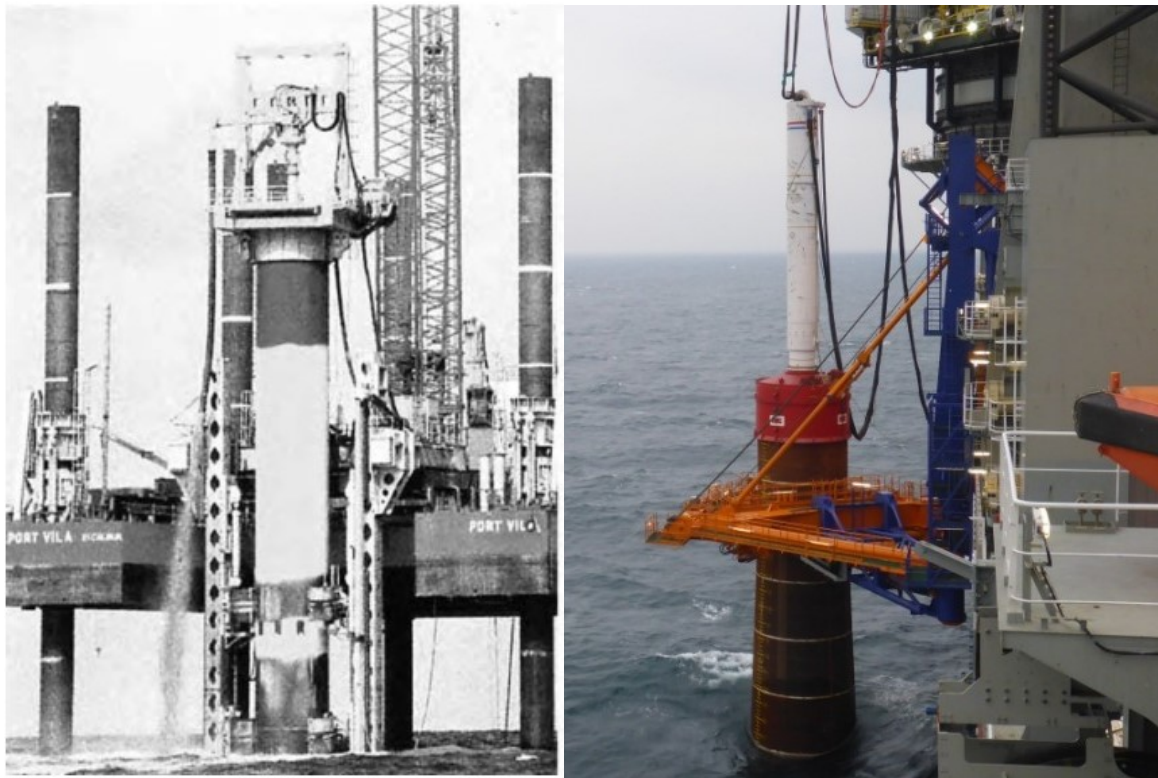


Figure 2.16 Pile driving guides. Sources: (Tomlinson et al. 2008, Martijn van Delft 2016)

When using this system, there is a chance of misalignment due to the hammer support system, especially when working with battered piles. A trestle guide is applied when driving steel piles. This avoids eccentric blows, that may result in high stresses in the driven section. In any case, the stress has to be monitored to make sure that bending stresses from the hammer weight and driving stresses are in the allowable limits. This is normally conducted onboard a vessel or barge for offshore pile driving.

2.4.2 Hammers

Different equipment has been developed for pile driving in the last century. Hammers are the most common and old equipment. Based on their source of impact energy, all hammers can be broadly classified as internal combustion hammer (ICH) and external combustion hammers (ECH). Diesel hammers are ICH, since the driving system is run by internal combustion in the chamber. All other hammers are ECH hammers. Choice of the appropriate hammer are affected by many factors. Pile makeup details (types and specifications), the type of soil to be driven done through, availability of space in the site, provision of cranes and noise limitations imposed on the area are some of the governing factors for the choice of a hammer (The Constructor 2017). Hannigan et al. (Hannigan et al. 2006) classifies the pile driving equipment as shown in Figure 2.17.

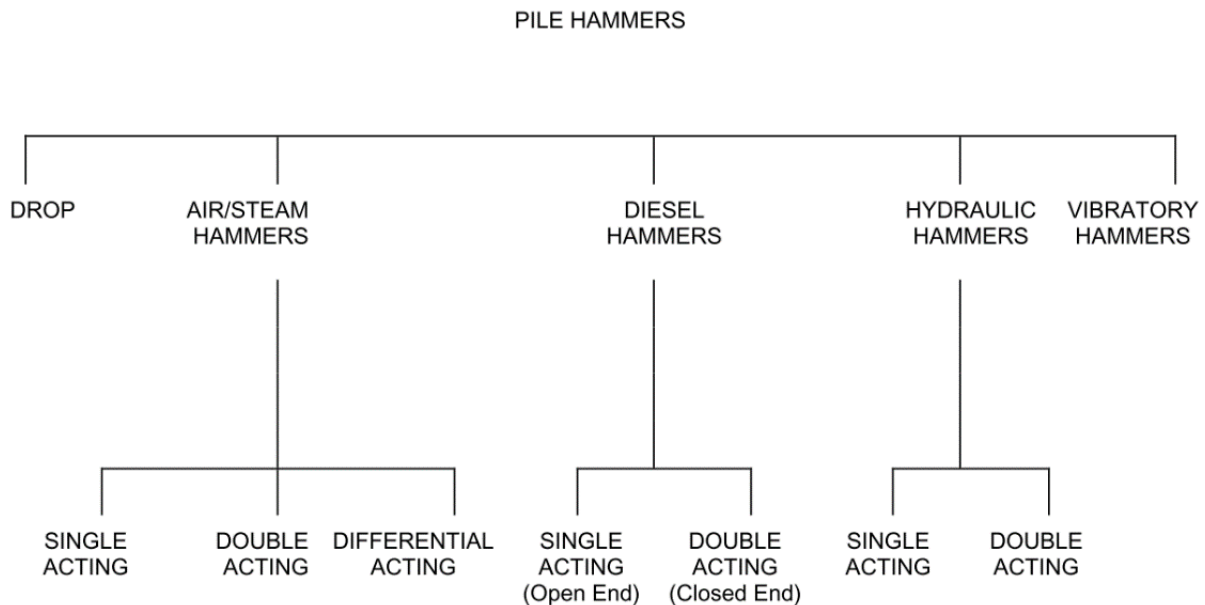


Figure 2.17 Pile hammer classification. Source: (Hannigan et al. 2006)

A **drop hammer** is a forged steel with solid mass ranging from 1000 to 5000 Kg. It is fitted with lifting eye and lugs for sliding in the leaders. It is usually applied to initial test piles (The Constructor 2017).

Single acting steam or compressed air hammer consist of a ram weight ranging from 2500 to 20000 Kg with a cylinder shape. The power source (steam or compressed air) would lift the ram to a specified height and then released it, which subjects it to a free fall and striking the pile helmet. The maximum hammer height available is 1.37 m and no higher 1.2 m in case of heavier pile (The Constructor 2017). The single-acting hammer is best suited to driving timber or precast concrete piles, since the drop of each blow of the hammer is limited in height and

is individually controlled by the operator. It is suitable for driving all types of pile in stiff to hard clays, where a heavy blow with a small drop is more efficient and less damaging to the pile than a large number of lighter blows (Tomlinson et al. 2008).

Double-acting (or differential-acting) hammers are steam- or air-operated both on the upstroke and down stroke, and are designed to impart a rapid succession (up to 300 blows per minute) of small-stroke blows to the pile. The double-acting hammer exhausts the steam or air on both the up- and down-strokes. In the case of the differential acting hammer, however, the cylinder is under equal pressure above and below the piston and is exhausted only on the upward stroke (Tomlinson et al. 2008). These hammers are most effective in granular soils where they keep the ground 'live' and shake the pile into the ground, but they are not so effective in clays (Tomlinson et al. 2008).

The principle of a **diesel hammer**, shown in Figure 2.18, is that as the falling ram compresses air in the cylinder, diesel fuel is injected into the cylinder and this is atomized by the impact of the ram on the striker plate. Ranging from 4500 to 15000 Kg, diesel hammers have different types (The Constructor 2017). They are generally suitable for all types of ground except soft clays. They have the advantage of being self-contained without the need for separate power-packs, air compressors or steam-generators. They work most efficiently when driving into stiff to hard clays, and with their high striking rate and high energy per blow they are favored for driving all types of bearing piles up to about 2.5 m in diameter (The Constructor 2017).

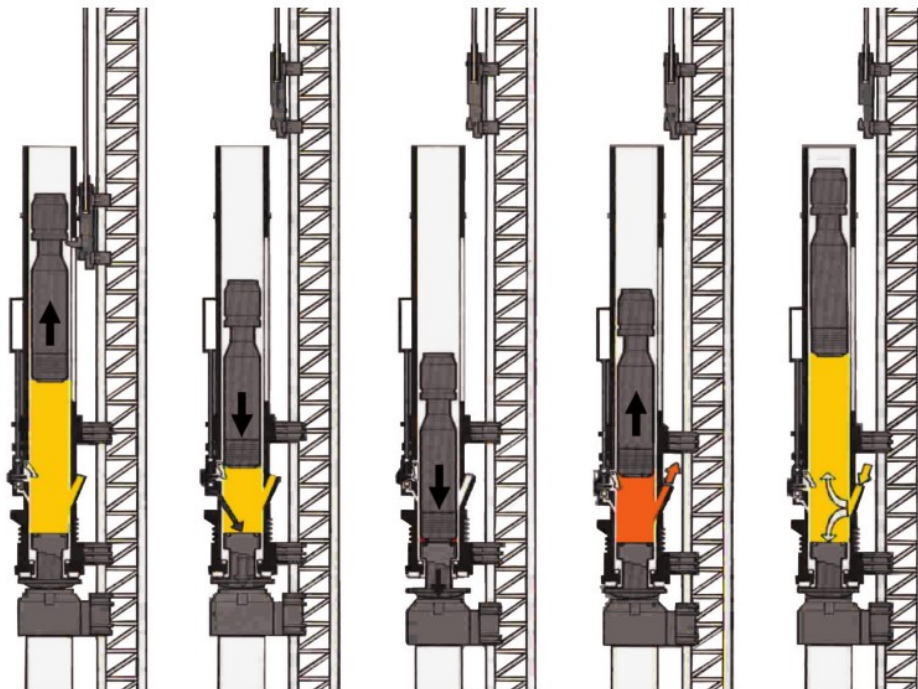


Figure 2.18 Diesel hammer operation schematic (left to right). Source: (Bauer-Pileco Inc. 2016)

Vibrators consist of pairs of exciters rotating in opposite directions which can be mounted on piles when their combined weight and vibrating energy cause the pile to sink down into the soil. The two types of vibratory hammers, either mounted on leaders or as free hanging units, operate most effectively when driving small displacement piles (H-sections or open-ended steel tubes) into loose to medium-dense granular soils. Vibrators have an advantage over impact hammers in that the noise and shock wave of the hammer striking the anvil is eliminated. They also cause less damage to the pile and have a very fast rate of penetration in favorable ground (Tomlinson et al. 2008).



Figure 2.19 P-23 Vibro Hammer. Source: (BAUER-Pileco Inc. 2015)

All **hydraulic hammers** use an external hydraulic power source to lift the ram (Hannigan et al. 2006). The simplest version is the single acting hammer. Hydraulic cylinders lift the ram and quickly retract, fully releasing the ram allowing it to free fall under gravity. The ram impacts the striker plate and the hammer cushion, which is located in the helmet. The hydraulic cylinder then lifts the ram again and the cycle is repeated. Another types are double-acting hammers (Figure 2.20a). Some types of double-acting hammers use hydraulic accumulators during the down stroke to store a volume of hydraulic fluid. This is used to speed up the ram lifting operation after impact (Hannigan et al. 2006). These types of double-acting hammers usually have a small double acting effect. Other more complicated models (Figure 4.7) have nitrogen charged accumulator systems, which store significant energy allowing a shortened stroke and

increased blow rate due to the applied pressure from the nitrogen chamber, in addition to free fall (Hannigan et al. 2006).

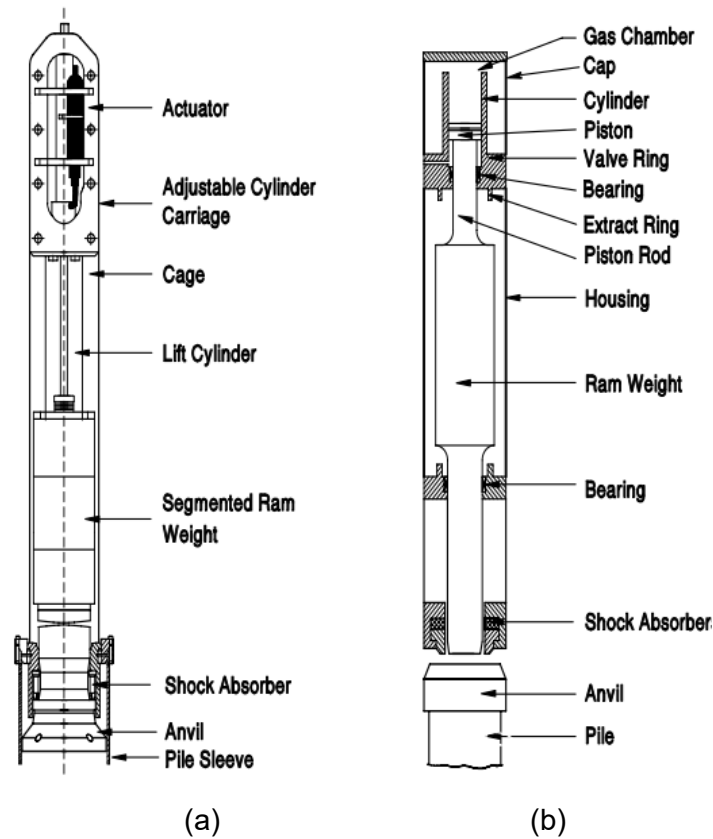


Figure 2.20 Schematics of single and double acting hydraulic hammers.

Source: (Hannigan et al. 2006)

Pile driving these hammers can also be equipped with add-ons for noise reduction (Figure 2.21). This compliments the concepts of environmental considerations during pile driving operations which is discussed in the next section.



Figure 2.21 Noise shroud for IHC hydrohammer. Source: (Hannigan et al. 2006)

2.5 Environmental Impact of Offshore Pile Driving

Countries found in the North Sea are all allowed to declare 12 nautical miles (12*1.852 km) from their coastline as territorial waters, with the boundary of the territorial sea for each state dividing the exclusive economic zone (EEZ) (Mockler et al. 2015). Environmental impact is a main criterion which is considered in the initial stage of an offshore wind farm development. According to Det Norske Veritas (DNV), these developments have to go through a consent process which enforces the awareness of marine/navigational safety and environmental impacts. Most European countries have a governing body making this regulations and enforcing them (Mockler et al. 2015).

The United Kingdom has the most operating offshore wind energy plants in Europe, with 2000 wind turbines spread out in 69 wind farms (EWEA 2014). EU law requires that every offshore wind farm development has to undergo two environments evaluation phases. They are Environmental Impact Assessment (EIA) and Strategic Environmental Assessment (SEA) (Mockler et al. 2015). Environmental repercussions of offshore wind projects are assessed before approval using the EIA. Det Norske Veritas (Mockler et al. 2015) reports that food chain disturbance, bird collision, stress and reduction of biological fitness, loss of habitat loss due to fish migration and others are some of the possible environmental effects and socio- economic problems that result from the development of offshore wind-farms The EIA mainly serves to create awareness with regards to the environment, by pointing out the potential damage that may occur because of the development (Mockler et al. 2015). Hence the assessment guarantees that all precautions to preserve the environment should and must be taken by the developer and all parties involved (Mockler et al. 2015).

Therefore, EU countries need to have an EIA and use it as an Environmental Statement (Mockler et al. 2015). Any offshore development project has to also present its EIA along with its application (Mockler et al. 2015). The second assessment process is the Strategic Environmental Assessment (SEA) Evaluation of environmental effects during the preparation of policies, plans, programs and legislations (including executive regulations) is done in the SEA (Mockler et al. 2015). An SEA Statement requires preparation of an Environmental Report. A potential offshore developer needs to prepare this report and input additional environmental considerations in the programme to have a competes SEA statement (Mockler et al. 2015).

As part of the EIA, the marine/navigational safety assessment or known as collision risk analysis is also carried out (Mockler et al. 2015). This mainly focuses on the influence of ships and vessels on the offshore development project. The major causes of this safety assessment

are providing search and rescue for vessels sailing through the wind farm, recreational or fishing vessels that are sailing near the farm, freight ships that have diverged from their normal route (Mockler et al. 2015).

From the different offshore wind projects being developed in Europe, Germany has a considerable amount of investment. As an example, environmental regulatory bodies of Germany, for offshore wind developments can be examined. In Germany, the bureau responsible for the approval of offshore wind farm developments is the German Bundesamt für Seeschifffahrt und Hydrographie (BSH). It facilitates all the proceedings for wind farms located in the German EEZ, as this is where most offshore developments are taking place. However, the regional authorities have the power to decide on the final approval of the wind farm development (Mockler et al. 2015).

One major requirement of the BSH, during the process for approval, is the environmental requirement. The development should not debilitate the safety and efficiency of traveling birds and cause harm to the marine environment. The standard outline of the BSH (StUK4) dictates that an investigation on the impacts of offshore wind developments on the marine environment should be done, as part of the environmental impact assessment. Additionally, a geological/geophysical and geotechnical site investigation has to also be carried out as a pre-requisite. After approval is given, the developer has to start construction within 2.5 years and the approval is valid for the next 25 years. This means an extension must be applied by the developer at the end of the 25 years to keep operating (Mockler et al. 2015).

In detail, the impact assessment studies consider different subjects. Often mentioned in relation to offshore developments is the state of marine life and the water body itself. These are usually contained in the national environmental regulations. According to Bailey et al. (Bailey et al. 2014), main environmental issues as a direct and indirect result of offshore wind developments are:

- noise pollution
- birds bumping onto the blades,
- habitats changes to benthic and pelagic,
- changing to food chains, and
- contamination by vessel who sail through and from seabed sediments.

During construction, noise emission from pile driving disturbs marine mammals, making them flee their habitat or causing auditory damage. Vessel movements for equipment mobilization and surveying procedures also cause disturbances in the marine life. Analysing the environmental effects of a proposed offshore development requires extensive data. When

considering marine life, the variety and habitat, population and life trend has to be known (Thomsen et al. 2006). This is however subjective since sound can travel to an unspecified distance and may affect species outside the study area. This will lead to a migration of the marine species affected. This means that the effect of the construction is simply not known. For example, disruption may be observed in marine mammals and fish located in a large area away from the proposed construction site (Thomsen et al. 2006).

However, at the end of construction and when the turbines start operating, noise pollution has little or no effect to the marine inhabitants. But the running turbines may cause birds to fatally collide to the blades or lose their path. Furthermore, the cables used for power transmission emit electromagnetic fields which also interfere with animals who use magnetic fields for direction. Aside from the previously mentioned impacts, these studies also address concerns such as gas emission due to vessel transits and helicopter journeys, dismantling of structures onshore/near shore, disposal/recycling of materials post dismantling, protection of marine archaeology and other site specific issues. And hence, the impact assessment studies for offshore wind farm projects undertake extensive environmental studies (Bailey et al. 2014).

It is the opinion of Bailey et al. (Bailey et al. 2014) that the impact studies should be done broader, considering a home range of population. Since these offshore developments are increasing, there is a great chance that there will be a number of them in a location. Hence, the impact assessment should also be done in a cumulative manner: a cumulative impact assessment.

To monitor this environmental impact, different countries have regulations. For example, national environmental regulations for offshore developments of three European countries are:

- Denmark: Danish Energy Agency (DEA)
- United Kingdom: Guidelines of the Convention for the Protection of the Marine Environment of the North-East Atlantic (OSPAR)
- Germany: Standards for the Environmental Impact Assessment issued by the Bundesamt für Seeschifffahrt und Hydrographie (BSH)

Even though the specific standards are slightly different from country to country, Danish Maritime Authority DNV-GL (Mockler et al. 2015) lists some of the guidelines of mitigation measures used to tackle the effect of noise caused during construction on animals.

- slow-start of pile driving,
- dispatching mammal watchers and postponing driving if mammals are present in the area,

- using noise creating devices to emit sounds that keep the mammals away during piling operations, e.g. pingers, seal scarers (Figure 2.22), bubble curtain systems (Figure 2.23) and shell-in-shell systems,
- prohibiting piling operations during some seasons, e.g. fish reproduction times,
- prohibiting wind farm developments in the Natura 2000 sites, which are sites found in the EU region and protected 'nature protected areas',
- restricting the allowable noise emission, and
- restricting parallel piling operations

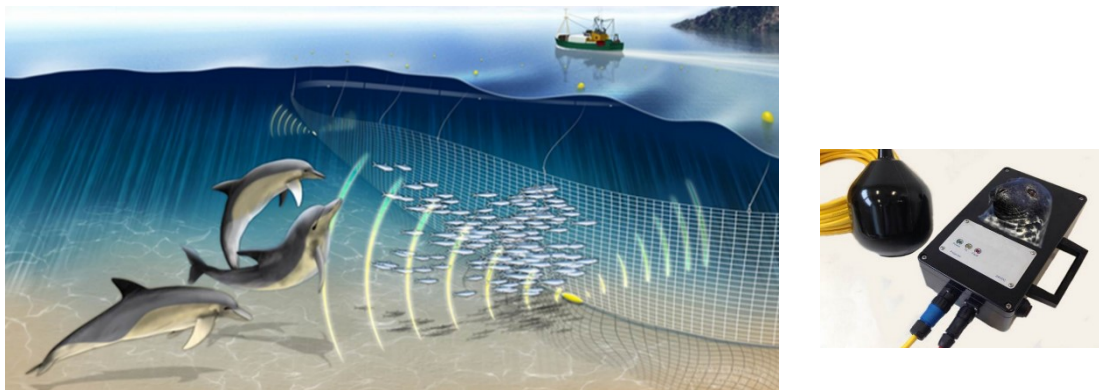


Figure 2.22 Acoustic mitigation devices (AMD). Source: (OSC 2018)



Figure 2.23 Bubble curtains used for noise mitigation. Source: (Rumes et al. 2016)

In order to reduce these environmental impacts, using floating foundations is also recommended (Mockler et al. 2015). This floating foundations systems are designed for deep water areas where the water depth is greater than 50 m (Figure 2.13). The European Wind Energy Association (EWEA 2013) also believes that this foundation method will most likely help bring about an environmental impact reduction. However, the technology is at its initial stages of popularity. An example for such developments is the 30-MW Hywind Scotland project of Station ASA involving five floating wind turbine installations, each with a 6 MW capacity. It is located off the coast of Powerhead in Aberdeenshire, Scotland. The adaptation

of these floating foundation systems as opposed to the conventional offshore foundation systems benefits the environment in the installation methods. The fixation of the floating structures to the seabed reduces noise impacts on mammals greatly. However this may be true, since this floating foundation systems are installed in higher water levels, the knowledge of the marine life distribution and the environment generally decreases (Bailey et al. 2014).

3. Driveability Analysis with PDI GRLWEAP

3.1 Pile Driving Analysis Background

Probably no branch of civil engineering depends more on the judgment and experience of its practitioners than geotechnical engineering, and this applies nowhere more than with deep foundations in general and driven piles in particular (Warrington 1997). Methods of approaching the analysis of pile driving does not date back so many years. However, because of the complexity and variability of ground conditions and soil mechanics, this process proceeded more slowly in geotechnical engineering than with any other branch of civil engineering. In the early 1950s E.A.L. Smith used a finite difference method to solve the wave equation, for carrying out dynamic pile analysis (Pile Dynamics 2010). The classical one-dimensional wave equation is given by the formula:

$$u_{tt}(x, t) = c^2 u_{xx}(x, t) \quad (1)$$

Where $u(x, t)$, $u(x, t')$, $u(x, \omega)$ is the displacement of pile particle, m

x is the distance from pile top, m

t is the time from zero point, sec

c is the acoustic speed of pile material, m/sec

For longitudinal vibrations, the constant c is the acoustic speed of the material of the bar, given by the equation

$$c = \sqrt{\frac{E}{\rho}} \quad (2)$$

Where E is the pile young's modulus of elasticity, Pa

ρ is the pile density, kg/m³

Impact velocity and ram mass define the energy available at impact. Consider a pile that is directly struck by a ram, without cushion or helmet mass considered between ram and pile top. In the first instant of contact, the top surface particles of the pile will assume the velocity, v_i , of the ram (Rausche 2000). Based on the wave theory, the corresponding force acting against the falling ram and the still motionless lower pile particles can be calculated as:

$$F = v_i Z \quad (3)$$

$$Z = EA/c \quad (4)$$

Where, Z is the pile impedance, kg/sec

A is the cross sectional area, m²

c is the wave speed given in Eq. (2)

When present, the cushions reduce the transfer rate of the impact force and prolong it over time. A helmet mass has a similar cushioning effect (Rausche et al. 1972). Regardless of cushion presence, the impact force is mainly dependent on the impact velocity. The impact force is also governed by the mass of the ram. The higher the mass, the longer the impact force will cause a long lasting pulse in the pile. This sustains a downward pile penetration. After impact, the wave of the impact force travels through the pile. It travels for a time of L/c to reach the pile bottom and the bottom pile particles start descending. Here, L is the pile length and c is the wave speed. When the wave has rebounded and reached the pile top it has a travel time of 2L/c.

In the 18th century St. Venant used a closed form solution to solve the wave equation. The solution assumes that a rigid mass impacts the elastic pile top directly and that the pile top is supported by a rigid foundation (Rausche 2000). Due to these assumptions, it was inevitable that another theory would be developed to explain the penetration of piles driven by impact. The first theory employed was that of Newtonian impact mechanics. The main aspects of this theory were assumptions of rigid body mechanics and conservation of momentum or energy, which were used to formulate dynamic formulas (Warrington 1997). From these dynamic formulas the most common one is the Engineering News formula (EN), Eq. (5), after A.M. Wellington. Even though this method was reasonable to use for pile driving analysis, it had its shortcomings. It fails to consider the soil-pile interaction and can just be applied for short timber piles. Main failures for the dynamic approach can be summarized as weakness in theory and changes in the application. The former includes the assumption of the pile as a rigid body, pile-soil interaction modelling for energy transfer and usage of a plastic soil model. Developments of reinforced concrete elements and steel started to be used as piles. This allowed the installation of longer piles, and hence this approach proved more inaccurate. Concrete pile driving was also problematic due to failure when subjected to higher stress, which made stress analysis very important. The EN formula is:

$$R_a = \frac{2W_h H_e}{S_h + C_{ENR}} \quad (5)$$

Where R_a = Allowable load on pile, pounds

W_h = Ram weight of hammer, pounds

H_e = Effective fall of hammer, ft.

s_h = Average penetration per blow under last few blows, inches

C_{ENR} = EN (Engineering News) formula constant = 1 for drop hammers, 0.1-0.3 for steam hammers

In the 1930's D.V. Isaacs made experiments to prove his reservation about dynamic formulas and the application of the Newtonian impact theory for analysis of longer sections. In his study, Isaacs analyzed issues like tension stresses in concrete piles, weight of the driving cap (helmet) and ram, and effect of cushion material stiffness. He also outlined the sophistication of dynamic pile analysis (Warrington 1997). This further paved way to the dominance of dynamic pile driving formulas for the next 50 years. Isaacs was able to show that stress waves exist in pile but at the same time their calculation is not an easy task (Warrington 1997).

In general, dynamic formulas are fundamentally incorrect. Pile rigidity, soil dynamic resistance and the variability of equipment performance are the main considerations that make dynamic formulas unreliable. Problems associated with pile driving formulas can be traced to the modeling of each component within the pile driving process: the driving system, the soil, and the pile. Dynamic formulas also assume a rigid pile, thus neglecting pile axial stiffness effects on driveability. Furthermore, they assume that the soil resistance is constant and instantaneous to the impact force (Hannigan et al. 2006).

3.2 WEAP Analysis Model and PDI GRLWEAP

3.2.1 Introduction

After E.A.L. Smith introduced the wave theory in the 1950's computer programs were developed to perform dynamic analysis on piles. GRLWEAP was developed out of the WEAP program of 1976 (Pile Dynamics 2010).

GRL WEAP has three main analysis methods. Depending on the purpose of analysis, different input methods and parameters are required. The level of their accuracy is subjective and maybe related to the importance of the analysis output. It is recommended to use the best possible input values emerging from reliable soil investigation data, local site conditions and the designer's engineering judgment for any analysis when use PDI GRLWEAP software.

1. Bearing Graph Analysis: outputs bearing capacity and blow count as a function of the penetration depth (Pile Dynamics 2010). In addition, tension and compression stress maxima can be plotted vs. blow count. A total ultimate capacity is assumed and

distributed on shaft and toe as per the input, followed by blow count calculation. A higher total ultimate capacity value is chosen next and shaft and toe resistance are proportionally increased to match the capacity usually equal to the expected or required R_{ult} (ultimate resistance). Here, the static geotechnical analysis is used for analyzing the percent distribution of the R_{ult} acting on the along shaft of the pile. The remaining percentage R_{ult} of the is assigned to the toe resistance. This is followed by the dynamic analysis (Pile Dynamics 2010). For the analysis, it is possible to input ten capacity values for consideration. After these capacity values are calculated, the bearing graph is created (Pile Dynamics 2010).

2. Inspector's Chart: relates the stroke height used with the blow count required to attain a certain ultimate capacity value. The stroke can be used as an equivalent energy value to monitor a driving process (Pile Dynamics 2010). This analysis can also be used for back calculation methods, such as refined wave equation analysis. Controlling of stresses is usually done by varying the stroke height. In the event that stroke height cannot be controlled, a blow count criteria may be applied which matches the stroke desired (Pile Dynamics 2010). For proper application of the inspector's chart (IC), it is vital that the actual hammer stroke energy level is known (Pile Dynamics 2010).
3. Driveability Analysis: This option calculates blow counts, stresses and transferred energy versus pile penetration without running separate bearing graph analyses for each depth. In other words, the driveability analysis performs numerous bearing graphs. This analysis option is the main focus of this thesis and will be covered in detail in section 3.3 (Pile Dynamics 2010).

For most engineers, the term wave equation refers to a partial differential equation. However, for the foundation specialist, it means a complete approach to the mathematical representation of a system consisting of hammer, cushions, helmet, pile and soil and an associated computer program for the convenient calculation of the dynamic motions and forces in this system after ram impact (Hannigan et al. 2006). In the first moment, after a hammer has struck the pile top, only the pile particles near the ram-pile interface are compressed. This compressed zone, or force pulse, as shown in Figure 3.1, expands into the pile towards the pile toe at a constant wave speed, C . This is dependent on the pile's elastic modulus and mass density (or specific weight). When the force pulse reaches the embedded portion of the pile, its amplitude is reduced by the action of static and dynamic soil resistance forces. Depending on the magnitude of the soil resistances along the pile shaft and at the pile toe, the force pulse reflects from the pile toe either as a tensile or a compressive force pulse, which travels back to the pile head. Both, incident and reflected force pulses cause a pile toe motion and produce a

permanent pile set if their combined energy and force are sufficient to overcome the static and dynamic resistance effects of the soil (Hannigan et al. 2006).

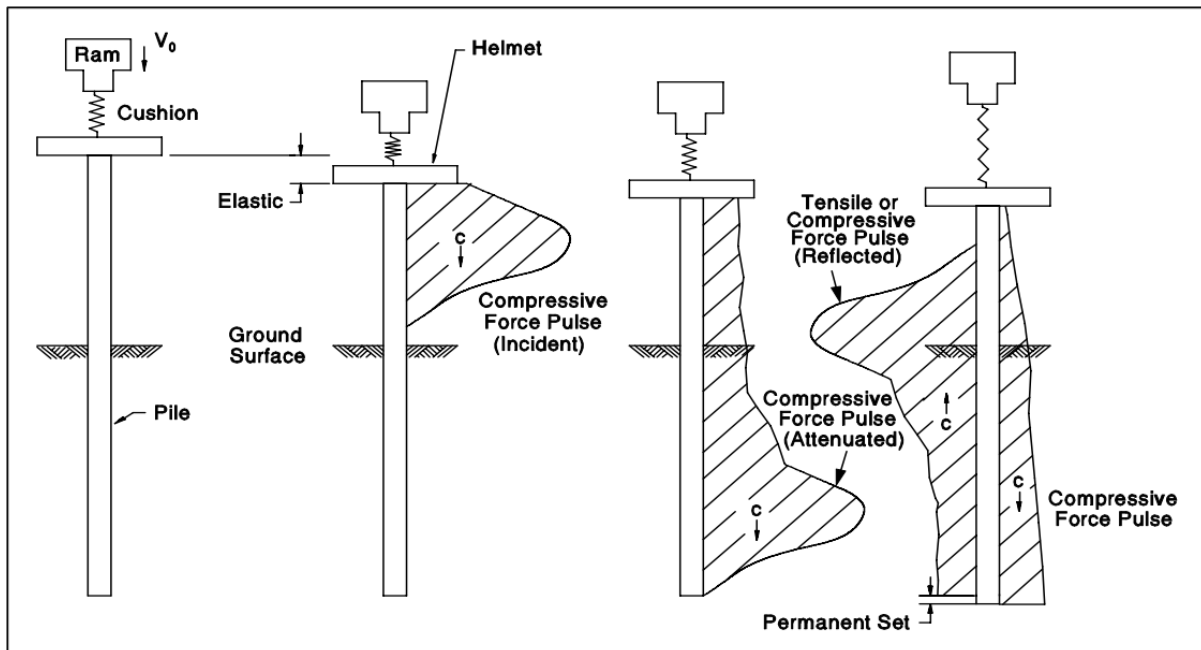


Figure 3.1 Wave propagation in a pile. Source: (Hannigan et al. 2006)

GRL's WEAP is a program that analysis dynamic pile driving using a hammer or vibrator and the corresponding forces and displacements that come as a result of (Pile Dynamics 2010). Analysis result in blow counts for impact hammers, time per unit penetration in for vibratory hammers, axial stress in a pile section, bending stress (offshore wave version), pile velocity and displacements, hammer-pile energy transfer, pile velocity and displacements and residual stress in the pile between hammer blows. The analysis also enables the calculation of the pile's bearing capacity at the time of driving or in case of a restrike. For a predetermined static bearing capacity, it also gives the stresses in the pile during pile driving; both for a given blow count and an expected blow count (Pile Dynamics 2010).

Energy is a measure of the work that can be done. It can be pushing a mass over a rough surface, lifting a weight, compressing a volume of gas, accelerating a mass to a certain speed, compressing a spring, etc (Rausche 2000). The pile driving process readily provides information regarding the soil resistance. The smaller the permanent set, s (unit length/number of blows), the greater the ultimate soil resistance, R_u , which opposes pile penetration (Pile Dynamics 2010). The pile is subjected to a hammer blow with kinetic energy, E_k . GRLWEAP does not directly work with the energy approach but these basic principles still apply. In general, the dynamic analysis can be given as:

$$E_s = R_u s_l \quad (6)$$

Where E_s is the energy available to do work on the soil

R_u is the ultimate soil resistance

s_l represents “losses” in the soil, e.g. due to damping

An equation relating the kinetic energy of the ram immediately preceding ram impact, E_k and E_s is given as:

$$E_s = E_k - E_{ds} - E_{pl} - E_{sl} \quad (7)$$

Where E_{ds} is the energy converted and lost in the driving system

E_{pl} is the energy converted and lost in the pile

E_{sl} is the energy converted and lost in the soil

E_k is usually approximated from the rated energy E_r , which is provided by the manufacturer. A hammer efficiency factor, e_h , is usually applied on rated energy, i.e. $E_k = E_r e_h$. The driving system of modern hammers comprises the helmet and cushions. The loss in this system may also be given by an efficiency factor e_d . The resulting kinetic energy at the top of the pile can be formulated as:

$$E_k - E_{ds} = e_d e_h E_r \quad (8)$$

Equating (6), (7) and (8) results in:

$$e_d e_h E_r - E_{pl} - E_{sl} = R_u s_l \quad (9)$$

Assuming that E_r is known, an estimate of e_d , e_h , E_{pl} and E_{sl} yields the permanent set, s , given R_u or vice versa. A summary of the hammer-pile-soil system is shown in Figure 3.2. Unfortunately, the estimation of the energy converted and lost in the pile and soil and estimation of the efficiencies of the driving system is not an easy task. The main differences between the wave equation and the energy formula is the evaluation of the e_d , E_{pl} and E_{sl} values. The calculation with the wave equation is with mathematics, using finite difference method as a principle (Pile Dynamics 2010). However, the efficiency of the hammers is based on the type, mode of operation and pile inclination.

The calculation of “losses” in the driving system (e_d) using the wave equation requires the coefficient of restitution not the cushions, stiffness values and the weight of the helmet. For the calculation of E_{pl} the elastic modulus, length, specific weight of the pile and a coefficient of restitution of the pile top are considered. Consideration of the soil stiffness and a soil damping factor are done to calculate the “losses” in the soil (E_{sl}).

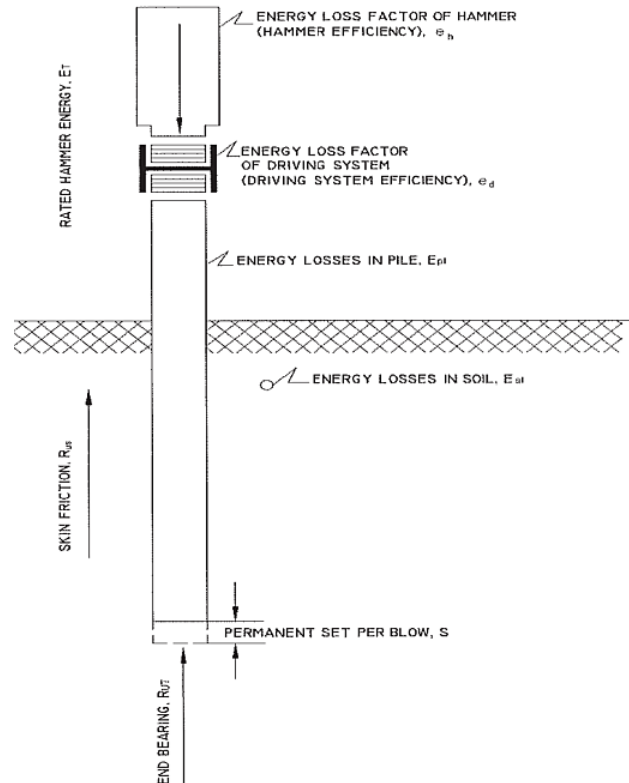


Figure 3.2 Energy balance in the Hammer-Pile-Soil system. Source: (Pile Dynamics 2010)

3.2.2 External Combustion Hammers (ECH) Model

3.2.2.1 The Ram and Assembly of EC Hammers

The ram is a component of the impact creating element of the hammer. Initially, to reduce analysis time Smith performed manual calculations with relatively long segments (e.g. 2.4 m) (Rausche et al. 2004). While representing shorter rams as a lumped mass model is sufficient, slender rams are divided into a maximum of 1 m segments. Very small segments may cause numerical instabilities because the critical time increments would become very small and hence should be checked if such problems arise during analysis. The segment weight is given as:

$$W_{ri} = \gamma_i A_i \Delta L_i \quad (10)$$

Where, γ_i is specific weight, kN/m^3

A_i is the cross-sectional area, m^2

ΔL_i is the length of each segment i , m

i , segment number, $i, = 1, 2 \dots m$

A ram spring is attached under each segment mass and has stiffness:

$$K_{ri} = E_i A_i / \Delta L_i \quad (11)$$

E_i is the elastic modulus of the ram. Note that γ_i , A_i and E_i may need to be averaged over length ΔL_i .

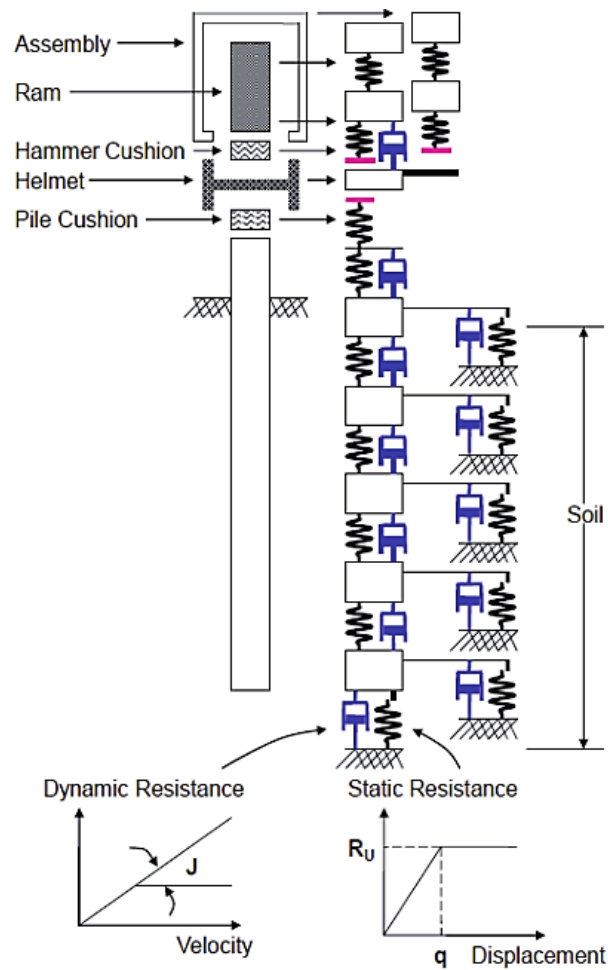


Figure 3.3 Scheme and model of a typical ECH hammer, pile and soil. Source: (Pile Dynamics 2010)

Aside from the ram, remaining parts of the hammer are collectively known as the assembly. An assembly is only considered for EC hammers. Their model usually consists of two assembly segment masses and springs. Input values for the assembly weight can be obtained by $0.5 \cdot (\text{hammer weight} - \text{ram weight})$, and assigned to the two segments.

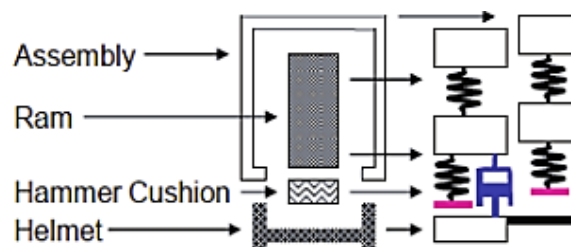


Figure 3.4 ECH ram and assembly Model. Source: (Pile Dynamics 2010)

Furthermore, to simulate the deformation behavior as non-linear springs representing cushions, impact block/helmet, and pile top, GRLWEAP uses a splice/slack model (Figure 3.5). Three parameters are used by this model. A tension slack, d_{st} , a coefficient of restitution,

c_a , and a round-out deformation or compressive slack, d_{sc} (Pile Dynamics 2010). During the compression stage, the force increases quadratically (stiffness increases linearly), compared to the deformation until the round-out deformation, d_{sc} , is attained. The equivalent force to this deformation is F_{lim} . After this point, there is a linear increase in force with a slope equal to the spring stiffness (k) (Pile Dynamics 2010). Further expansion will lead to a decrement in the compressive force, linearly. But in this case the model gives a slope which is based on the coefficient of restitution and wave speed, k/c_a^2 . Coefficient of restitution (c_a) represents the remaining energy in the spring after impact or during expansion, which solely depends on the property of the material (Pile Dynamics 2010).

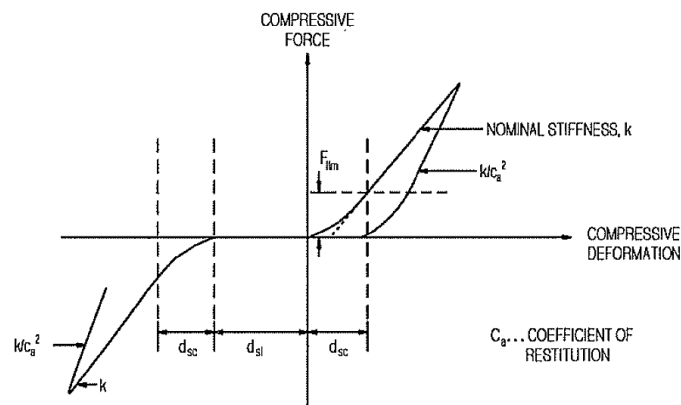


Figure 3.5 Force deformation curve for slack model. Source: (Pile Dynamics 2010)

3.2.2.2 Hammer Losses of Double Acting and ECH Hammers

Hammer efficiencies account for the losses prior and during impact. For ECH hammers, prior to impact, losses emerge from friction, power assist and fall height. During impact, a misaligned striking of the pile might also cause “energy loss”. An overstrike may also occur caused by the use of excess energy, in which case there will be an efficiency greater than 1. Calculation of the ram impact velocity is required when dealing with impact hammers analysis using the wave equation. Initially, as the ram is falling, there is no dynamic force applied on the pile. However, the weights of assembly and helmet create a static force in pile and soil. Thus, the dynamic analysis only has to cover the time period during and after impact (Pile Dynamics 2010). Because of the uncertainty of actual the hammer behavior, GRL WEAP (Pile Dynamics 2010) recommends to analyze conservatively for stresses at a somewhat higher efficiency than normal or for bearing capacities and/or blow counts with a slightly lower efficiency. The hammer efficiency values for ECH recommended in GRLWEAP are:

$e_h = 0.80$ for hydraulic hammers, single acting or power assisted but not double acting and without impact velocity measurement

$e_h = 0.95$ for hammers whose rating is based on measured impact velocity

Closed end or double acting hammers operate at a higher blow rate than open or single acting units. Applied force from the top of the ram in addition to gravity results in a higher number of impact blows. For ECH the downward force on the ram is often created by active pressure. In the case of hard driving conditions, the hammer assembly tends to uplift which leads to unstable driving conditions. The operator will then reduce the pressure which in turn leads to a reduced impact energy. This is the main reason why double acting air/steam/hydraulic hammers have lower GRLWEAP efficiencies than their single acting counterparts (Pile Dynamics 2010).

Impact velocity calculation in GRLWEAP is different for a double, differential or compound acting ECHs. It does not know in what proportions is the impact energy composed from. Besides the free fall, the additional pressure on the ram is not differentiated. To solve this problem, the program calculates an equivalent stroke height from the hammer's rated energy and the ram weight.

$$h_e = E_r/W_r \quad (12)$$

Where, E_r is the hammer's rated energy, kN/m, and

W_r is the weight of the ram, kN

The impact velocity is then given by

$$V_{ri} = \sqrt{2gh_e e_h} \quad (13)$$

Where, e_h is the hammer efficiency

Modern hydraulic hammers have been designed with a variety of other power assisting mechanisms during the down stroke. For example, the IHC hammers work with an adjustable downward directed nitrogen gas pressure which can be used to adjust the hammer impact velocity and blow rate.

3.2.3 Driving System Model

The driving system is simulated by a two non-linear springs and a mass for the system. Over all, the driving system is composed of the striker plate, hammer cushion, helmet, helmet insert and, for concrete piles, a pile cushion (Pile Dynamics 2010). In this system the spring for the hammer cushion and ram are connected in series. If the hammer cushion is not used the lower ram spring is connected directly on the helmet (Pile Dynamics 2010). For systems without helmet mass, the ram's bottom spring acts directly on the pile top spring for ECH (Pile Dynamics 2010).

The pile helmet (cap) is found between the pile and the hammer. To consider their weight, inserts between the helmet and pile, pile or hammer cushions or any other related add-ons can be included together with the helmet weight (Pile Dynamics 2010).

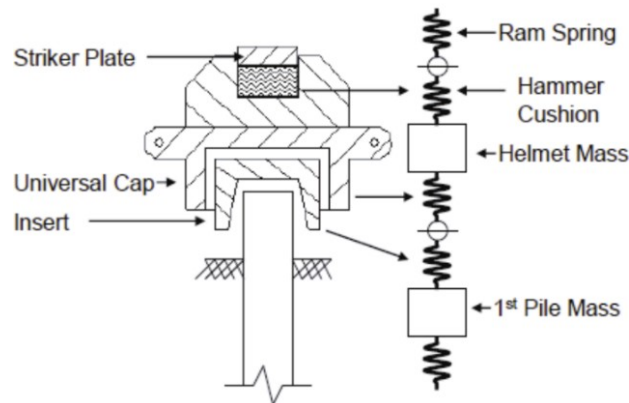


Figure 3.6 Driving system model. Source: (Pile Dynamics 2010)

The driving system model also contains a dashpot in parallel with the hammer cushion spring. Its damping constant c_{dh} is computed from:

$$c_{dh} = \frac{1}{50} c_{dhi} \sqrt{k_r m_a} \quad (14)$$

Where c_{dhi} is a non-dimensionalized input value

k_r is the hammer cushion stiffness and,

m_a is the helmet (ECH) mass

The default value of c_{dhi} is 1 and can be altered or removed by entering other multipliers.

3.2.4 Pile Model

The pile is divided into segments. It is equipped with linear and non-linear springs, masses and dashpots. A segment length of 1 m is automatically chosen, but based on the analysis of interest different values can be chosen when using the software. The length of the pile segments ($i=1, 2, 3 \dots N$) is calculated by:

$$L_i = \alpha_i L; \sum \alpha_i = 1, \quad (15)$$

Where, L is the total pile length and,

α_i is the multiplier (the program assumes it to be $1/N$)

GRL WEAP has an option to consider pile and hammer weights under different conditions. It is possible to manually assign a separate gravitational acceleration for the pile g_p and the hammer g_h . For mass calculation, the program uses the corresponding input weights and divides them by $g=9.81 \text{ m/s}^2$. The results are multiplied by the corresponding gravity values g_h and g_p . This results in an effective static weights for equilibrium analysis giving an initial soil

and pile deformation analysis. The input gravity values may be altered for cases like the consideration of pile batter or buoyancy (e.g. offshore pile driving). The spring stiffness is given by Eq. (11) and each segment of the pile has a mass calculated by the assignment shown in Figure 3.7.

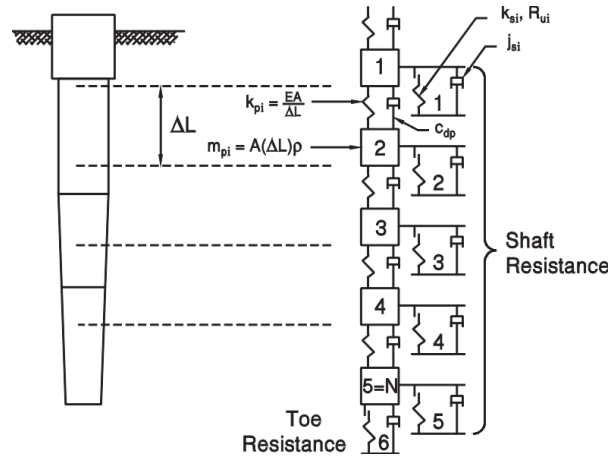


Figure 3.7 Pile-Soil model. Source: (Pile Dynamics 2010)

A pile damping value is also specified to account for the structural damping. Since the loss of energy in the pile is small compared to soil damping, c_{dp} , a simple model is used. It is given as:

$$C_{dp} = \left(\frac{1}{50}\right) C_{dpi} \left(\frac{EA}{c}\right) \quad (16)$$

Where c_{dpi} is an input number

EA/c is the impedance (dynamic damping) of the pile top

Additional parameter inputs are also used for different analysis options. Perimeter and toe area inputs are required for driveability and static geotechnical analyses. The perimeter may be altered to consider the internal friction of the pipe. Toe area may be used with full pipe area in some layers to account for soil plugging effects. Furthermore, pile size and pile type are used for the assignment of pile toe quakes and to find the appropriate manufacturer's recommended driving system.

3.2.5 Soil Model

3.2.5.1 Static Resistance Model

GRLWEAP's soil model is basically a Smith static resistance model approach (Pile Dynamics 2010). As shown in Figure 3.8, it consist of a spring and a dashpot. The spring represents the static resistance and the dashpot represents the dynamic resistance. Generally, the static soil resistance has the relation:

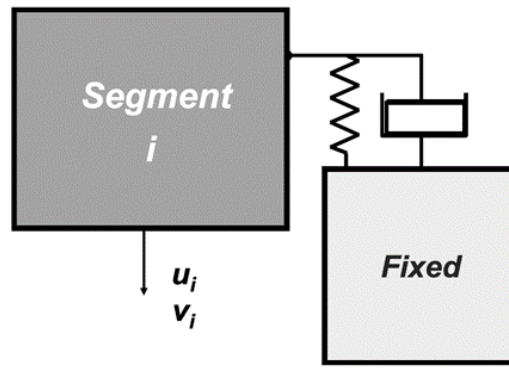


Figure 3.8 Soil Model. Source: (Rausche 2009)

$$R_{Total} = R_{si} + R_{di} \quad (17)$$

Where, R_{si} is the static resistance at segment i

R_{di} is the dynamic resistance at segment i

A slow moving pile encounters only static resistance. Whereas a fast moving pile encounters both static and dynamic resistance (Hannigan et al. 2016).

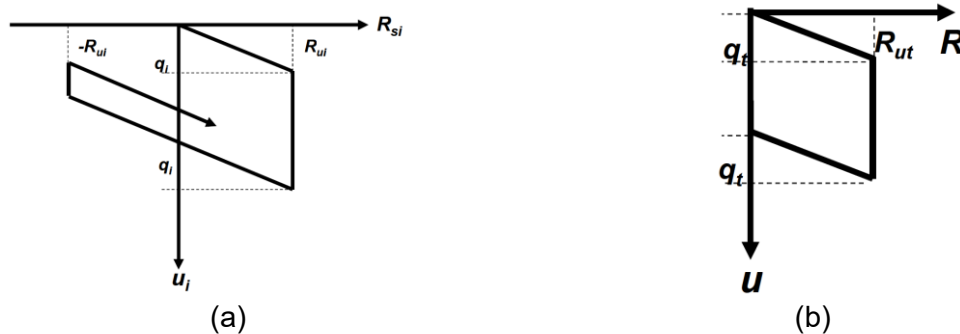


Figure 3.9 Static shaft and toe quake resistance. Source: (Rausche 2009)

The static shaft resistance is shown in Figure 3.9a. An elastic spring is used to simulate the stress-strain behavior. Considering a pile segment under loading, there will first be an linearly elastic deformation. At a deformation which is equal to the quake (q_i) the pile will yield. After this point the model assumes a perfectly plastic stress-strain behavior. Which means that there is an increase in deformation for a constant stress value. This stress value is called the ultimate resistance, R_{ui} . For a deformation value below the quake, R_{si} is proportional to the R_{ui} , Eq. (18). For a deformation value greater than the quake value, the ultimate resistance (R_{ui}) and shaft resistance (R_{ui}) are equal. These two cases hold, as long as the pile segment's velocity is positive (downward). For a case of stress reduction, i.e. when the stress wave returns from the pile bottom, the deformation rate of the spring is the same as the loading one. But the maximum negative value which can attain is equal to the ultimate resistance value, $-R_{ui}$. The same system holds true for the static toe resistance. But during unloading the R_{ui} cannot get below zero (Figure 3.9b). Hence the lowest static toe resistance is zero.

$$R_{si} = (u_i/q_i) * R_{ui} \text{ for } u_i \leq q_i \quad (18)$$

$$R_{si} = R_{ui} \text{ for } u_i > q_i \quad (19)$$

Shaft quakes have been found to vary little among different soil types. Clear relationships between soil type and shaft quake or pile size and shaft quake have not been established. A 2.5 mm (0.1 inch) shaft quake is reasonable and generally accepted. In contrast to the shaft quakes, toe quakes can vary widely (Pile Dynamics 2010). In general, hard soils or rocks are stiffer and the toe quake is therefore smaller than in softer soils. Furthermore, displacement piles such as closed ended pipe piles require much larger displacements to activate the ultimate toe resistance than non- displacements piles. The reason is that activating the ultimate capacity requires a much larger pile toe penetration, often leading to pile size dependent failure criteria (Pile Dynamics 2010). GRLWEAP recommends the quake values as tabulated in Table 3.1. Further descriptions can be found in Appendix C. It is recommended that these values are merely guidelines and should be complimented with experience and engineering judgement.

Table 3.1 GRLWEAP recommendations of shaft and toe quakes. Source: (Pile Dynamics 2010)

Shaft quake (mm)	Toe quake (mm)			
	Non-displacement		Displacement piles	
2.5	Other soil types	Hard Rock	Very dense/ hard soils	Soft/ loose soils
		2.5	1.0	D/120

3.2.5.2 Dynamic (damping) Resistance Model

The dynamic soil resistance is the resistance of the soil to rapid pile penetration produced by a hammer blow (Hannigan et al. 2006). Driving is resisted not only by static friction and cohesion, but also by the soil viscosity (damping), which is comparable to the viscous resistance of liquids against rapid displacement under an applied force (Hannigan et al. 2006). GRLWEAP has different options for damping. The standard option is similar to Smith's original model (Figure 3.8). Referring to the dashpot representation for the dynamic response of the soil mass, the damping resistance R_{di} is given as:

$$R_{di} = j_{si} R_{si} v_i \quad (20)$$

Where, j_{si} is the Smith damping factor at segment i , s/m,

v_i is the pile segment velocity at segment i , m/s and,

R_{si} is the static resistance force at segment i , kN/m²,

Recommendations for damping values, based on soil type, for shaft and toe have been given by Smith. The same values are adopted and given in the GRLWEAP software as default and are shown in Table 3.2 They are further described in Appendix C.

Table 3.2 Recommended damping factors after Smith. Source: (Pile Dynamics 2010)

Shaft (s/m)				Toe (s/m)
Clay	Sand	Silts	Layered Soils	All soils
0.65	0.16	intermediate value	Weighted average	0.5

In a bearing graph analysis, constant values are merely generated by the software. For the best results, the weighted average of the values should be taken. Better results are obtained if values are entered manually for each layer. In a driveability analysis, the damping factors are chosen for each layer according to their soil type. It is recommended that these values should be monitored by the designer.

3.2.6 Numerical Procedures and Integration

As we are dealing with a finite difference problem, the time increment is very important. Smith's lumped mass model is mathematically stable only if the computational time increment is chosen shorter than the shortest (critical) wave travel time of any segment i . The critical time increment is the time that it takes the stress wave to travel through the pile segment (Pile Dynamics 2010), and is given as:

$$\Delta t_{cri} = L_i/c_i \quad (21)$$

For a lumped mass with the wave speed of the segment c , given as $c_i = \sqrt{E_i/\rho_i}$, the critical time increment is given as:

$$\Delta t_{cri} = \sqrt{m_i/k_i} \quad (22)$$

Where m_i is the segment mass

$$K_i \text{ is the stiffness with } k = E_i A_i / L_i = E_i V_i / L_i^2$$

$$\rho \text{ is the unit mass (density) with } \rho = m_i / V_i$$

These properties may be different for a pile with changing properties, within a segment length. In this case the segment properties are averaged.

To make the analysis stable, the time increment, Δt , is taken as:

$$\Delta t = \min(\Delta t_{cri}) / \varphi \quad (23)$$

$\min(\Delta t_{cri})$ is the minimum critical time increment of all hammer and pile segments. GRLWEAP used $\varphi = 1.6$ as a default value. A higher value can be chosen if instability is observed in the analysis (Pile Dynamics 2010).

While the critical time of the hammer-driving system-pile model is normally determined from the stiffest segment in the hammer or driving system, the program also checks the other pile segments. This is to consider the effects of soil resistance on the stiffness of the pile segments. As a result, GRLWEAP may select the computational time increment with smaller values for high capacities than for low capacities (Pile Dynamics 2010).

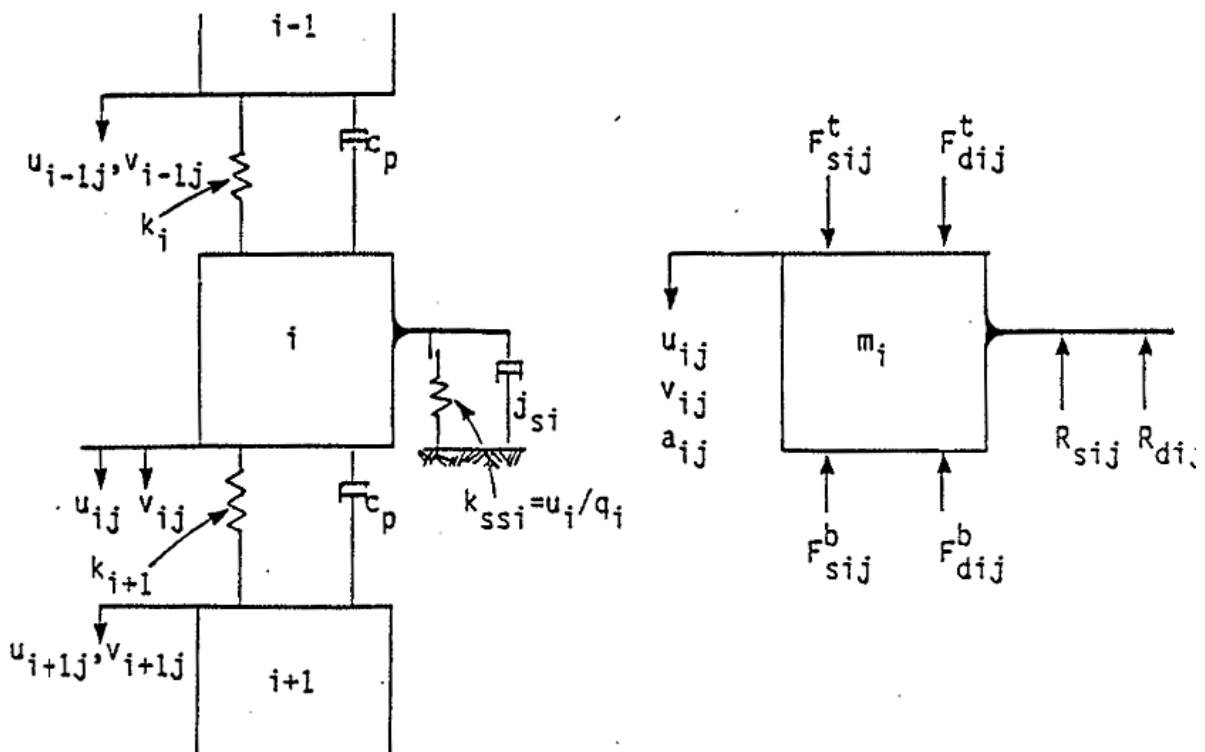


Figure 3.10 Schematic of model of segment i (left) and free-body diagram (right) (Source: Goble and Rausche 1986)

With a defined time, increment, the initial conditions for the finite difference scheme can be set. Referring to the pile segment (Figure 3.10), initially the velocity of the segment is equal to the ram velocity, and the acceleration is equal to the gravitational acceleration. The displacement, velocity, acceleration and forces of a segment are predicted by a Euler integration as follows:

$$\text{Initial conditions: } u_{ij-1} = 0; \quad V_{ij-1} = V_{ri}; \quad a_{ij-1} = g; \quad m_i = W_i/g$$

$$\text{Pile displacement: } u_{ij} = u_{ij-1} + \Delta t * V_{ij-1} \quad (24)$$

$$\text{Velocity of pile: } V_{ij} = V_{ij-1} + \Delta t * a_{ij-1} \quad (25)$$

Using the external resistance forces, R_{sj-1} and R_{dj-1} , calculated at the end of a previous time step, and the gravitational acceleration of the segment, g , it is now possible to compute the acceleration of a pile segment, i , during the current time step, j (Pile Dynamics 2010).

$$\text{Acceleration: } a_{ij} = a_{i-1j} + [F_{sij} - F_{dij} - R_{sij-1} - R_{dij-1}] * \frac{1}{m_i} \quad (26)$$

Where F_{sij} is the sum of top (F_{si}^t) and bottom (F_{si}^b) spring force respectively, given by:

$$F_{sij}^t = k_i * (u_{i-1} - u_{ij}) + k_{i+1} * (u_{ij} - u_{i+1}) \quad (27)$$

F_{bij} is the sum of top (F_{di}^t) and bottom (F_{di}^b) dashpot forces respectively, given by:

$$F_{dij}^t = C_p * (V_{i-1} - V_i) + C_p * (V_i - V_{i+1}) \quad (28)$$

Furthermore, after the acceleration value has been calculated for a segment, its velocity and displacement values are corrected by integration under the assumption of a linearly increasing acceleration (Pile Dynamics 2010):

$$V_{ij} = V_{ij-1} + (a_{ij} + a_{ij-1}) * \Delta t / 2 \quad (29)$$

$$u_i = u_{i-1} + V_{ij-1} * \Delta t + (2a_{j-1i} + a_{ij}) * \Delta t^2 / 6 \quad (30)$$

These corrections result in a more accurate results of the displacement and velocity, and hence will result in a faster convergence. Using the new displacements new spring forces, and using the new velocities new dashpot forces are calculated. This process is repeated for all hammer, driving system and pile segments, except the hammer and driving segments would not have a resistance force component. The calculation of forces, accelerations, and then displacements can be repeated for the same time increment, with the newly computed a_i , v_i , and u_i values taking the place of the previous prediction. Iterations are stopped if either the number of required iteration steps has been exceeded (since maximum number of iterations can be set) or if convergence of the velocities of the top and bottom pile elements had been achieved. After convergence of the pile variables, the resistance forces are calculated for the next interval (Pile Dynamics 2010). Summary of the calculation steps is shown in Figure 3.11.

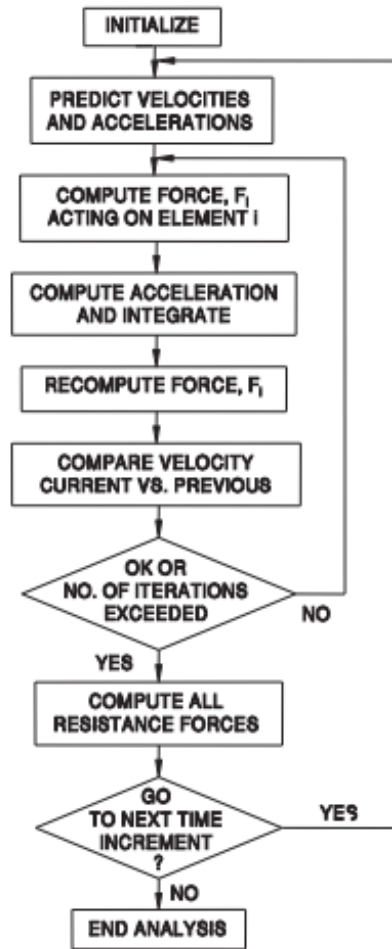


Figure 3.11: Block diagram of predictor-corrector analysis. Source: (Pile Dynamics 2010)

3.2.7 Blow Count Computation

For blow count calculations, the difference between the maximum toe displacement, u_{mt} , and the average quake is calculated. The average quake is:

$$q_{av} = \sum[R_{ui}(q_i)] / R_{ut} \quad (31)$$

Where, R_{ui} is the segment ultimate resistance

q_{ui} is the segment quake and

R_{ut} is the total ultimate capacity

The summation is from $i=1$ to $N+1$, where N is the number of pile segments. The resistance $N+1$ represent the end bearing. The predicted permanent pile set is given as,

$$s = u_{mt} - q_{av} \quad (32)$$

And hence, the blow count is given by:

$$B_{ct} = 1/s \quad (33)$$

This analysis step applies for the ECH driven piles. Two pile analysis, and vibratory hammer driven piles have further modifications and hence GRLWEAP background report (Pile Dynamics 2010) should be referred for detailed description.

3.2.8 Static Geotechnical Analysis

In the GRLWEAP software there are four input options to perform static soil analysis and fill the S1 (Soil Property Input for Driveability Analysis) form. The accuracy however is dependent on the accuracy of the soil investigation report, type of tests and many other factors which can be a major source of error. However, these input methods are not the only methods of input. It is also possible to calculate the unit shaft and toe resistance using other methods. GRLWEAP (Pile Dynamics 2010) suggests trying other methods of static geotechnical analysis, e.g. computerized methods such as UNIPILE, DRIVEN and SPT97. Local experience may indicate which methods of static pile analysis work and which do not work in a particular geology. After calculating, the user can insert the data using the 'Paste Special' option of the GRLWEAP program.

In general, two widely used methods are considered for the unit resistance calculations. The α – method and the β – method. The α – method uses a total stress analysis and is appropriate for short-term capacity calculation of a pile. It is applied for cohesive soils and uses the undrained shear strength parameter as an input. To calculate the unit shaft resistance, this method assumes proportionality between the skin friction and the undrained shear strength S_u . It also assumes that the interface shear stress f_s between the pile surface and the surrounding soil is proportional (Wrana 2015).

$$f_s = \alpha S_u \quad (34)$$

Where α is an adhesion coefficient depending on pile material and clay type, and S_u is the undrained shear strength.

The unit base resistance for cohesive, using Terzaghi's bearing capacity equation, is formulated as (Wrana 2015):

$$q_t = N_c (S_u)_t \quad (35)$$

Where N_c is the bearing capacity coefficient, and $(S_u)_t$ is the undrained shear strength of the cohesive soil under the pile bottom.

The other analysis option is the β – method. The method uses an effective stress analysis and is appropriate for long-term (drained) capacity calculations. The method can be employed for either cohesionless or cohesive soil types (Wrana 2015).

$$f_s = \beta p_o', \beta = k_o \tan \delta \quad (36)$$

Where β is the Bjerrum-Burland beta coefficient,

p_o' is the average effective overburden pressure along the pile shaft,

k_o is an earth pressure coefficient, and

δ is the pile-soil interface friction angle.

The unit toe resistance is calculated as:

$$q_t = N_t (p_o')_t \quad (37)$$

Where N_t is the toe bearing capacity coefficient, and

$(p_o')_t$ is the average effective overburden pressure at the pile bottom.

In addition to the static resistance values, the GRLWEAP static geotechnical analysis methods also provide a help for dynamic parameters, shaft damping and toe quake (toe damping and shaft quake are always considered independent of soil or pile type). For the driveability analysis, also rough estimates of the soil parameters pertaining to the soil resistance's gain/loss behavior are provided (setup factor, relative energy and setup time) (Pile Dynamics 2010).

3.2.8.1 Soil Type Based Method (ST)

This method of soil profile input used basic soil inputs and classifies according to the information provided by Bowles and Fellenius mentioned in (Hannigan et al. 2006). The inputs of the program are simply the density and stiffness levels for non-cohesive and cohesive (granular) soils, respectively. GRLWEAP (Pile Dynamics 2010) and Hannigan et al. (Hannigan et al. 2006) both recommend inputting the different layers of analysis with a thickness of maximum 3 m and less.

The analysis method uses, a *modified* α -method (total stress method) for the calculation of unit resistance of cohesive soils. It relies on the unconfined compressive strength (q_u) of the soil layer. The q_u -value and, based on it, the unit shaft resistance and end bearing values are given as a function of both soil type and a representative SPT N-value (Hannigan et al. 2006) as annexed in Table B-1. This are recommended values after Bowles (Bowles 1997). Unlike the normal α -method, undrained shear strength and the α coefficient for skin friction and the N_t value for unit base resistance are not required for this input method.

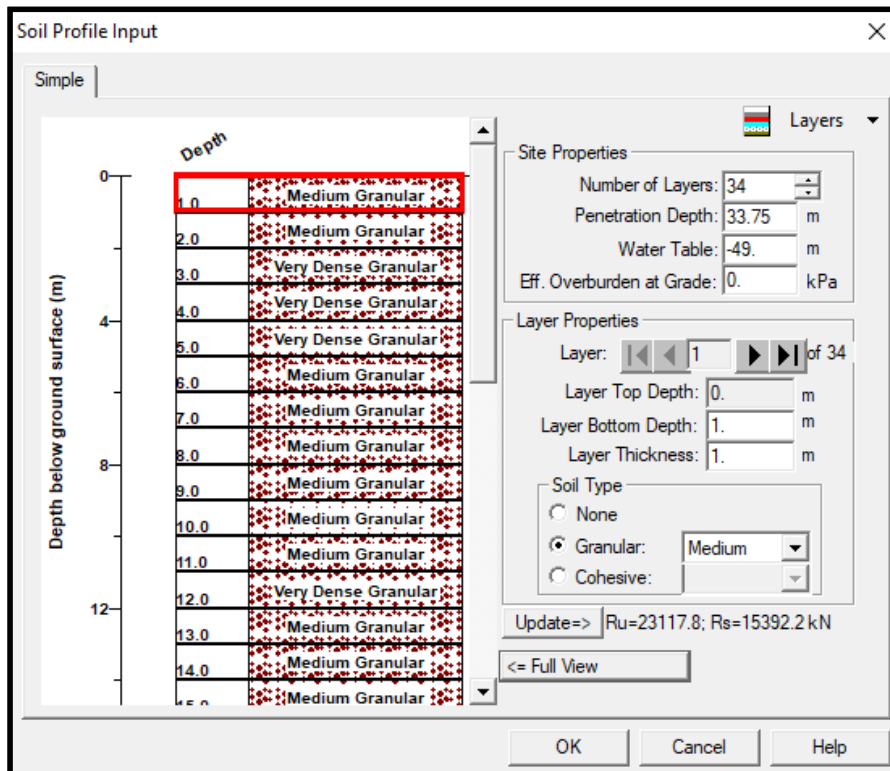


Figure 3.12: GRLWEAP's ST analysis method input window. Source: (Pile Dynamics 2010)

For the calculation of the unit shaft and quake resistance for non-cohesive soil layers, the ST input method uses the β -method (effective stress method). This method is similar to the one described in section 3.2.8. The β value for shaft resistance and the toe bearing capacity coefficient (N_t) are assigned based on Bowle's (Bowles 1997) recommendations (Table B-2). This is done based on the simple soil type classification input. The summary of calculation steps for resistance calculation and tables of recommended values can be found in Appendix B-i.

3.2.8.2 SPT N-value Based Method (SA)

This method is based on results from a SPT (soil penetration test). Robertson et al. (Robertson et al. 1983) defines SPT as a soil investigation test made by dropping a "free" falling hammer weighing 63.5 kg onto the drill rods from a height of 0.76 m. The number of blows, N , necessary to achieve penetration of 0.3 m of a standard sample tube, is regarded as the penetration resistance. In the SA method, instead of the N value, it is also possible to enter the undrained shear strength and friction angle. Direct input of unit shaft and toe inputs is also possible, for rock layers for instance. The SPT-N value input is corrected for energy (N_{60}) but not for the usual correction, which is for overburden pressure. In effect, this is a normalization which increases the N -value for hammers with high transfer efficiency (greater than 60%) and

lowers them for poorly performing hammers (those with transfer efficiencies less than 60%) (Pile Dynamics 2010).

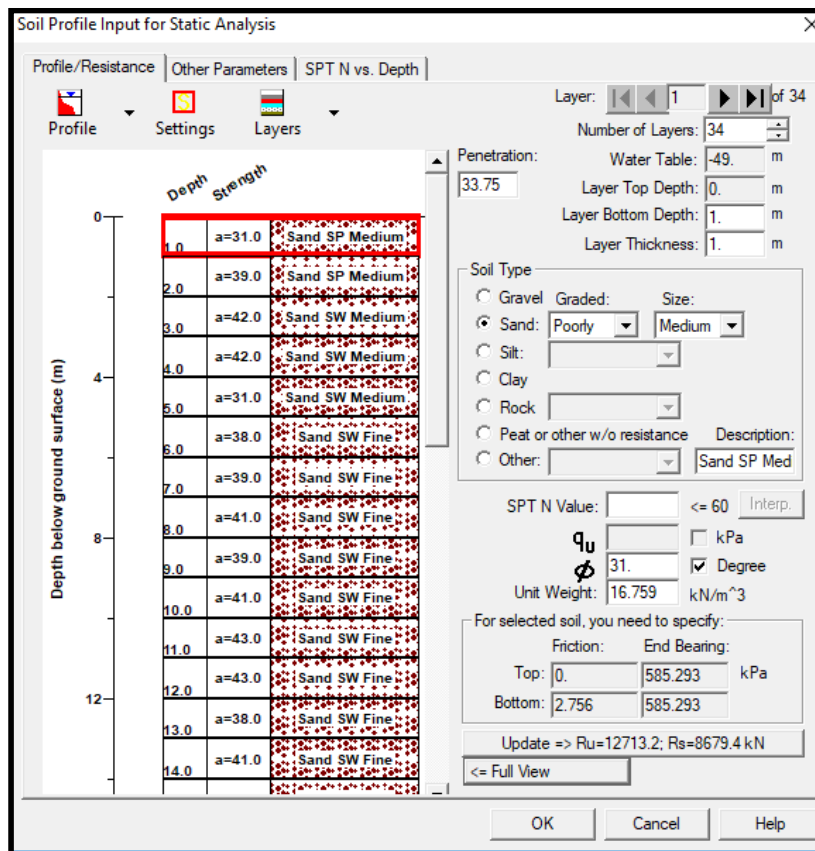


Figure 3.13: GRLWEAP's SA analysis method input window. Source: (Pile Dynamics 2010)

This analysis method considers an effective stress method for both cohesionless and cohesive soils. This means, the resulting resistance values are the short term values. Using Table 3.3, it is possible to analyze which input method is available for the data at hand.

Table 3.3 Soil parameters input possibility for SA analysis

Soil Type	Gravel	Sand	Silt	Clay	Rock	Peat/No resistance	Other
SPT-N	✓	✓	✓	✓	✗	✗	✗
q_u	✗	✗	✗	✓	✗	✗	✗
ϕ (°)	✓	✓	✓	✗	✗	✗	✗
Unit weight (γ)*	✓	✓	✓	✓	✓	✓	✓
Shaft Friction & End bearing	✗	✗	✗	✗	✓	✗	✓

*Unit weight recommendations are also automatically assigned based on (Bowles 1997) for an inputted SPT-N, unconfined compressive strength or friction angle value.

However, soil strength from N-value and soil type is always only an estimate because SPT N-values are inherently inaccurate and soil type information is subjective and the pile driving process itself changes the properties of the soils and, therefore, affects long term soil resistance and soil resistance to driving (SRD). And hence, the designer should be cautious of this drawback when applying this method of static geotechnical analysis. The calculation steps of the shaft and toe resistance for the different soil classifications options according to the SA method, as given in (Pile Dynamics 2010) are annexed in Appendix B-ii.

3.2.8.3 The Cone Penetration Test (CPT) Method in GRLWEAP

Cone penetration test is a test used to determine the resistance of soil and soft rock to the penetration of a cone and the local friction on a sleeve (EN 1997-2 2007). It consists of pushing the standard cone into the ground at a rate of 20 mm/s and recording the resistance. The total cone resistance is made up of side friction on the cone shaft perimeter and tip pressure (Bowles 1997). It gives a continuous soil profile and can collect up to 5 independent readings in a single sounding. These readings, notably the cone tip resistance (q_c), sleeve friction (f_t), and penetration pore water pressure (u_2) are interpreted to give the soil parameters used to analyze subsurface stratigraphy (Rocscience Inc. 2016). In a way, it simulates a pile and it is also a relatively quick and simple test.

The preferred Dutch Cone configuration has a cone tip area of 10 cm² and a cone angle of 60 degrees. GRLWEAP's method for calculating pile unit shaft friction, q_s , and unit end bearing, q_t , programmed in GRLWEAP assumes that the cone tip resistance, q_c , and the cone's sleeve friction, q_s , have been measured with such a standard cone. The soil type determination is based on Robertson et al. (Robertson and Campanella 1986) and the resistance calculation is as proposed by Schmertmann (1978) (Pile Dynamics 2010). However, CPT data can only be imported into GRLWEAP from a text file (Pile Dynamics 2010). Hence a numerical summary of the CPT with q_c , q_s values are required to use this input method in GRLWEAP (Figure 3.14).

The summary of calculation steps for resistance calculation and tables of recommended values can found to in Appendix B-iii.

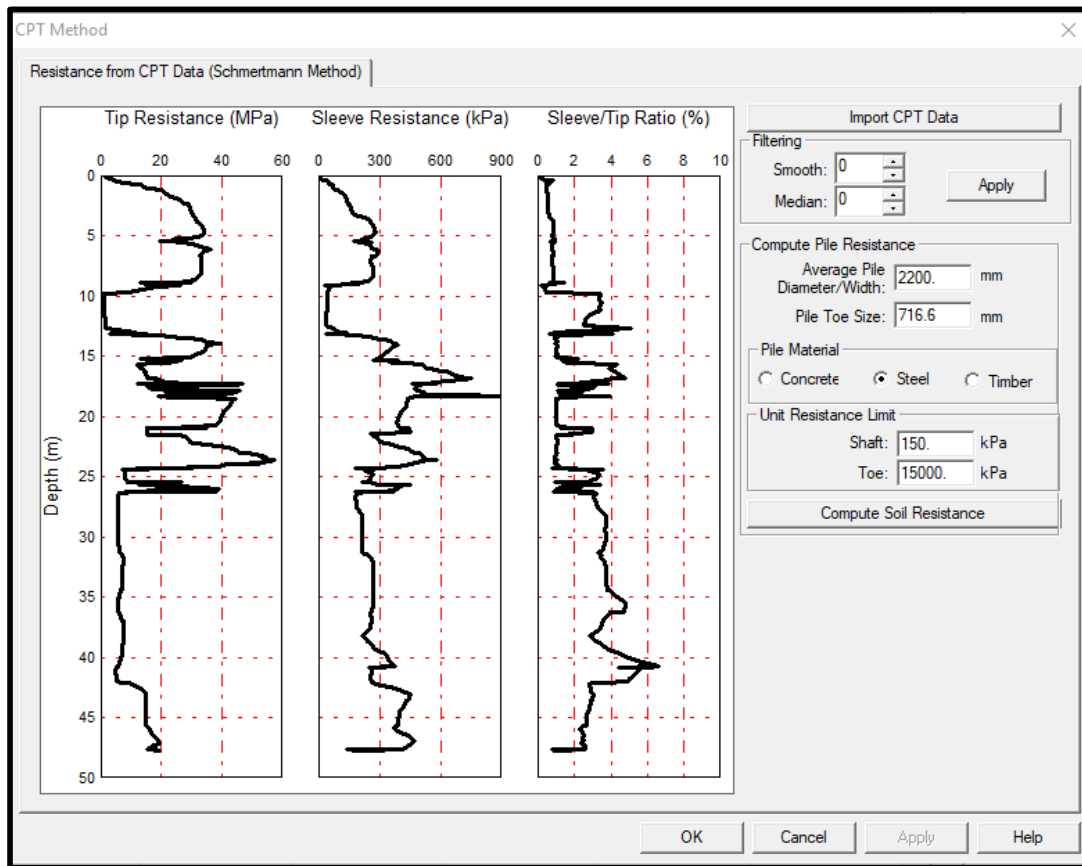


Figure 3.14: GRLWEAP's CPT analysis method input window. Source: (Pile Dynamics 2010)

3.2.8.4 The API Method in GRLWEAP

The method is based on (API 1993). In GRLWEAP software it is a feature that is fully available in the 'Offshore Wave Version' of the software. Note that this is an approximate method and that API recommends instead using high quality soil strength information where available (Pile Dynamics 2010). Furthermore, this method is specifically applicable to pipe piles.

The analysis assumes an effective stress analysis for cohesionless soils and total stress. Soil strength input for GRLWEAP's routine is undrained shear strength (S_u) for cohesive soils and a general density classification for non-cohesive soils (Figure 3.15) (Pile Dynamics 2010). The density classification also contains a soil description. From this input values, for cohesionless soils, API (API 1993) assigns parameters of effective friction (ϕ') and bearing capacity factor (N_c) values for resistance calculations (Table B-4).

For performing a static geotechnical analysis input using the API method, available soil types with corresponding methods are shown in Table 3.4. The summary and intermediate corresponding calculation steps are annexed in Appendix B.

Table 3.4 Soil parameters input possibility for API - GRLWEAP analysis

Soil Type	Gravel	Sand	Sand-Silt	Silt	Cohesive
ϕ [°]	✓	✓	✓	✓	✗
Unit weight (γ)*[kN/m ³]	✓	✓	✓	✓	✗
Undrained shear strength (q_u)[kPa]	✗	✗	✗	✗	✓

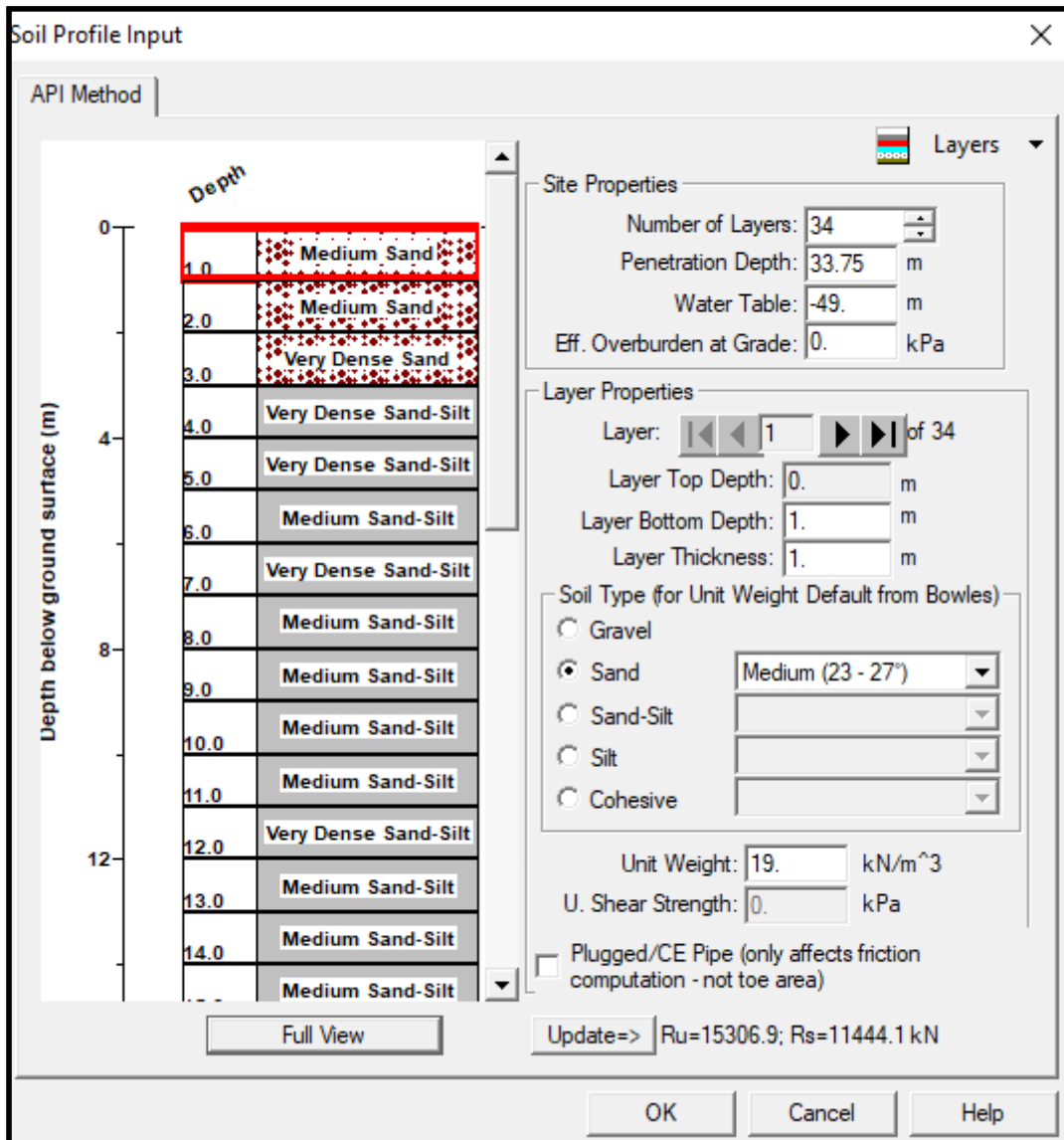


Figure 3.15: GRLWEAP's API analysis method input window. Source: (Pile Dynamics 2010)

To generally summarize, the four input methods to perform static geotechnical analysis with their respective basic analysis assumptions are tabulated in Table 3.6.

Table 3.5 Soil parameters input possibility for SA analysis

Analysis method	Input	Basic Analysis
Soil type based method (ST)	Soil Type	Effective Stress, Total Stress
SPT N-value based method (SA)	SPT N-value	Effective Stress
CPT based method (CPT)	Resistance at the cone tip and sleeve	(Schmertmann 1978)
API method in GRLWEAP (API)	ϕ , S_u	Effective Stress, Total Stress

After the static geotechnical analysis using any of the above four input methods the unit shaft resistance is multiplied by the perimeter and length for shaft resistance and the unit end bearing is multiplied by the toe area to give the ultimate resistances in kilo-newton.

$$R_{ui,shaft} = f_s * P * L \quad (38)$$

Where f_s is the unit shaft resistance,
 P is the perimeter of the shaft, and
 L is the length of the soil layer.

$$R_{ui,toe} = q_t * A_t \quad (39)$$

Where q_t is the unit toe resistance, and
 A is the toe area.

Pile driving changes the soil properties and pile material has an effect on the shaft resistance. Effects such as predrilling or jetting, an oversized toe plate, driving of nearby piles causing heave and densification, group effects, time effects like setup and relaxation, variable water table elevation, excavations or refilling around and in the neighborhood of the pile, and many other phenomena have a significant effect on shaft resistance and end bearing.

GRLWEAP's static geotechnical analysis methods should merely be seen as an aid for the program user in estimating very basic soil resistance input parameters. When performing the soil layer input, the program also displays the calculated capacity and the shaft resistance. This additional information may be used as a check on how reasonable the basic assumptions are and whether or not the intended pile capacity can indeed be achieved. Again, this capacity value should not serve for design purposes.

For the open-ended pipes, the question of internal friction is difficult to answer. It would be expected that an unplugged pile (the soil remains at its location, i.e., it does fill the pile and does not move with the pile – the cookie cutter effect) has some internal soil resistance.

However, unless diameter to embedment is relatively large, the effective stresses will be relatively low inside the pipe and the driving process will reduce the internal friction. Thus for most unplugged analyses only partial internal friction is normally considered (Pile Dynamics 2010).

For the toe area, the user must determine whether plugging can occur for open profiles or not. In very dense sands or during restrrike testing after a long waiting time, plugging may be expected unless the pile diameter is very large (say greater than 900 mm or 30 inches) or the penetration into the bearing layer is very shallow (say less than 3 diameters). In general, the GRLWEAP's default value for the pile toe area is that of the closed end condition (Pile Dynamics 2010). In addition, it is also strongly recommended to perform optimistic (unplugged) and pessimistic (plugged) driveability analyses to establish lower and upper bound driving resistance values (Pile Dynamics 2010).

Some recommendations of analysis for open ended pipe piles given in PDI GRLWEAP are described as follows.

- I. Open ended pipe piles driven into
 - a) All non-plugging soil types, i.e., not for hard, dense, very dense or moderately hard rock which the pile can penetrate,
 - b) Extremely large diameter open-ended pile piles (diameter greater than 96 inches or 2500 mm) in all soil types, and
 - c) Hard rock (all diameters).

Since these piles are expected to have relatively low end bearing relative to the skin friction, it is not too critical for a driveability analysis whether or not they plug. Also extremely large diameter pipe piles will not plug. They therefore can be analyzed as open ended with some internal friction. Similarly, when piles cannot penetrate into a hard rock, then end bearing will act against the steel annulus only. Note that driving pipes to non-uniform hard rock surfaces may create non-axial high stress concentrations which cannot be analyzed/predicted by GRLWEAP (Pile Dynamics 2010).

Table 3.6 Recommended analysis for non-plugging pile with partial internal friction

Unit end bearing	As per static analysis
Toe area	Steel area
Toe quake	0.10 inches or 2.5 mm or 0.04 inches or 1mm for hard rock
Perimeter	Double circumference over bottom 5 diameters and outer circumference for the rest of the section
Unit shaft resistance	As per static analysis

- II. Open ended large diameter (diameter 30 to 96 inches or 760 to 2500 mm) pipe piles driven into moderately hard rock, dense or very dense non-cohesive soils:

It is recommended to perform an upper and lower bound analysis (even though piles with diameters between 60 to 96 inches or 1500 to 2500 mm probably rarely plug, it is still recommended to subject them to lower and upper bound analyses like the smaller piles). For the upper bound analysis of piles with more than 48 inches (120 mm) diameter it is considered that plugging may either be only partial or the end bearing over a large plugged area may be less than what is expected for smaller displacement piles (Pile Dynamics 2010).

A. Lower bound analysis

Table 3.7 Lower bound analysis of large diameter open-ended piles with partial plugging

Unit end bearing	As per static analysis
Toe area	Steel area
Toe quake	0.10 inches or 2.5 mm
Perimeter	Double outer circumference over bottom 5 diameters and outer circumference for the rest of the section
Unit shaft resistance	As per static analysis

B. Upper bound analysis

Table 3.8 Upper bound analysis of large diameter open ended piles with full plugging

Unit end bearing	One and one half of unit resistance from static
Toe area	Closed bottom area
Toe quake	Diameter divided by 120
Perimeter	Outer circumference
Unit shaft resistance	As per static analysis

- III. Open-ended small diameter (diameter less than 30 inches or 760 mm) pipe piles driven into moderately hard rock, dense or very dense non-cohesive soils driven at least 3 diameters into the competent material:

Table 3.9 Recommended analysis for small diameter open-ended piles with full plugging

Unit end bearing	As per static analysis
Toe area	Closed bottom area
Toe quake	Diameter divided by 120
Perimeter	Outer circumference
Unit shaft resistance	As per static analysis

Due to the simplicity of GRLWEAP's static geotechnical calculation methods, ignores many conditions. For instance, effects of pile size, pile non-uniformity (such as a tapered pile which may have a relatively high shaft resistance), influence of upper lubricating soils on lower soil layers, the effect of pile material on the friction, and many other influences normally affecting friction and/or end bearing values were not necessarily considered in detail. The designer should therefore adjust the result based on the recommendations in the literature or their own experience and judgment when these methods are used (Pile Dynamics 2010).

Furthermore, Stevens (Stevens et al. 1982), studied four cases of driveability which simulate coring (unplugged) and plugging scenarios of an open ended pile. The study was done for hard clay, very dense sand and rock and assume continuous driving conditions. They are shown in Table 3.10.

Table 3.10 Recommended analysis for SRD after Stevens et al. (Stevens et al. 1982)

	Type	Analysis	Applicable soil type
1	Lower bound coring pile	$1.5 \cdot R_s + R_{an}$	in sand and clay
2	Upper bound, coring pile	$2 \cdot R_s + R_{an}$	in sand and clay
3	Lower bound, plugged pile	$R_s + R_e$	in sand and clay
4	Upper bound plugged pile	$1.3 \cdot R_s + 1.5 \cdot R_e$	in sand
		$R_s + 1.67 \cdot R_e$	in clay

Where R_s is outside shaft resistance,

R_{an} is end bearing on pile annulus (bottom-section area), and

R_e is full pile end bearing.

3.3 Driveability Analysis

3.3.1 Analysis Description

This option calculates blow count, stresses and transferred energy versus pile penetration without running separate bearing graph analyses for each depth. In other words, the driveability analysis performs numerous bearing graph analyses automatically for user specified pile tip penetrations. Input consists of unit shaft resistance and end bearing values along with toe area (for both plugged and unplugged conditions) obtained by static soil analysis, along with soil layer specific quake and damping values. In addition, the gain/loss factors modifying the unit shaft resistance or unit end bearing values, can be specified. These factors allow the user to model complete or partial loss of soil setup, relaxation effects or the long term soil resistance (Pile Dynamics 2010).

3.3.2 Soil Setup and Gain/Loss Factors

The Gain/Loss factors (f_{GL}) control the absolute change of static soil resistance, whereas the Setup Factor (f_s) controls the relative change of soil resistance among the various soil layers. The static resistance has to be estimated by geotechnical analysis of the soil. The result of this analysis is the Long Term Static Resistance (LTSR). However, during pile driving the soil properties change and the pile encounters the Static Resistance to Driving (SRD). The conversion of LTSR to SRD is accomplished in GRLWEAP using setup factors and gain/loss factors (Pile Dynamics 2010). For a particular soil type the long-term static soil resistance can be formulated as:

$$LTSR = f_s * SRD \quad (40)$$

Here, a distinction is made between the gain/loss factor and reduction factor with respect to the setup factor. A single layer of soil can be described using a reduction factor, which is the inverse of the setup factor. Whereas a gain/loss factor can represent a relative term consistent with the most sensitive layer (Pile Dynamics 2010). An example to describe the two cases adopted from (Pile Dynamics 2010) is as follows. Taking a single soil layer, e.g. a clay, with setup factor $f_s = 2.5$. The reduction factor applied is therefore $f_{RD} = (1.0/2.5) = 0.4$, which represents a full loss of setup. To simulate a worst-case driveability situation a reduction factor of 1 may be applied. Indirectly, this means the SRD and LTSR are equal, or there is no loss of strength. An intermediate value of reduction factor, i.e. $0.4 < f_{RD} < 1.0$, can be used to simulate an incomplete setup. This case may occur for an interruption time below the setup time. Hence, each depth analyzed, with the three gain/loss factors $f_{GL} = 0.4, 0.7$ and 1.0 specified as an input, a bearing graph would be calculated by the driveability analysis with three ultimate

capacity values, one bearing graph for each depth analyzed. For each of these analyses, an appropriate end bearing gain/loss factor could also be considered in the input (Pile Dynamics 2010).

Assuming two different soil layers, with different setup factors, of clay layer having $f_s = 2.5$ and sand layer $f_s = 1.25$. Reducing the soils layers to a full setup would result in the sand layer reduced by $f_{RD} = (1.0/1.25) = 0.8$ and the sand loses $f_{RD} = (1.0/2.5) = 0.4$. This variation in reduction factor is treated by considering a gain/loss factor which is consistent with the most sensitive layer. For less sensitive layers the reductions of resistance would be proportionate to the ratio of setup factors. Therefore, if we again analyze a gain/loss factor $f_{GL} = 0.4$ (to cover the set-up factor 2.5 of the most sensitive layer) and a gain/loss factor 0.7 (half loss of resistance of the most sensitive layer) and a gain/loss factor 1 for full setup (no loss of driving resistance) then the sand's corresponding reduction factors would be $f_{RD} = 0.8, 0.9$ and 1.0 while for the clay we would have $f_{RD} = f_{GL} = 0.4, 0.7$ and 1.0.

Mathematically, the capacity multipliers for the individual layers, f_{RD} , are calculated by GRLWEAP as follows.

I. A relative soil/pile sensitivity, f_s^* , is calculated from the set-up factors, f_s .

$$f_s^* = (1 - 1/f_s)/(1 - 1/f_{sx}) \quad (41)$$

Where, f_{sx} is the maximum set-up factor of all soil layers analyzed (2.5 in the example)

Therefore, for the sand with $f_s = 1.25$, $f_s^* = (1 - 1/1.25)/(1 - 1/2.5) = 0.333$, which means that the sand is only a third as sensitive as the clay because it loses 20% when the clay loses 60%.

II. The friction reduction factor during driving is calculated from the gain/loss factor, f_{GL} , and relative soil/pile sensitivity.

$$f_{RD} = (1 - f_s^* + f_s^* f_{GL}) \quad (42)$$

Therefore, the reduction factor for the sand will be; $f_{RD} = 1 - 0.333 + 0.333(0.7) = 0.9$. Which means, when the clay is analyzed with 70% of its long-term strength, the sand has 90% of its full capacity. Aside from the shaft resistance, the end bearing might also be subjected to different resistances during and after driving. A rising negative pore water pressure during driving in fine-grained soils like clay may increase the toe resistance (e.g. for clay; by 50%) of the soil temporarily during driving. Post driving the resistance will decrease following the pore pressure dissipation. The example above can be a good representation for ECH driven piles but not for vibrated ones. (Pile Dynamics 2010) explains that sands and clays often behave very differently with sands losing a very high and clays losing a very low percentage of their LTSR. It is recommended to do further reading on the subject matter before

assigning/accepting the generated gain/loss factors tabulated on Appendix B, which are recommended soil-setup factors found in the GRLWEAP background report.

If there is an interruption in setup due to re-striking or a new setup period is introduced while a layer is undergoing a resistance loss due to driving, then the capacity loss would commence from an intermediate level. Since driveability analyses considers the variations of soil resistance as the pile penetrates into the ground, it is also possible to include soil set-up effects that might occur during driving interruptions (Pile Dynamics 2010). This is called variable setup and can be considered in the program, in cases where an interruption in driving due to breakdown or most commonly welding of an add-on is carried out. Furthermore, whenever a driving interruption is introduced a refusal due to mobilization of setup may occur. However, the analysis may show in latter depths that a penetration is possible (non-refusal blow counts) result, which in reality is not practical (unless some mode of relief drilling, jetting other operations are done). Further recommendation for variable setup method can be referred to in (Pile Dynamics 2010).

In a post driving situation, a back calculation, referred to as a refined wave equation analysis, could be performed to acquire the assumed values (quake, damping and setup factor) for future driveability analysis in that area and also to reconfirm the design parameters such as bearing capacity. The records taken during pile driving give values that show the performance of the hammer and the pile. Further analysis of these results can give information about the soil parameters by using signal matching method (Rausche et al. 2009). This is however done with some alteration of the wave equation. This is because of the simplified assumptions used in the wave equation to begin with. The soil model, driving model and pile model are all simplified for the sake of analysis. After altering the wave equation, the resulting back calculation by signal matching is called a Refined Wave Equation Analysis (Rausche et al. 2009). This analysis will use the result of the signal matching method and use parameters to match them with the post driving data recorded (Rausche et al. 2009). In inconvenient locations, such as offshore pile installations, dynamic measurements (e.g. Pile Driving Analyzer (PDA)) may be combined with signal matching analysis (e.g. Case Pile Wave Analysis Program (CAPWAP/CW), can be used to replace static pile load tests (Rausche et al. 2009). This refined equation analysis eliminates the need to use assumptions and recommendations of different input parameters while performing dynamic pile analysis. This has resulted in its popularity in the pile driving industry (Webster et al. 2008).

3.4 Refusal

The main purpose of this research is to use PDI GRLWAP software as a prediction tool of refusal by performing driveability analysis. There are standards in different parts of the world setting the limit of pile driving in terms of blow count. For instance, API (API 1993) has set guidelines defining refusal of a pile being driven. Pile refusal is made as part of a contract. It sets a certain value of blow counts where driving should be stopped. After stopping, refusal may be followed by relief drilling methods to decrease the resistance from the soil. Furthermore, refusal also enables to control any damage that may be done on the hammer or pile due to excessive blows (API 1993). The definition of refusal should also be adapted to the individual soil characteristics anticipated for the specific location. Refusal should be defined for all hammer sizes to be used and is contingent upon the hammer being operated at the pressure and rate recommended by the manufacturer (API 1993).

API (API 1993) explains further that, for every pile driving project, a refusal criteria has to be defined beforehand. An example (to be used only in the event that no other provisions are included in the installation contract) of such a definition is:

"Pile driving refusal with a properly operating hammer is defined as the point where pile driving resistance exceeds either 300 blows per foot (0.3 m) for five consecutive feet (1.5 m) or 800 blows per foot (0.3 m) of penetration (This definition applies when the weight of the pile does not exceed four times the weight of the hammer ram. If the pile weight exceeds this, the above blow counts are increased proportionally, but in no case shall they exceed 800 blows for six inches [152 mm] of penetration) If there has been a delay in pile driving operations for one hour or longer, the refusal criteria stated above shall not apply until the pile has been advanced at least one foot (0.3 m) following the resumption of pile driving. However, in no case shall the blow count exceed 800 blows for six inches (152 mm) of penetration." (API 1993)

In establishing the pile driving refusal criteria, the recommendations of the pile hammer manufacturer should be considered (API 1993). Summarizing the refusal criteria:

- 300 blows/0.3 m for 5 consecutive 0.3 m intervals (for continuous driving)
- 800 blows/0.3 m
- 800 blows/0.152 m (setup case)

*The most stringent of the above shall be applied to determine the pile refusal

As mentioned above, the refusal criteria are specific for a particular installation and should be stated in the contract. Another example of refusal could be one used for a driveability study on a wind farm in the North Sea (Anusic et al. 2016). At this specific location refusal is encountered when one of the following criteria is met: 125 blows per 0.25 m in six intervals of

0.25 m (500 bl/m), 200 blows per 0.25 m in two intervals of 0.25 m (800 bl/m), 325 blows per 0.25 m in one interval of 0.25 m (1300 bl/m) or 325 blows per 0.25 m in two intervals of 0.25 m (1300 bl/m) (Anusic et al. 2016).

- 125 blows per 0.25 m for 6 consecutive 0.25 m intervals (500 bl/m)
- 200 blows per 0.25 m for 2 consecutive intervals 0.25 m (800 bl/m)
- 325 blows per 0.25 m in 1 interval of 0.25 m (1300 bl/m)
- 325 blows per 0.25 m in 2 consecutive intervals of 0.25 m (1300 bl/m)

4. Driveability Analysis of BOWL

4.1 Project Overview

In the long term, wind energy is the most important and economical renewable energy source in the field of electricity. The majority of offshore wind farms, such as the Beatrice, that are at the initial stage or being constructed are located in the North and Baltic Seas (BauerNews 2017). Beatrice Offshore Wind farm Limited (BOWL) is a share of three stake holders. The SSE Renewables, Copenhagen Infrastructure Partners, and Red Rock Power, each having 40%, 35% and 25% respectively (BOWL 2011). It will be situated in the northern part of Scotland. With a total generating capacity of 588 MW, it will consist of 84 jackets, each equipped with Siemens turbines with a capacity of 7 MW (BOWL 2011). The Crown Estate has endowed BOWL with the development of the offshore wind farm project in 2009 (BOWL 2011). In May 2016, all proceedings with the finance were finished and led way to the commencement of the construction (BOWL 2011).

BAUER Renewables Ltd. is involved in the foundation work with an underwater drilling rig specially designed for use on the high seas in order to relief drill the foundation piles. For each of the 84 turbines, four foundation piles with a diameter of 2.2 meters each and lengths between 32 and 54 meters are required. The subsoil consists of sand and hard clay with scattered boulders. All piles will be installed by the client, Seaway Heavy Lifting (SHL), using

the pile-driving method. Sometimes, in difficult soil conditions, the piles could experience early refusal. Then Bauer may drill inside to relief the piles from excess friction (BauerNews 2017). A specially designed drilling rig from BAUER Maschinen GmbH – the BAUER Dive Drill C40 – will be used as part of the current [BOWL] project. The drilling rig is designed especially for fast use underwater at an optimal drilling speed (BauerNews 2017).



Figure 4.1 BAUER Dive Drill C40. Source: (BAUER Renewables Ltd. 2018)

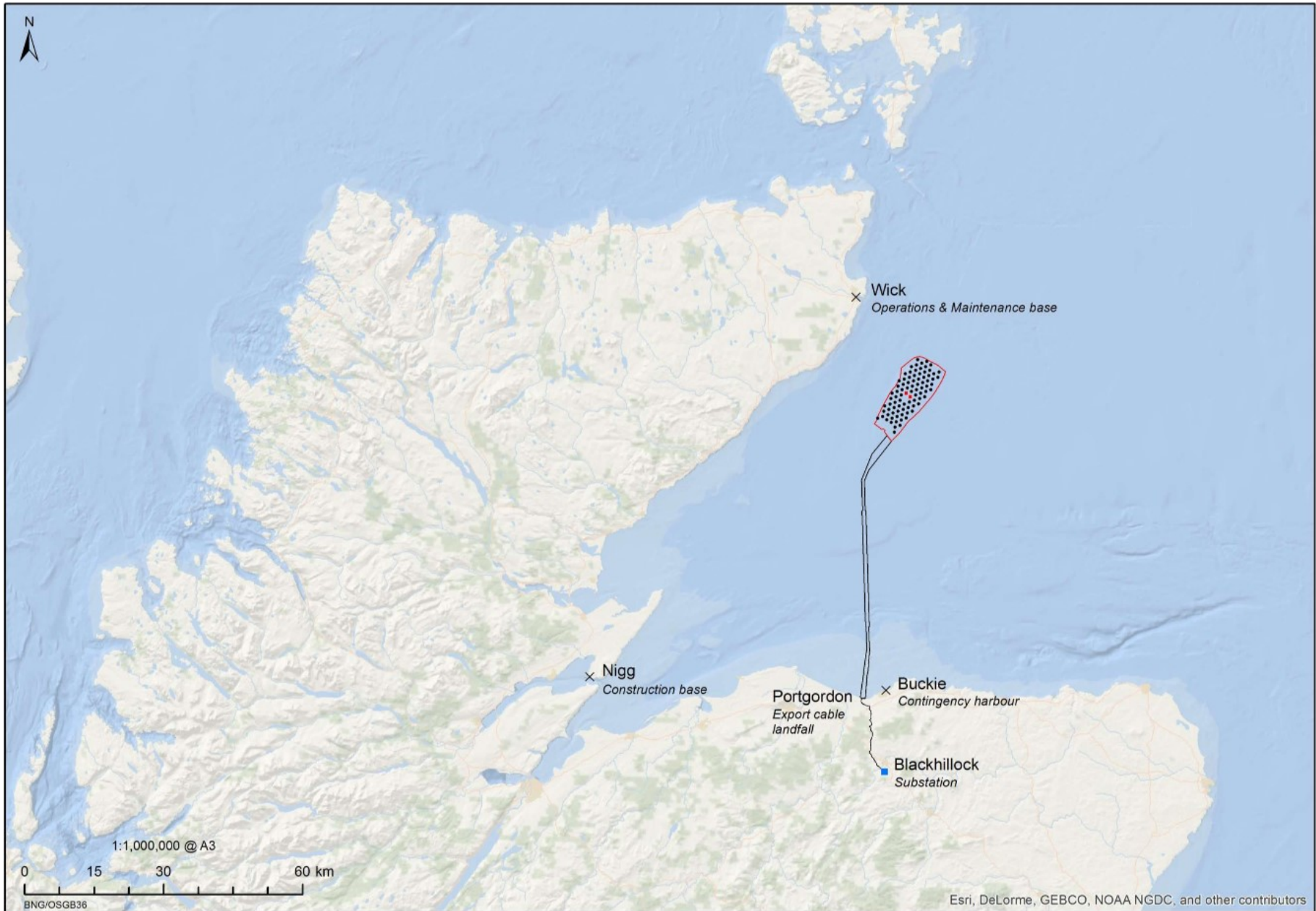


Figure 4.2 Beatrice Offshore Wind farm Ltd. installation layout. Source: (BOWL 2017))

The various preparation and execution of different work items involve different machineries, equipment and professionals. The work flow, according to the operational scheme document, can be simply summarized as;

- I. Setting up the vessel
- II. Installing piles
- III. Pile driving
- IV. Relief drilling (if necessary)
- V. Installing Jackets
- VI. Relocating the vessel



Figure 4.3 The vessel with PIF, Hammer and BAUER DD C40. Source: (BOWL 2017)

One of the vessels used (Figure 4.3), is equipped with a 2.500 t crane which is used for main on-site operations including lifting and lowering the steel piles, the pile installation frame (PIF) and the driving hammer. The relief drilling machine DD-C40 is also fixed and ready for drilling. After the vessel is positioned on the drilling location site, mooring to the seabed is done using anchors. Next, surveying operations to inspect water properties (salinity and density) and geometric survey on PIF and tidal survey is done. Following, pre-Surveying of sub-sea conditions by ROV (Remotely Operated Vehicle) is done. This is to find any obstacles such as boulders, rock or else. This is done after boulder clearing operations have been conducted in 50-meter water depth. The surveying of the sea bed is also used to initially adjust relative elevations of the four legs of the PIF before deployment.

The Pile Installation Frame (PIF) (Figure 4.4), is used to install piles in the correct location, at the appropriate inclination and stick-up height prior to installing the jacket. It is first lifted by the an Internal Lifting tool (ILT) (Figure 4.5) and then lowered by the main crane in to the waters and placed as a template for the pin piles. ROV and beacons will assist an auxiliary winch in the alignment and orientation. The piles are then prepared for placement. The main crane and the ILT will lift the pile, after which it will be guided by a frame on the vessel and shims inside the PIF to be stabbed in the seabed. Here, the ROV is used for assistance and visualization.



Figure 4.4 Pile Installation Frame (PIF). Source: (BOWL 2017)

Once all four piles are stabbed, hammering operations begin. Before hammering operations commence, information is sent for the “Mammal-Watchers”, to inspect and report if there is a screaming of mammals. This will dictate if hammering has to be delayed or not. In the latter case, due to the same reason, a soft start (low energy to minimize the impact noise) will be done. Accordingly, the hammer is placed and hammered to either the final depth or an intermediate depth. Hence, latter method requires 8 rounds of driving.

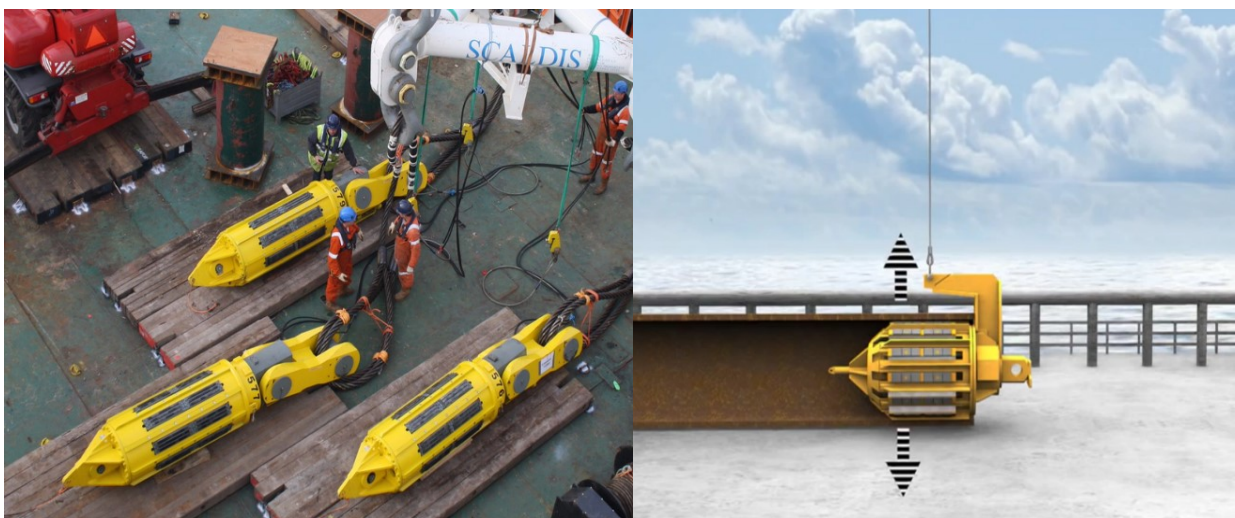


Figure 4.5 Internal Lifting Tool (ILT). Source: (BOWL 2017)

According to the operational scheme of BOWL, the hammering method used for the project mainly dictates to have a constant blow count per 25 cm. By manipulating the hammer energy input for control. The blow count measurement is done using laser indicator in the PIF (Figure 4.5) which targets the pile markings which are marked every 25 cm. Hence, the hammer runs with constant blow rate and the mechanic adjusts the energy input. After this procedure, the pile driving work is done. The final step is to remove the PIF, using the ROV and bring on board the vessel. The same procedure is done for the remaining jackets. The jacket placement and other work follow with another vessel and crew.



Figure 4.6 Stabbed piles ready for hammering. Source: (Journal John O’Groat 2017)

For this project three hammers were considered. IHC’s S-1200, S-1800 and S-2500. The first two, were used mostly as a backup, while the S-2500, with an additional spare, was mainly used for the pile driving operations. An additional 55t of weight was also attached on this particular hammer. This is done to insure the contact between the pile and hammer is not lost due to buoyancy forces. According to (SHL 2017), the S-2500 has a rated energy of 2500 kNm. The energy can be adjusted from 5 to 100% using a computer. This means that the stroke height and other parameters of the hammer can be controlled as desired and monitored accurately. The computer also registers each blow, which makes reporting and post driving analysis very accurate. The hammer is computer controlled, which enables the operator to adjust the hammer’s performance parameters very precisely. The computer registers every blow so that an accurate pile report can be created.

The S-2500 hammer is a double acting hydrohammer. The ram weight, ram pin and piston rod are forged into one piece. The operating principle is governed by a hydraulic system to lift the ram and an additional pressure on the top from a confined nitrogen gas. Referring to Figure 4.7, initially the pressure line is closed at P (inlet valve) and opened at R (return valve). This allows for the ram to be lifted with a hydraulic pressure. The ram rises until the stroke height

is reached. At the same time the ram is compressing the nitrogen gas located above. During the fall of the ram, after reaching the stroke height, the R valve is opened and the P valve is closed. The ram will fall due to gravity; at the same time the confined nitrogen gas will apply pressure on the top of the ram. According to Seaway Heavy lifting (SHL 2017), the ram will reach a maximum acceleration equal to twice the gravitational acceleration (2g). This fact allows for a higher impact frequency increasing the blow rate (SHL 2017) The specifications of the IHC S-2500, according to the manufacturer data are as follows.

Table 4.1 IHC S-2500 Specification. Source: (SHL 2017)

General		
Name - IHC S-2500 Hydrohammer		
Operating Data		
Max. pile energy/blow	kNm	2500
Min. pile energy/blow	kNm	270
Blow rate (max. energy)	bl/min	29*
Weights		
Ram	tons	126
Hammer (incl. ram, in air)	tons	254
Hammer (incl. ram, in salt water) (only if fully submerged)	tons	200
Hydraulic Data		
Operating pressure	bar	250
Maximum pressure	bar	350
Maximum oil flow	L/min	4800

*In relation to the oil flow

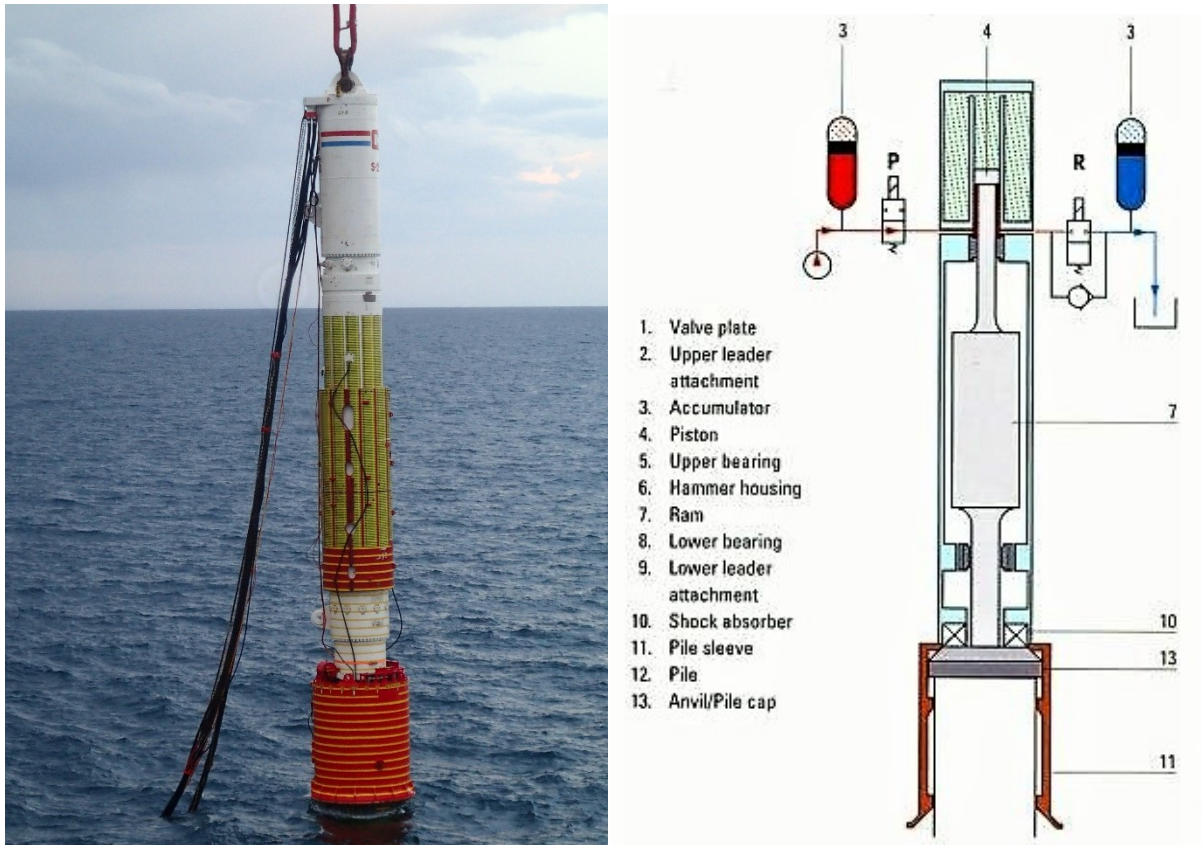


Figure 4.7 IHC S-2500 Hydrohammer and section detail. Source: (SHL 2017)

As mentioned at the beginning there are 84 jackets, each with a set of four piles. Open ended steel pipes are used for this section. However, they have a section change, majorly from a thickness of 60 mm to 50 mm from top to bottom. The pile specifications as follows

Table 4.2 BOWL pile specification

Pile Specification	
Length [m]	36 - 55
Outer diameter (OD) [m]	2.2 to 2.24
Thickness (WT) [mm]	55-80
Stick-up height [m]	2-6
Shear key area from top of pile [m]	1.325
Length of shear key area [m]	5.4
Thickness of shear key [mm]	18
Number of piles [-]	344 (86 Jackets)

All the steel pipes used are grade P-E46, except for the section from the top of the pile up to 2 m below the bottom shear key is a grade SP-F46 steel. 13 shear keys spaced at 45 cm are provided to each pile (Figure 4.8 shows detail of cluster - 3 piles). Shear keys are provided to

increase the axial load carrying capacity at the interface between steel and grout. Weld beads are welded on the required section according to the specification in shown in Figure 4.8. The transition zone will be part of the connection between the jacket and the pile.

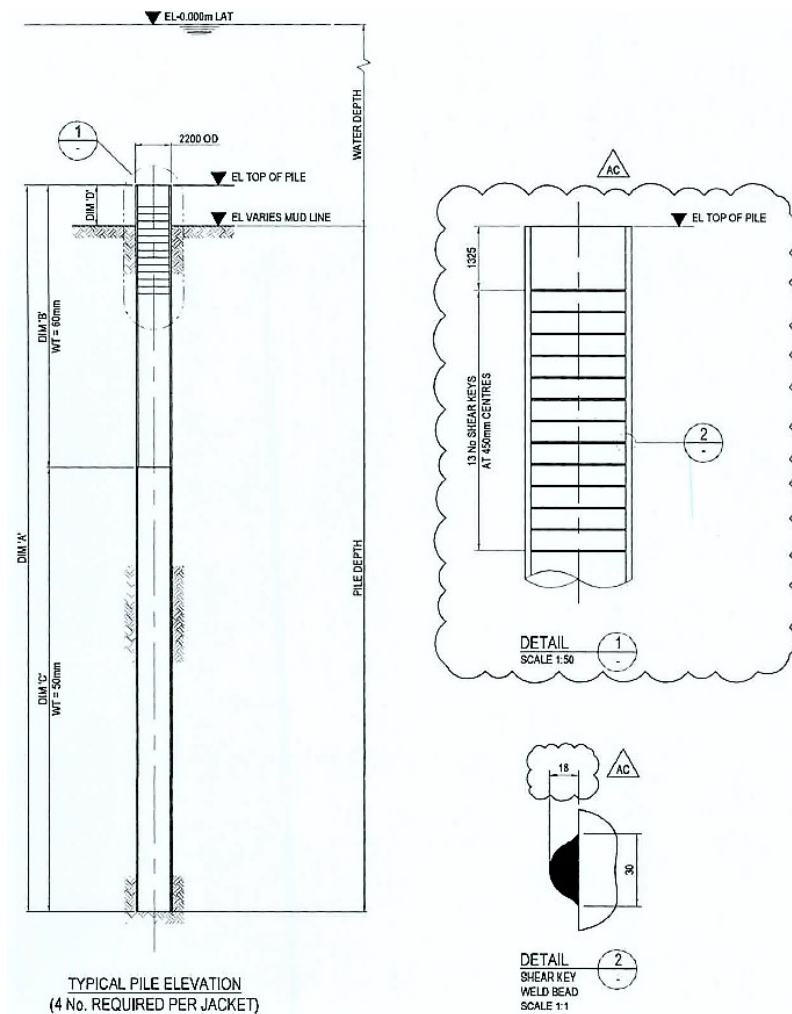


Figure 4.8 Cluster - 3 steel pipe detail partially. Source: (BOWL-project documents)

As the steel will be exposed to water throughout its service life, corrosion protection is also specified. Besides the temporary corrosion protection during storage, Zinc Silicate primer coating is applied 4 m below the nominal original sea bed and 1 m above for the external section, and 1m below and above the nominal original sea bed level for the internal section of the open-ended steel pile. Additionally, as the steel pipe is composed of welded pieces of steel, monitoring of fatigue is done. The process of initiation and propagation of cracks through a structural part due to action of fluctuating stress is known as Fatigue (BS EN 1993-1-9: 2005 / EN 1993-1-9: 2005).



Figure 4.9 Steel pile production and storage. Source: (BOWL 2011)

4.2 Input Data Summary

4.2.1 Overview

The range of the required input data varies strongly, depending on the complexity of the problem to be solved. For example, the input for a simple bearing graph analysis can be entered on the Main Input Screen while a driveability with static analysis of a non-uniform, spliced pile may require data in at least 6 different screens. However, it has been attempted to make the input procedure as simple as possible. For this reason, the program calculates pile model details like springs and masses and distributes the shaft resistance to the various pile segments. For further simplification of the input preparation, the program database includes the models of hammer and driving systems. However, very basic soil and pile information must be supplied by the user (Pile Dynamics 2010).

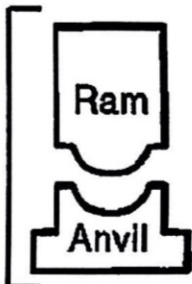
A format for acquiring all the necessary data is shown in the Appendix C. For our problem, the completed version of this form is shown in Figure 4.10, This format is termed as “Pile and Driving Equipment Data Form”, and it is recommended that it should always be used as a pre-requisite to gather the required information before running the program. For the driveability analysis, several piles were considered based on the data acquired. The type of soil investigation results, the depth of the logs, proximity of a pile to the test borehole and post driving data for comparison were the main criteria used for the choosing a pile for analysis. Figures and describe show the layout of the piles.

As a first step, the different options of static geotechnical analysis possibilities with GRLWEAP program were compared with the data at hand. A set of borehole log data from a cone penetration test (CPT) and intermediately withdrawn samples, which are shown in red and blue circles in Figure 4.12, were acquired. The red bore logs acquired have data comprising depth vs plot of undrained shear strength (S_u) in kPa, which was estimated from the CPT data (with $N_{kt}=15-20$) along with few sets of lab and in-situ tests (torvane, laboratory vane, undrained triaxial, in-situ vane, remolded in-situ vane, pocket penetrometer, fall cone, unconfined compressive strength, direct shear test), relative density (D_r) in % also estimated from CPT data ($K_o=0.5$ and 2.0), cone resistance (q_c) in MPa, moisture content in % and unit weight (γ) in kN/m^3 . The blue bore logs have the same parameter plots vs depth except the cone resistance values.

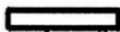
Form 1: Pile and Driving Equipment Data Form

Contract No.: _____ Structure Name and/or No.: BE-L9
 Project: Beatrice Offshore Windfarm Ltd. Pile Driving Contractor or Subcontractor: SHL
 County: _____ (Piles driven by)

Hammer Components



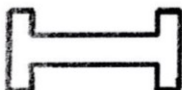
Hammer
 Manufacturer: IHC Model No.: 2500
 Hammer Type: ECH Serial No.: _____
 Manufacturers Maximum Rated Energy: 2499999.99 (Joules)
 Stroke at Maximum Rated Energy: 2.04 (meters)
 Range in Operating Energy: 270000 to 2500000 (Joules)
 Range in Operating Stroke: 0.22 to 2.04 (meters)
 Ram Weight: 125,000 (kg)
 Modifications: Assembly weight already added by the program as two segments.



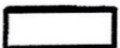
Striker Plate
 Weight: N/A (N) Diameter: N/A (mm)
 Thickness: N/A (mm)



	Material #1	Material #2
	(for Composite Cushion)	
Hammer Cushion	Name: <u>N/A</u>	Name: <u>N/A</u>
	Area: <u>N/A</u> (cm ²)	Area: <u>N/A</u> (cm ²)
	Thickness/Plate: <u>N/A</u> (mm)	Thickness/Plate: <u>N/A</u> (mm)
	No. of Plates: <u>N/A</u>	No. of Plates: <u>N/A</u>
	Total Thickness of Hammer Cushion: <u>N/A</u>	



Helmet (Drive Head)
 Weight: 181.68 (kN) + 55t add-on (539.37 kN)
539.37
721.05 kN (insert)



Pile Cushion
 Material: N/A
 Area: N/A (cm²) Thickness/Sheet: N/A (mm)
 No. of Sheets: N/A
 Total Thickness of Pile Cushion: N/A (mm)



Pile
 Pile Type: Steel
 Wall Thickness: 600-500 (mm) Taper: _____
 Cross Sectional Area: 40 (cm²) Weight/Meter: _____
 Ordered Length: 39 (m)
 Design Load: _____ (kN)
 Ultimate Pile Capacity: _____ (kN)
 Description of Splice: N/A

Driving Shoe/Closure Plate Description: N/A

Submitted By: _____ Date: _____
 Telephone No.: _____ Fax No.: _____

Figure 4.10 Pile and Driving Equipment data for BE-L9. Source: (BOWL-project documents)

The cone resistance values and undrained shear strength values are used for the static geotechnical analysis. The cone resistance values were considered for the non-cohesive soils whereas the clay and silty layers are analyzed according to the undrained shear strength. For the cohesive soils, friction angle was used for classification derived from the cone resistance values. Different correlations and recommendations were applied and compared for some of the geotechnical analysis methods used (SA and API).

The jacket chosen for analysis is BE-L9, consisting of four piles with assumed same characteristics. The corresponding bore log used for identifying the different layer and parameters for the analysis is BHI-69. The pile is a non-uniform pile where the upper 15 m has a wall thickness of 60 mm, whereas the lower art (24 m) has 50 mm thickness. The post driving data from BE-L9 2 will also be used for comparing the blow counts results of the analysis.

The hammer used is the ICH S-2500, which is described in detail in section 4.1. The hammer weight and assembly weight are already included in the program. But since all autofill or values which come in by default should be checked, the weights have been confirmed. The helmet weight however is manually inserted. For the helmet weight considered, a manufacturer's recommendation window (Figure 4.11). Since there was not a recommendation for hammer model (M/S-2500) and pile size (PS=2200 mm) available, hammer model (M/S-2300) and pile size (PS=2440 mm) was used instead.

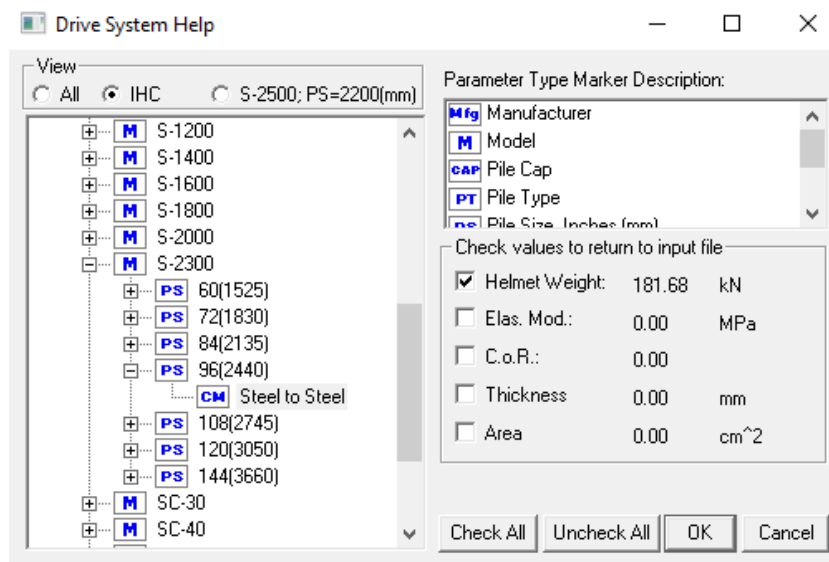


Figure 4.11 Manufacturer's recommended driving system

The recommended helmet weight of 181.68 kN was considered. Here, the reader should note that all means of acquiring the driving hammer data is recommended, and the measure taken above should be avoided for future practices. Furthermore, as mentioned in section 4.1. an

additional 55 t weight (539.37 kN) is attached to the hammer. This weight is considered with the helmet weight as an additional weight, shown in Figure 4.10. In summary, input parameters from Figure 4.10 and additional inputs are tabulated below.

Table 4.3 General input parameters used

Hammer parameters	
Efficiency (-)	0.95
Stroke (m)	2.04
Max. rated energy (kJ)	2500
*Ram weight (kg)	125000
*Assembly weight (kg)	135000
Helmet weight (kN)	721.05
Pile parameters - L9_Pile2_R00	
Pile material	Steel
Pile diameter (mm)	2200
Pile thickness (mm]	60-50
Pile length (m)	39
Pile penetration (m)	33.75
Section area (cm ²)	4033.66 (top), 3377.21 (bottom)
Toe area (cm ²)	3377.21
**E=modulus (MPa)	210000
**Specific weight (kN/m ³)	77.2
Ground Condition	
Water depth (m)	- 49.44 LAT
***Gravity hammer (m/s ²)	7.724
***Gravity steel pile (m/s ²)	8.576

*Already considered in the program and can be checked in the hammer detail option

**Inserted from the reference table of the (Pile Dynamics 2010) by the program following OD input in the "Area Calculator" window.

***Back calculated to account for buoyancy force acting against

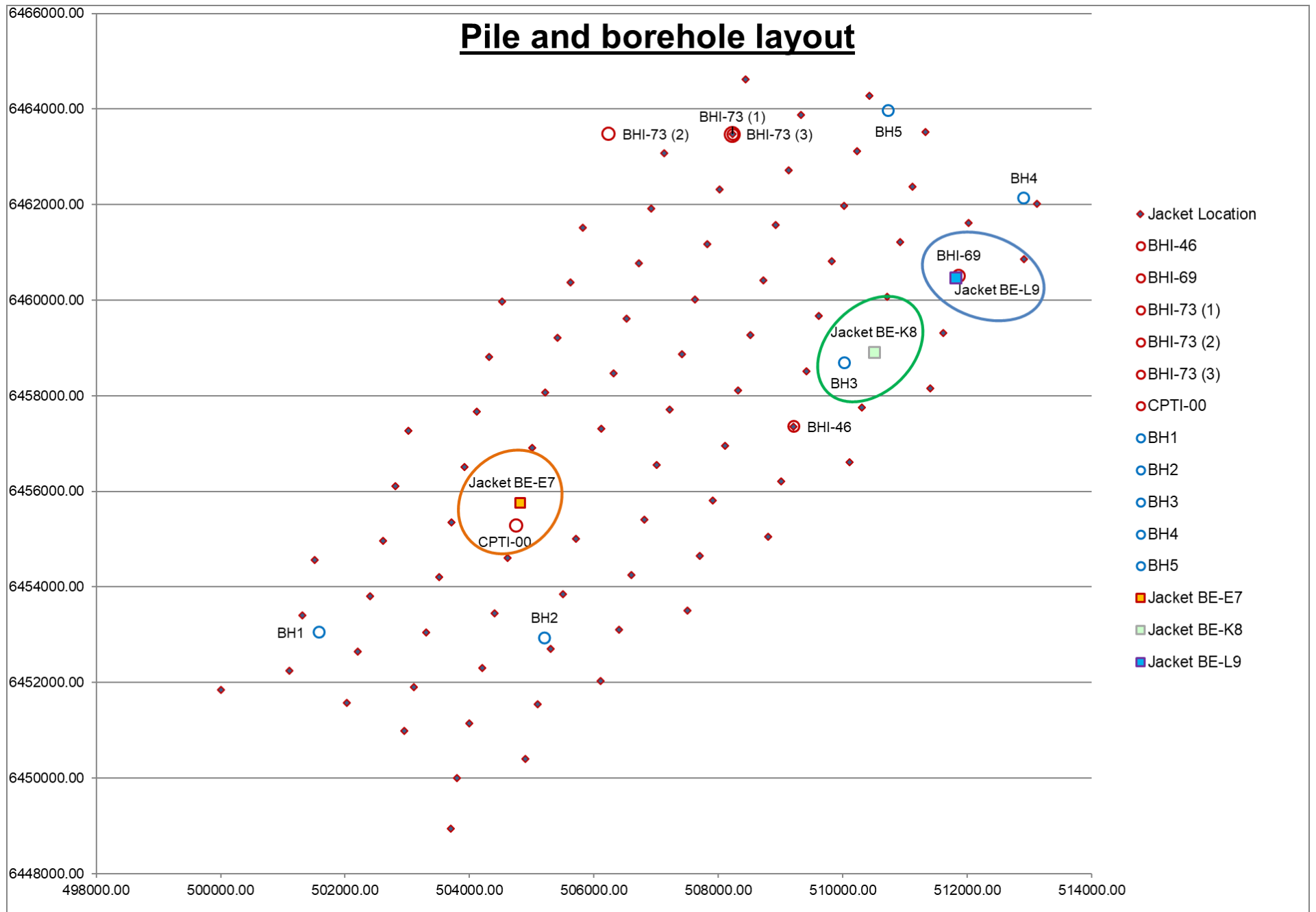


Figure 4.12 Steel pile production and storage

4.2.2 Static Geotechnical Analysis

PDI GRLWEAP software avails different options for the static geotechnical analysis, to determine the unit shaft and toe resistance values. ST, SA and the API method are the once that have been used for this case study. The soil layer input for the corresponding methods is shown in Table A-1, Table A-2 and Table A-3, respectively. The soil layers assigned for ST and API input methods are basically based on layer descriptions of the bore hole log for BHI- 69 (Figure 4.13). However, the inputs for the SA method were made from correlations.

Soil type classifications available for the SA input are as shown in Table 3.3. From the available options, soil classification was done using derived friction angles based on cone resistance values (Table A-3). The correlation after Robertson and Campanelle (Robertson et al. 1983) was used. Applicable to sand, the correlation is given as:

$$\tan \varphi' = \frac{1}{2.68} * [\log \left(\frac{q_c}{\sigma_{vo}'} \right) + 0.29] \quad (43)$$

With regards to quake and damping for the shaft and toe of the pile, recommended values from Table C 1 and Table C 2 are used. They are used in the calculations of the static and dynamic resistance. These recommended values are also altered for the different considerations of plugging, to consider internal friction and plugging. These considerations are discussed in the next sub-section.

The resulting soil resistance distributions for shaft and toe resistance are shown in Figure 4.14. They are however on different scales and should not be compared proportionally. The SA input method has a visible difference in the distribution, giving a relatively variable resistance value of the S.F. (shaft friction) and E.B. (end bearing). However, is it much lower than the ST and API resistances. This is further explained in the next sections.

Depth below Platform Level (m)	Soil description
0.0 m - 0.5 m	loose to medium dense SAND
0.5 m - 1.2 m	loose to medium dense SAND with a thick bed of low strength clay
1.2 m - 2.0 m	loose to medium dense SAND
2.0 m to 4.7 m	very dense above brown lime to coarse SAND with fine to coarse gravel and shell fragments *4.5 m - 4.7 m: with a thin bed of lime to coarse gravel
4.7 m - 19.9 m	medium dense to dense grey to very dark grey slightly clayey silty fine to medium SAND with extremely closely to very closely spaced thin laminate of silty fine sand *10.8 m - 12.5 m: very dense
19.9 m to 50.0 m	dense to very dense dark grey to grey very silty fine to medium SAND *21.2 m: with possible cobbles *24.0 m - 26.0 m: medium dense *26.0 m - 30.4 m: medium dense -dark grey silty fine SAND *30.4 m - 34.9 m: dense to very dense dark grey silty fine SAND *34.9 m - 50.0 m: dense to very dense dark grey to grey very silty fine to medium SAND

Figure 4.13 Summary of the soil investigation bore log report for BHI-69

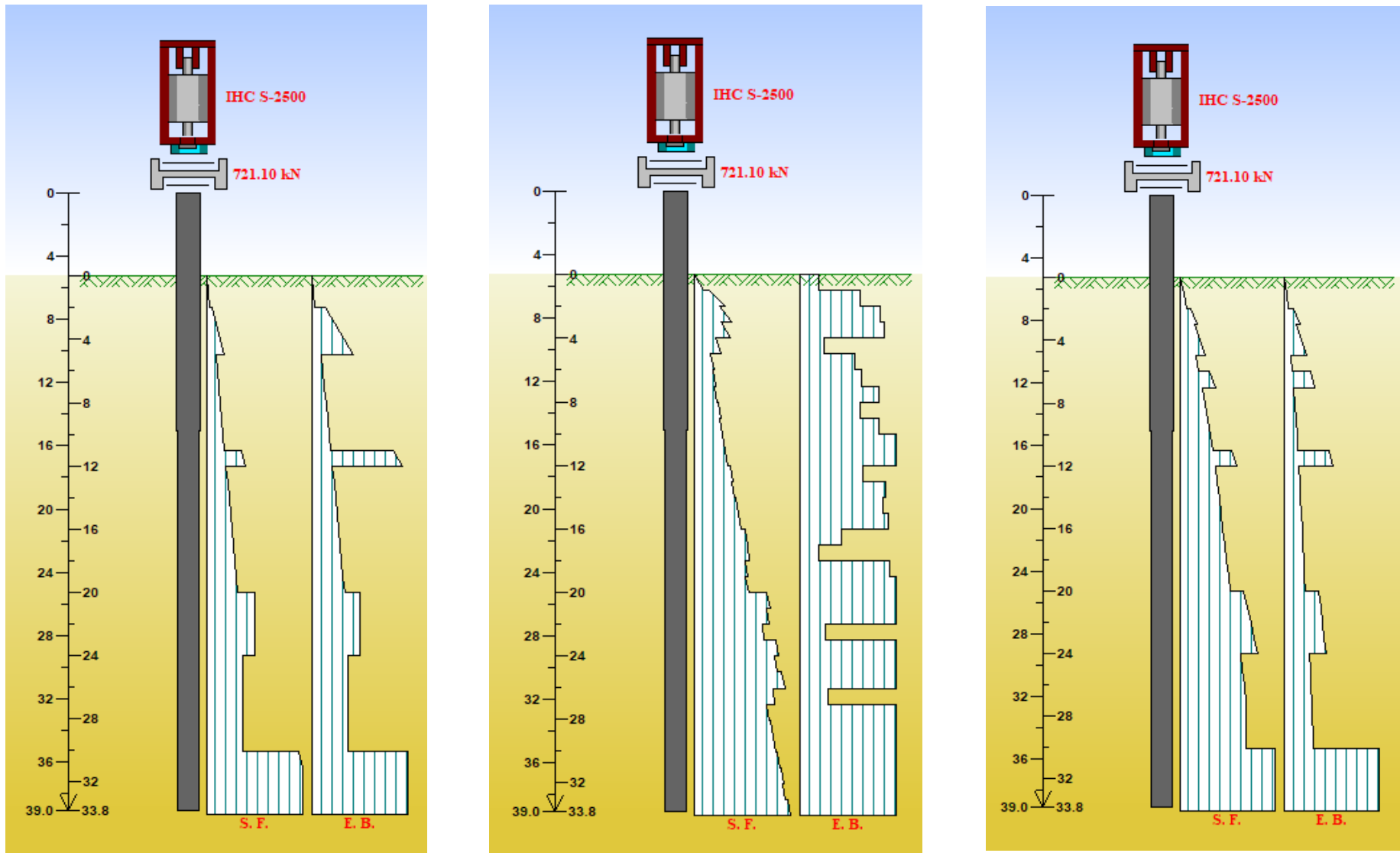


Figure 4.14 Shaft and toe resistance distributions for ST (left), SA (center) and API method in GRLWEAP (right)

4.3 Driveability Analysis Results and Discussion

Three different analysis types to determine SRD were carried out, for each ST, SA and API methods. These analyses are assuming continuous driving conditions. The analysis types were based on Stevens' (Stevens et al. 1982) recommendations are used since his driveability study was also for hard clay, very dense sand and rock. According to PDI (Pile Dynamics 2010), in very dense sands or during restrrike testing after a long waiting time, plugging may be expected unless the pile diameter is very large (say greater than 900 mm or 30 inches) or the penetration into the bearing layer is very shallow (say less than 3 diameters). Even though our OD is large (2200 mm), a lower bound plugged pile was analyzed to establish an upper bound for the driveability analysis. Hence type 1 (lower bound, coring (unplugged)), type 2 (upper bound, coring (unplugged)) and type 3 (lower bound, plugged) according to (Stevens et al. 1982) were run as described in Table 3.10. The results shown and discussed in this report show the first two types. Type 3, which is a lower plugged condition resulted in almost complete refusal in all input types and hence will not be discussed.

For the purpose of discussion, the soil stratum, according to the borehole log (Figure 4.13), can be briefly summarized as shown in Table 4.4.

Table 4.4 Brief summary of major soil types

Penetration depth (m)	Soil type description
0.0 - 2.0	Loose to medium dense SAND
2.0 - 4.7	Very dense SAND
4.7 - 10.8	Medium dense to dense SAND
10.8 - 12.5	Very dense SAND
12.5 - 19.9	Medium dense to dense SAND
19.9 - 34.0	Very dense SAND

To simulate actual driving conditions, an equivalent stroke height was back calculated according to Eq. (12), from post driving transferred energy recordings. A driveability analysis is usually carried out by using the maximum values of stroke and rated energy. This allows one to determine the choice of hammer and if it is appropriate for driving the pile to the desired penetration depth. The equivalent stroke height calculated from the post driving data, makes the driveability analysis comparable (Anusic et al. 2016). The transferred energy comparison between the post driving data and the three analysis types is shown in Figure A-1. Additionally, quake values are taken from GRLWEAP (Pile Dynamics 2010) recommendations (Table C-1).

Furthermore, the ultimate resistance calculation also gets the contribution from the dynamic response of the soil. In GRLWEAP (Pile Dynamics 2010) dynamic resistance is calculated using Smith's damping factor (Eq.(20)). Recommended values of damping factor (Table C-2) were used.

Consideration of setup is also done through gain/loss factors. The gain loss factors that are used for the shaft are dependent on the setup factors of the most sensitive layer. All layers are predominantly composed of sand and hence the setup factor is taken as 1.2 (Table C-3). Which means that the inverse value ($1/1.2=0.8333$) is the first shaft gain loss factor input, representing a full loss of setup. Here, gain/loss factor used for the toe is 1, which means that the toe resistance is assumed not to be affected by the driving process and hence the LTRD and SRD are equal. A second gain loss entry was assigned with a gain loss factor of 1.0 for both shaft and quake. This analysis output represents a fully mobilized setup, worst case driveability scenario or possibly a restrike case, giving an upper limit of the overall analysis.

4.3.1 Analysis Type-1 (T1-Lower_bound_unplugged (coring))

This analysis simulates the pile as fully (coring), also known as the cookie cutter effect, unplugged open-ended non-displacement pile with partial internal friction. The latter consideration is due to the non-uniformity of the pile. Since the soil mass cored into the pile will be squeezed into the upper section where the internal diameter decreases from 2100 mm to 2080 mm, friction is assumed to develop in that section. Hence, it is considered that the shaft resistance acts on the full external section and another 50% is assumed to act on the internal section of the pile. The toe resistance acts on the bottom-section area. Therefore, the SRD calculation was calculated according to the values in Table 4.5.

Table 4.5 Analysis type-1, lower bound, coring (unplugged)

Unit end bearing	1.5*as per static analysis
Toe area	3377.21 cm ²
Shaft/Toe quake	2.5 mm/2.5 mm
Shaft/Toe damping	0.164 s/m/0.5 s/m
Unit shaft resistance	As per static analysis

As it can be observed in Figure 4.15, type 1 analysis results in lower blow counts in all sections. This can be interpreted as an underestimation of the soil resistance values. But generally ST method shows relatively better predictions than SA and API methods, especially for the restrike case (Figure 4.16), even though inaccuracies are clearly visible.

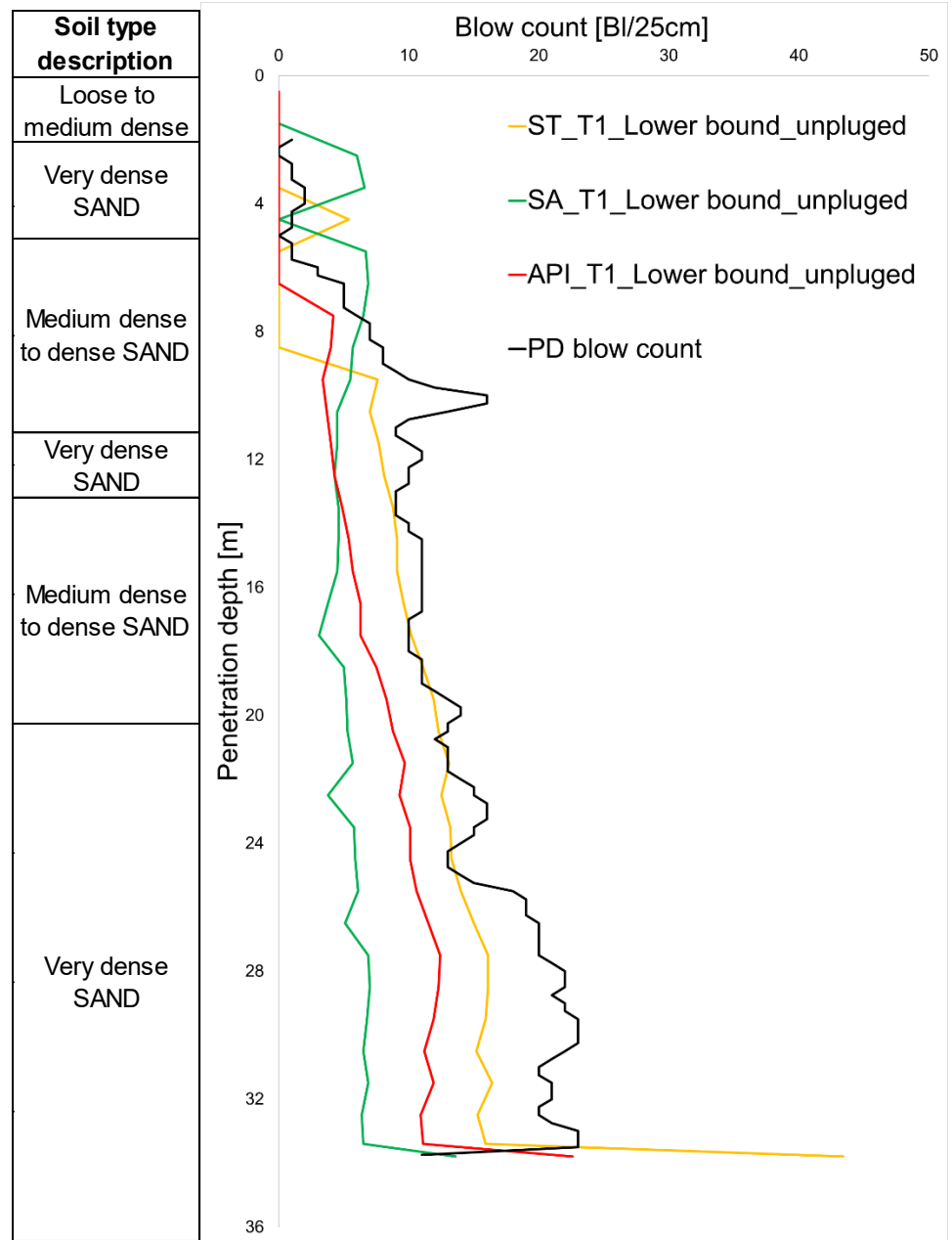


Figure 4.15 Type 1-driveability prediction of BE-L9 with G/L-0.833/1.000

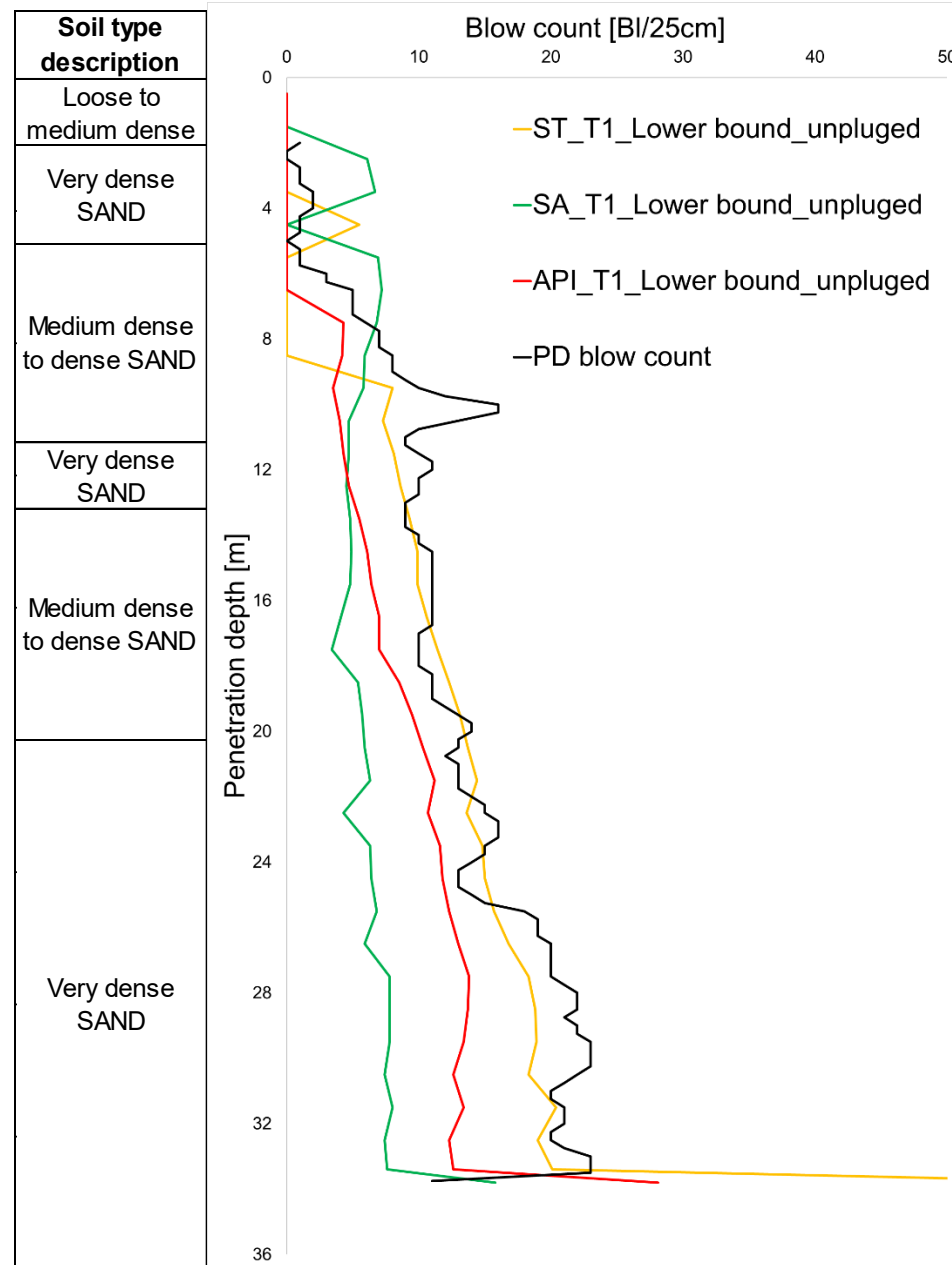


Figure 4.16 Type 1-driveability prediction of BE-L9 with G/L-1.000/1.000

4.3.2 Analysis Type-2 (T2-Upper_bound_unplugged (coring))

This analysis simulates the pile as fully (coring), also known as the cookie cutter effect, unplugged open-ended non-displacement pile with equal external and internal friction. Hence, the shaft resistance is assumed to be present in the external and external section of the pile equally. The toe resistance acts on the bottom-section area. Therefore, the SRD calculation was calculated according to the values in Table 4.5.

Table 4.6 Analysis type-2, upper bound, coring (unplugged)

Unit end bearing	2*as per static analysis
Toe area	3377.21 cm ²
Shaft/Toe quake	2.5 mm/2.5 mm
Shaft/Toe damping	0.164 s/m/0.5 s/m
Unit shaft resistance	As per static analysis

The driveability predictions are shown in Figure 4.17 and Figure 4.18. The ST and API methods show good predictions. The ST method shows an over prediction in the very dense sand layer (10.8 m and below) for the restrike case. Additionally, the ST method comes to a blow count of 233.6/25 cm (934.4 bl/m), at the penetration depth of 33.8 m. However comparing this value with the refusal criteria of API (API 1993) and Anusic (Anusic et al. 2016), described in section 3.4, it is not a refusal blow count and will can be driven until finish.

The SA predictions show an underestimation in both cases. This can result from different factors. In this study, a graphical cone resistance plot from a CPT was first transferred into figures. This values were used to acquire the effective friction angle, using Robertson and Campanelle's (Robertson et al. 1983) correlation. This has resulted in underestimation of the resistance. Since the SA method uses the effective friction angle for calculation of shaft resistance (Appendix B), the majority of the underestimation comes from the shaft resistance. Comparing the shaft resistance values shows an underestimation within the range of 46-61 % from ST and API SRD values.

The overall prediction is acceptable but shows a low quality, in terms of curve fitting. This is due to many factors. The layer thickness, accuracy of the soil type and input parameters, SRD calculation methods, and unknown values (quake, damping and setup factors) are the major reasons. Unknown values such as quake, damping and setup factors are used based on recommended values by GRLWEAP (Pile Dynamics 2010). This should be further developed by the design engineer while performing back analysis or refined wave equation analysis. This back analysis results in quake, damping and setup factors values from a post driving data.

This is very useful for future projects in the vicinity and also to give the designer an upper hand in performing realistic driveability analyses in the future. It will also enable better understanding of the PDI GRLWEAP software.

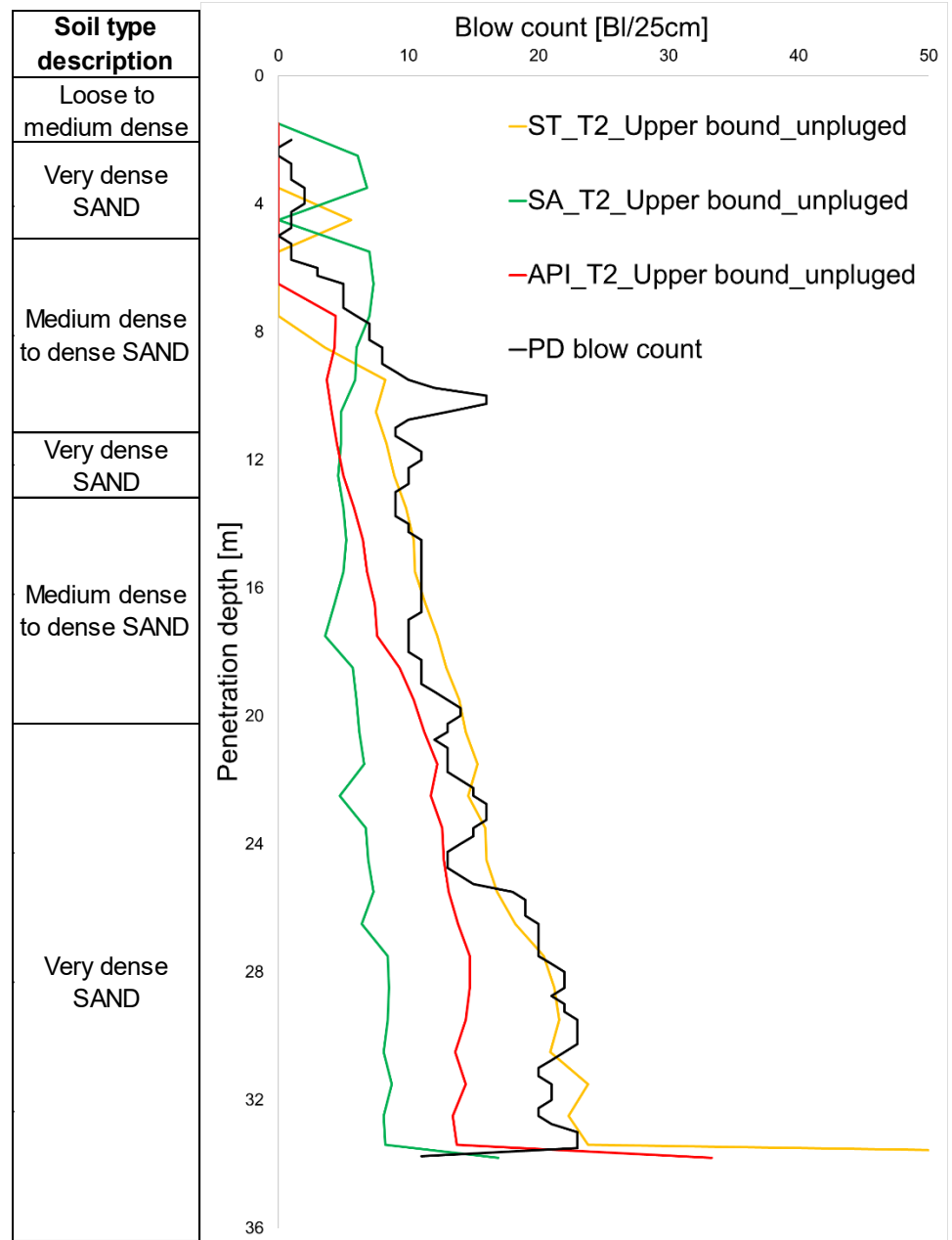


Figure 4.17 Type 2-driveability prediction of BE-L9 with G/L-0.833/1.000

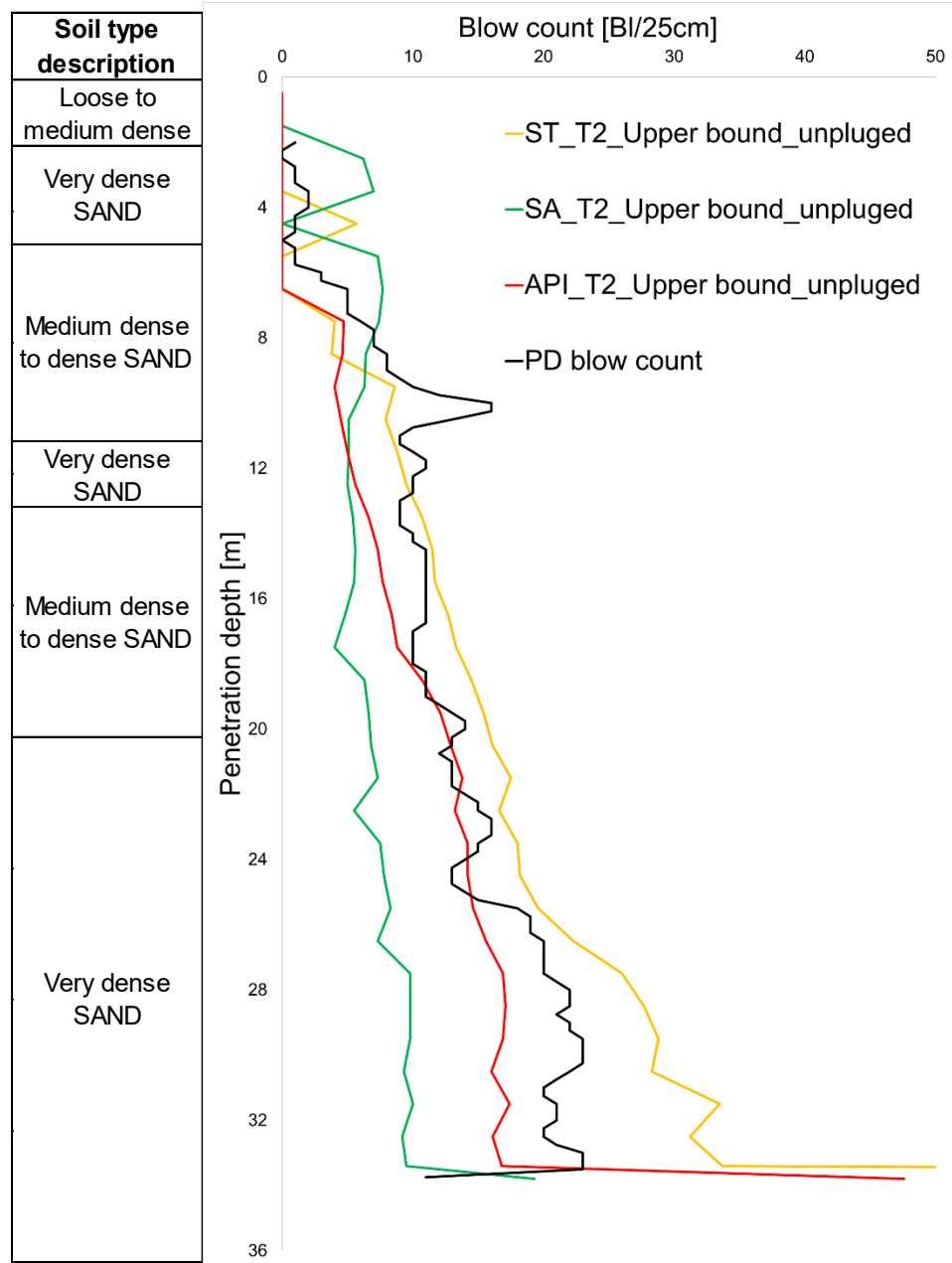


Figure 4.18 Type 2-driveability prediction of BE-L9 with G/L-1.000/1.000

5. Conclusions

During offshore pile driving operations, driving to the desired penetration may not be achieved due to higher soil resistance, hence it is said that a refusal has occurred. This refusal can be overcome by reducing the soil resistance along the shaft. One of the methods employed is relief drilling. A drilling machine bores through the inner section of the open-ended pile, reducing the internal friction. It is also possible to simulate the driving process during the initial stages of the project. A driveability analysis allows to predict this refusal scenario and also simulate the driving process as a whole. However, a driveability analysis should be done with caution. Unless aided with experience, the prediction of the SRD (static resistance to driving), and unknown parameters such as quake, damping and setup values may be very difficult and lead to underestimation or overestimation.

A driveability study based on data from the Beatrice Wind Farm Ltd. Project was done. The chosen pile location had a stratum that is mainly composed of very dense to dense sand. Three static geotechnical analysis methods, ST (soil type method), SA (SPT N-value method) and API (American Petroleum Institute) in GRLWEAP methods, using PDI GRLWEAP software were carried out and compared. Three possible scenarios were applied to each case: Lower bound unplugged (coring) (T1), upper bound unplugged (coring) (T2) and lower bound plugged (T3). All three were analyzed for each static geotechnical analysis, but only results from T1 and T2 are presented in this study. Furthermore, two gain loss factors were applied to simulate cases of end of driving resistance and the worst case driveability or restrike case.

T1 results in lower blow counts for all input methods. This can be interpreted as an underestimation of the soil resistance values. In general, the ST method shows relatively better predictions than SA and API methods, especially for the restrike case. The ST and API methods show good predictions. The ST method shows an over prediction in the very dense sand layer for the restrike case. Refusal was not encountered for both T1 and T2 analyses. The SA predictions result in an underestimation in both analysis cases. The effective friction angle was obtained from a CPT cone resistance (q_u) by Robertson and Campanelle's (Robertson et al. 1983) correlation. This has resulted in a significant underestimation of the shaft resistance.

The overall prediction is acceptable but has a low quality in terms of curve fitting. The layer thickness, accuracy of the soil type and input parameters, SRD calculation methods, and unknown values (quake, damping and setup factors) are the major reasons. Refined wave equation analysis should be performed to acquire quake, damping, setup factor values and

other variables from a post driving data. This will give the designer an upper hand in performing realistic driveability analyses in the future and have a better engineering judgement.

Bauer Spezialtiefbau GmbH can use the PDI GRLWEAP software for predicting driveability in pile driving operations, both onshore and offshore. The analysis should be done based on a solid soil investigation data, which is the basics for the static geotechnical analysis. Bauer engineers should perform driveability analysis based on past projects involving different soil types, complexity and installation methods. This will greatly improve the understanding and limitations of the PDI GRLWEAP software. Furthermore, when considering only the driveability predictions, deciding on the necessity of relief drilling operations can be decided by considering two factors. One factor is the designer's judgement and confidence in the driveability predictions, while the other is proximity of the results with respect to the refusal criteria. This shows, the decision to employ a relief drilling machinery for an offshore pile driving operation is very subjective. Furthermore, when considering project executions, considerations of project schedule and cost can also be a governing factor to deploy a relief drilling machine.

Bibliography

- Anusic, I., Eiksund, G. R., and Liingaard, M. A. (2016). "Comparison of pile driveability methods based on a case study from an offshore wind farm in North Sea." *Proceedings of the 17th Nordic Geotechnical Meeting Challenges in Nordic Geotechnic*, 1037–1046.
- API. (1993). *Recommended Practice for Planning, Designing and Constructing Fixed Offshore Platforms-Load and Resistance Factor Design*. American Petroleum Institute, Washington.
- Bailey, H., Brookes, K. L., and Thompson, P. M. (2014). "Assessing environmental impacts of offshore wind farms: lessons learned and recommendations for the future." *Aquatic biosystems*, BioMed Central, 10(1), 8.
- Bauer-Pileco Inc. (2016). "Diesel Hammers and Leads."
- BAUER-Pileco Inc. (2015). "Vibro Hammers."
- BAUER Maschinen GmbH. (2017). "MC Seilbagger - MC Duty-Cycle Cranes."
- BAUER Renewables Ltd. (2018). "BAUER Renewables Ltd." <<http://www.bauer-renewables.co.uk/en/index.html>> (Feb. 7, 2018).
- BauerNews. (2017). "Next step in the future market of renewable energy."
- BOWL. (2011). "Beatrice Offshore Windfarm Ltd (BOWL) Overview and Summary." (June), 1–36.
- BOWL. (2017). "Project Update." *BOWL: Project Update - March 2017*, (March), 1–6.
- Bowles, J. (1977). *Foundation analysis and design*. McGraw-Hill.
- Bowles, J. E. (1997). *Foundation Analysis and Design. Engineering Geology*, The McGraw-Hill Companies, Inc., Singapore.
- BS 8004. (1986). "BS 8004:1986 Code of practice for foundations." *British Standard Institution, London*, (March), 186.
- Buza, J. (1999). *Builder 3 & 2, Volume 2*. Naval education and Training Professional Development and Technology Center, Pensacola, Florida.
- EN 1997-2, E. N. (2007). "Geotechnical design - Part 2: Ground investigation and testing." *Eurocode 7, 2(2007)*, 1–197.
- EWEA. (2013). "Deep water - The next step for offshore wind energy." *European Wind Energy Association report, Brussels*. See <http://www.ewea.org>, (July), 51.
- EWEA. (2014). *The European Offshore Wind Industry - Key Trends and Statistics 2013*. January, Brussels.
- Fellenius, B. H. (2006). *Basics of Foundation Design*. Electronic edition, Calgary, Alberta.
- FinnRA, F. N. R. A. (2000). *Steel pipe piles. Bridge Engineering*, Finnish National Road Administration, Helsinki, Finland.

- Goble, G. G., and Rausche, F. (1986). *Wave Equation Analysis of Pile Foundations: WEAP86 Program*. Department of Transportation, Federal Highway Administration, Offices of Research and Development, Implementation Division.
- Hannigan, J. P., Goble, G. G., Thendean, G., Likins, G. E., and Rausche, F. (2016). "Design and Construction of Driven Pile Foundations." *Workshop Manual, Volume - II Publication No. FHWA-HI-97-014*, I(September).
- Hannigan, P. J., Goble, G. G., Likins, G. E., and Rausche, F. (2006). "Design and Construction of Driven Pile Foundations Reference Manual – Volume II." II(132021).
- Jaky, J. (1944). "The coefficient of earth pressure at rest 1944, 10: 355-358." *Journal for Society of Hungarian Architects and Engineers*, 10(2), 355–358.
- Journal John O’Groat. (2017). "Final piles installed at Beatrice offshore wind farm." <<https://www.johngroat-journal.co.uk/News/Final-piles-installed-at-Beatrice-offshore-wind-farm-04122017.htm#>> (Feb. 14, 2018).
- Kulhawy, F. H., Jackson, C. S., and Mayne, P. W. (1989). "First-Order Estimation of K_o in Sands and Clays." *Foundation engineering: current principles and practices*, 121–134.
- Kulhawy, F. H., and Mayne, P. W. (1991). "Relative density, SPT, and CPT interrelationships." *Calibration Chamber Testing*, Elsevier New York, 197–211.
- Malhotra, S. (2011). "Selection, Design and Construction of Offshore Wind Turbine Foundations." *Wind Turbines*, InTech.
- Martijn van Delft. (2016). "Recorder function of PDR used for offshore PDA-test." <<http://allnamics.eu/tag/offshore/>> (Feb. 20, 2018).
- Mockler, S., Eikeland, H., Lasselle, S., and Jørgen Johnsrud Capt Stephen Bligh, H. (2015). "Review of Maritime Regulations and Standard for Offshore Wind - Summary report on North Sea regulation and standards Søfartsstyrelsen / Danish Maritime Authority." (December).
- OSC, O. science C. (2018). "Ocean Science Consulting." <<http://www.osc.co.uk/>> (Feb. 2, 2018).
- Pile Dynamics, P. (2010). *GRLWEAP Procedures and Models*. Pile Dynamics Inc.
- Rausche, F. (2000). "Wave Mechanics And The Wave Equation." *Pile Driving Contractors Association*.
- Rausche, F. (2009). "GRLWEAP™ Fundamentals."
- Rausche, F., Liang, L., Allin, R. C., and Rancman, D. (2004). "Applications and Correlations of the Wave Equation Analysis Program GRLWEAP." *Proceedings of the Seventh International Conference on the Application of Stresswave Theory to Piles*, (C), 107–123.
- Rausche, F., Naggy, M., Webster, S., and Liang, L. (2009). "Omae2009-80163 Capwap and Refined Wave Equation Analyses for Driveability Predictions and Capacity Assessment of Offshore Pile." *Omae*, 1–9.
- Rausche, F., Thendean, G., Abou-matar, H., and Likins, G. Goble, G. (1997). *Determination of Pile Driveability and Capacity from Penetration Tests*. Federal Highway Administration.

- Robertson, P. K., and Campanella, R. G. (1986). *Guidelines for Use, Interpretation and Application of the CPT and CPTU*. Hogentogler & Company.
- Robertson, P. K., Campanella, R. G., and Wightman, A. (1983). "SPT- CPT correlations." *Journal of Geotechnical Engineering - ASCE*, 109(11), 1449–1459.
- Rocscience Inc. (2016). "CPT Data Interpretation Theory Manual." 1, 18.
- RTG Rammtechnik GmbH. (2016). "RG-System."
- Rumes, B., Erkman, A., and Haelters, J. (2016). "Chapter 4 Evaluating Underwater Noise Regulations for Piling Noise in." 37–48.
- Schmertmann, J. H. (1975). "Measurement of in situ shear strength, SOA Report." *Proceedings, ASCE Spec. Conference on In Situ Measurement of Soil Properties, Raleigh, NC, 1975*, 57–138.
- Schmertmann, J. H. (1978). *Guidelines for Cone Penetration Test - Performance and Design*. United States. Federal Highway Administration, Florida, USA.
- Scottish Power Renewables. (2012). "Offshore Wind and Supply Chain Opportunities." *Workshop in Bilbao*, <<https://www.slideshare.net/bemadrid/offshore-wind-supply-chain-bilbao-alan-28-feb-2012>> (Feb. 2, 2018).
- SHL. (2017). "IHC S-2500." Seaway Heavy Lifting.
- Stevens, R., Wiltsie, E., and Turton, T. (1982). "Evaluating Drivability for Hard Clay, Very Dense Sand, and Rock." *Offshore Technology Conference*.
- The Constructor. (2017). "Types of Pile Driving Equipments -Applications, Advantages and Details." <<https://theconstructor.org/geotechnical/pile-driving-equipment-types-uses/17605/>> (Feb. 20, 2018).
- Thomsen, F., Lüdemann, K., Kafemann, R., and Piper, W. (2006). *Effects of offshore wind farm noise on marine mammals and fish*. Biola, Hamburg: Germany.
- Tomlinson, M. J. (1994). *Pile design and construction practice-Fourth edition*. McGraw-Hill handbooks, London, UK.
- Tomlinson et al., M. J. (2008). *Pile design and construction practice-Fifth edition*. *Canadian Journal of Civil Engineering*, McGraw-Hill handbooks.
- Volume, W. H., and American Welding Society. (2004). *Welding Handbook, Welding Processes, Part 1. AWS WHB-1.9*, Miami, Florida.
- Warrington, D. C. (1997). "Closed Form Solution of the Wave Equation for Piles." *University of Tennessee at Chattanooga*, University of Tennessee at Chattanooga, Engineering.
- Webster, S., Givet, R., and Griffith, A. (2008). "Offshore pile acceptance using dynamic pile monitoring." *Technology*, 655–661.
- Wind Europe. (2016). "Wind in Power: 2016 European Statistics." *Wind Europe: Brussels, Belgium*, (February), 1–24.
- Wrana, B. (2015). "Pile Load Capacity – Calculation Methods." *Studia Geotechnica et Mechanica*, 37(4).

Appendices

Appendix A Driveability Analysis Input and Results

- i. Soil classification input and S1 table for ST input method
- ii. Soil classification input for SA input method
- iii. Soil classification input for API input method

Appendix B Calculation Steps for Resistance Output

- i. Simple soil type classification (ST)
- ii. SPT N-value based method
- iii. The CPT Method in GRLWEAP
- iv. The API Method in GRLWEAP

Appendix C Reference Tables and Formats

- i. Recommended quake and damping values
- ii. Recommended setup factors
- iii. Pile and driving equipment data form

Appendix D Raw and Correlated Data

- i. BHI-69 - Original soil investigation bore log report
- ii. Cone resistance approximation
- iii. Driving monitoring data with plots

Appendix A Driveability Analysis Input and Results

I. Soil Classification Input and S1 Table for ST Input Method

Table A-1 Sub-soil layering input for ST method

Layer thickness (m)	Soil Type	Density/Cohesivity
0	Granular	Medium dense
1	Granular	Medium dense
2	Granular	Medium dense
3	Granular	Very dense
4	Granular	Very dense
5	Granular	Very dense
6	Granular	Medium dense
7	Granular	Medium dense
8	Granular	Medium dense
9	Granular	Medium dense
10	Granular	Medium dense
11	Granular	Medium dense
12	Granular	Very dense
13	Granular	Medium dense
14	Granular	Medium dense
15	Granular	Medium dense
16	Granular	Medium dense
17	Granular	Medium dense
18	Granular	Medium dense
19	Granular	Medium dense
20	Granular	Medium dense
21	Granular	Dense
22	Granular	Dense
23	Granular	Dense
24	Granular	Dense
25	Granular	Medium dense
26	Granular	Medium dense
27	Granular	Medium dense
28	Granular	Medium dense
29	Granular	Medium dense
30	Granular	Medium dense
31	Granular	Very dense
32	Granular	Very dense
33	Granular	Very dense
34	Granular	Very dense

II. Soil Classification Input for SA Input Method

Table A-2 Sub-soil layering input for SA method

Layer thickness (m)	Soil Type	Grading	Size	SPT-N	Qc (Cone Resistance) (Mpa)	Friction angle (ϕ) ($^{\circ}$)	Unit weight (kN/m^3)
0.0	Sand	Poorly	Medium	-	2.0	0	19
1.0	Sand	Poorly	Medium	-	1.0	43	19
2.0	Sand	Poorly	Medium	-	13.8	51	19
3.0	Sand	Well	Medium	-	23.5	52	19
4.0	Sand	Well	Medium	-	25.0	51	19
5.0	Sand	Well	Medium	-	2.5	39	19
6.0	Sand	Well	Fine	-	11.7	46	19
7.0	Sand	Well	Fine	-	12.5	46	20
8.0	Sand	Well	Fine	-	20.0	47	19
9.0	Sand	Well	Fine	-	14.3	45	19
10.0	Sand	Well	Fine	-	20.0	46	19
11.0	Sand	Well	Fine	-	33.0	48	20
12.0	Sand	Well	Fine	-	32.5	47	20
13.0	Sand	Well	Fine	-	10.5	42	19
14.0	Sand	Well	Fine	-	20.0	45	19
15.0	Sand	Well	Fine	-	19.0	44	19
16.0	Sand	Well	Fine	-	20.0	44	19
17.0	Sand	Well	Fine	-	5.0	36	19
18.0	Sand	Well	Fine	-	1.5	28	19
19.0	Sand	Well	Fine	-	20.0	43	19
20.0	Sand	Well	Fine	-	32.1	46	18
21.0	Sand	Well	Medium	-	40.0	46	19
22.0	Sand	Well	Medium	-	27.0	44	18
23.0	Sand	Well	Medium	-	2.0	29	18
24.0	Sand	Well	Medium	-	36.0	45	18
25.0	Sand	Well	Medium	-	22.5	43	19
26.0	Sand	Well	Medium	-	30.0	44	19
27.0	Sand	Well	Fine	-	2.5	29	19
28.0	Sand	Well	Fine	-	50.0	46	19
29.0	Sand	Well	Fine	-	52.0	46	19
30.0	Sand	Well	Fine	-	32.1	44	18
31.0	Sand	Well	Fine	-	28.0	43	19
32.0	Sand	Well	Fine	-	27.0	42	19
33.0	Sand	Well	Fine	-	30.6	43	18
34.0	Sand	Well	Fine	-	21.3	41	19
35.0	Sand	Well	Fine	-	18.2	40	19
36.0	Sand	Well	Medium	-	22.8	41	18
37.0	Sand	Well	Medium	-	27.5	42	19
38.0	Sand	Well	Medium	-	33.2	43	18
39.0	Sand	Well	Medium	-	22.2	40	18
40.0	Sand	Well	Medium	-	32.1	42	18
41.0	Sand	Well	Medium	-	28.0	41	19
42.0	Sand	Well	Medium	-	27.0	41	19
43.0	Sand	Well	Medium	-	30.6	41	19
44.0	Sand	Well	Medium	-	21.3	39	19
45.0	Sand	Well	Medium	-	18.2	38	19

III. Soil Classification Input for API Input Method

Table A-3 Sub-soil layering input for API method in GRLWEAP

Layer thickness (m)	Soil Type	Density/ Cohesivity	Unit weight (kN/m ³)
0.0	Sand	Dense	19
1.0	Sand	Medium	19
2.0	Sand	Very dense	19
3.0	Sand	Very dense	19
4.0	Sand	Very dense	19
5.0	Sand	Dense	19
6.0	Sand	Very dense	19
7.0	Sand	Very dense	20
8.0	Sand	Very dense	19
9.0	Sand	Very dense	19
10.0	Sand	Very dense	19
11.0	Sand-Silt	Very dense	20
12.0	Sand-Silt	Very dense	20
13.0	Sand-Silt	Very dense	19
14.0	Sand-Silt	Very dense	19
15.0	Sand-Silt	Very dense	19
16.0	Sand-Silt	Very dense	19
17.0	Sand-Silt	Very dense	19
18.0	Sand-Silt	Dense	19
19.0	Sand-Silt	Very dense	19
20.0	Sand-Silt	Very dense	18
21.0	Sand-Silt	Very dense	19
22.0	Sand-Silt	Very dense	18
23.0	Sand-Silt	Dense	18
24.0	Sand-Silt	Very dense	18
25.0	Sand-Silt	Very dense	19
26.0	Sand-Silt	Very dense	19
27.0	Sand-Silt	Dense	19
28.0	Sand-Silt	Very dense	19
29.0	Sand-Silt	Very dense	19
30.0	Sand-Silt	Very dense	18
31.0	Sand-Silt	Very dense	19
32.0	Sand-Silt	Very dense	19
33.0	Sand-Silt	Very dense	18
34.0	Sand-Silt	Very dense	19
35.0	Sand-Silt	Very dense	19
36.0	Sand-Silt	Very dense	18
37.0	Sand-Silt	Very dense	19
38.0	Sand-Silt	Very dense	18
39.0	Sand-Silt	Very dense	18
40.0	Sand-Silt	Very dense	18
41.0	Sand-Silt	Very dense	19
42.0	Sand-Silt	Very dense	19
43.0	Sand-Silt	Very dense	19
44.0	Sand-Silt	Very dense	19
45.0	Sand-Silt	Very dense	19

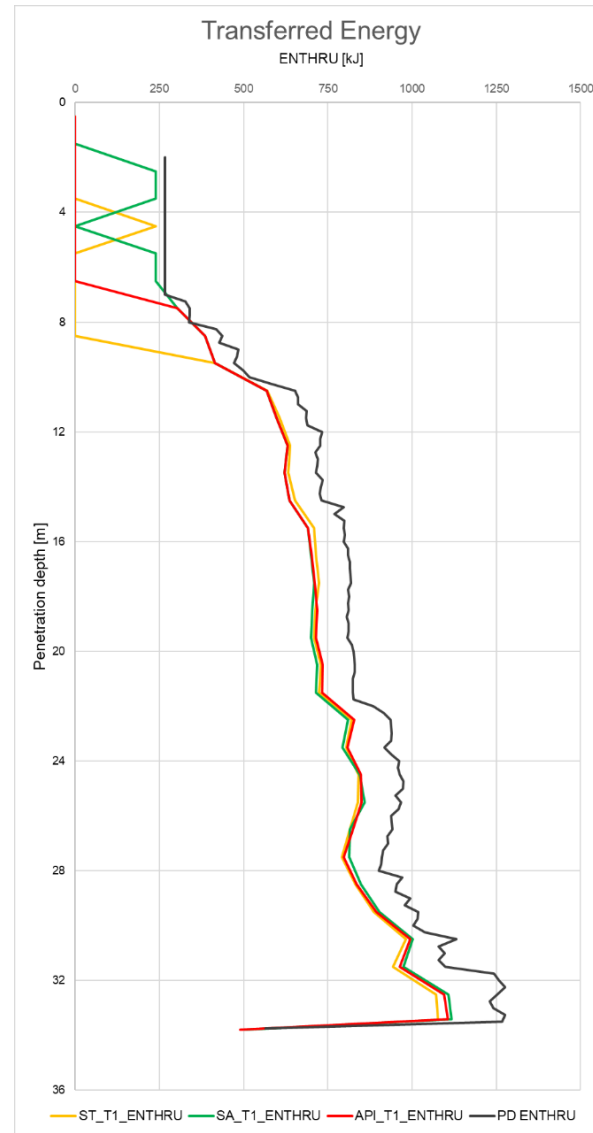
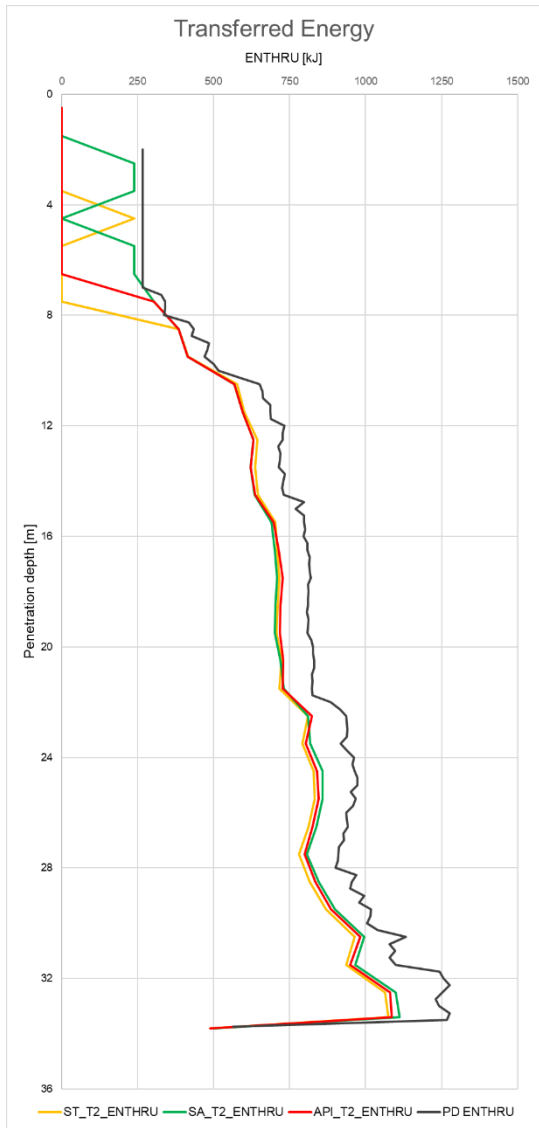


Figure A-1 Transferred energy comparison for T1 (left) and T2 (right)

Appendix B Calculation Steps for Resistance Output

i. Simple Soil Type Classification (ST)

This method processes each entry for non-cohesionless soils as

1. Converts inputs according to the soil classification shown in the first tab of Table B-2. and assigns unit weight, β -value, and N_t -value.
2. Calculates overburden pressure (under consideration of buoyancy).
3. With the assigned β and N_t values of the table finds the unit shaft resistance and end bearing and these values are limited according to Table B-2.

Table B-1 Soil parameters in ST analysis for cohesive soil types after Bowles (Bowles 1997)

Soil Type	SPT-N	q_u (kPa)	Unit Weight (kN/m ³)	f_s (kPa)	q_t (kPa)
Very Soft	1	12	17.5	3.5	54
Soft	3	36	17.5	10.5	162
Medium	6	72	18.5	19.0	324
Stiff	12	144	20.5	38.5	648
Very Stiff	24	288	20.5	63.5	1296
Hard	>32	>384	19-22	77.0	1728

Table B-2 Soil parameters in ST analysis for non-cohesive soil types after Bowles (Bowles 1997)

Soil Type	SPT-N	Friction Angle (°)	Unit Weight (kN/m ³)	β	N_t	Limit f_s (kPa)	Limit q_t (MPa)
Very Loose	2	25-30	13.5	0.203	12.1	24	2.4
Loose	7	27-32	16	0.242	18.1	48	4.8
Medium	20	30-35	18.5	0.313	33.2	72	7.2
Dense	40	35-40	19.5	0.483	86	96	9.6
Very Dense	>50	38-43	22	0.627	147	192	19

ii. SPT N-value based method

The calculation steps for an entry using the SPT-N input method is as follows are taken from (Pile Dynamics 2010).

0. As a basis for the calculation of several of the following quantities, the vertical effective stress is calculated first, as follows:
 - 0.1. Find the soil's unit weight (γ) based on Bowles (Bowles 1977).
 - 0.2. Find the vertical effective stress, p_o , in the layer based on the overburden on the layer, layer thickness, γ from Step 1, and the water table depth.

1. Shaft resistance for sands and gravels

- a. Find relative density, D_r , from Kulhawy (Kulhawy et al. 1989) and (Kulhawy and Mayne 1991).
- b. Find friction angle, ϕ' , based on Schmertmann (Schmertmann 1975) and (Schmertmann 1978).
- c. Assume the pile-soil friction angle as $\delta = \phi'$.
- d. Find the earth pressure coefficient at rest, k_o , based on D_r , according to Robertson and Campanella (Robertson et al. 1983)

$$\text{with } \frac{1-\sin \phi'}{1+\sin \phi'} < k_o < \frac{1+\sin \phi'}{1-\sin \phi'}$$

- e. Calculate unit shaft resistance: $q_s = k_o \tan(\delta) \sigma_v'$ with $q_s \leq 250$ kPa

Note: (a) Depending on the grading of a sand and its coarseness, the calculations may be slightly modified. (b) If friction angle is entered in lieu of N-value, skip steps a and b.

2. Shaft resistance for clays

- a. Find the friction angle from $\phi' = 17 + 0.5N$ with $\phi' \leq 43^\circ$.
- b. Define the pile-soil friction angle as $\delta = \phi'$.
- c. Find the over consolidation ratio (OCR) from N and σ_v' [kPa]

$$\text{OCR} = 18N/\sigma_v'$$

- d. Find the normally consolidated and earth pressure coefficient according to Jaky (Jaky 1944); given as $k_{nc} = 1 - \sin \phi'$
- e. Find the earth pressure coefficient at rest as

$$k_o = k_{nc}(\text{OCR})^{1/2}$$

$$\text{Where, } \frac{1-\sin \phi'}{1+\sin \phi'} \leq k_o \leq \frac{1+\sin \phi'}{1-\sin \phi'}$$

- f. Calculate the unit shaft resistance from

$$q_s = k_o \tan \delta \sigma_v' q; \text{ With; } q_s \leq 75 \text{ (kPa)}$$

Note: if the unconfined compressive stress q_u is entered in lieu of the N- value, the program will calculate adhesion values according to Tomlinson (Hannigan et al. 2006).

3. Shaft resistance for silts

- a. Use the friction angle ϕ' from Step 1-b if it is non-cohesive or from Step 2-a if it is cohesive.
- b. Find the Bjerrum-Borland β coefficient according to Fellenius (Fellenius 2006) by linear interpolation. $\beta = (\phi' - 28) * \left(\frac{0.23}{6}\right) + 0.27$
with $0.27 \leq \beta \leq 0.5$
- c. Calculate $q_s = \beta \sigma_v'$, with $q_s \leq 75$ kPa (cohesive), $q_s \leq 250$ kPa (non-cohesive).

Note: if the unconfined compressive stress q_u is entered in lieu of the N-value, the program will calculate adhesion values according to Tomlinson (Hannigan et al. 2006).

4. Unit end bearing for sands and gravels

- a. Calculate the unit end bearing based on the uncorrected SPT N- value from $q_{toe} = 200$ N (kPa), with $q_{toe} \leq 12,000$ kPa.

If friction angle has been directly entered, find corresponding N-value from Bowles in Hannigan et al. (Hannigan et al. 2006) and then calculate as shown.

5. Unit end bearing for clays

- a. Calculate the unit end bearing based on the uncorrected SPT N-value from $q_{toe} = 54$ N (kPa) with $q_{toe} \leq 3240$ (kPa).

If q_u has been directly entered calculate unit end bearing as $4.5 q_u$

6. Unit end bearing for silts

- a. Find friction angle ϕ' from Step 1-b if it is non-cohesive or from Step 2-a if it is cohesive (or use directly entered friction angle).
- b. Find the toe capacity coefficient, N_t , according to Fellenius (Fellenius 2006) by interpolation.

$$N_t = (\phi' - 28) / (0.3 + 20), \text{ with } 20 \leq N_t \leq 40$$

- c. $q_{toe} = N_t \sigma_v'$ with $20 \leq N_t \leq 40$ and $q_{toe} \leq 6,000$ kPa.

iii. The CPT Method in GRLWEAP

The first step is classification of the different soil layers according to Robertson et al. (Robertson and Campanella 1986) with minor adjustment.

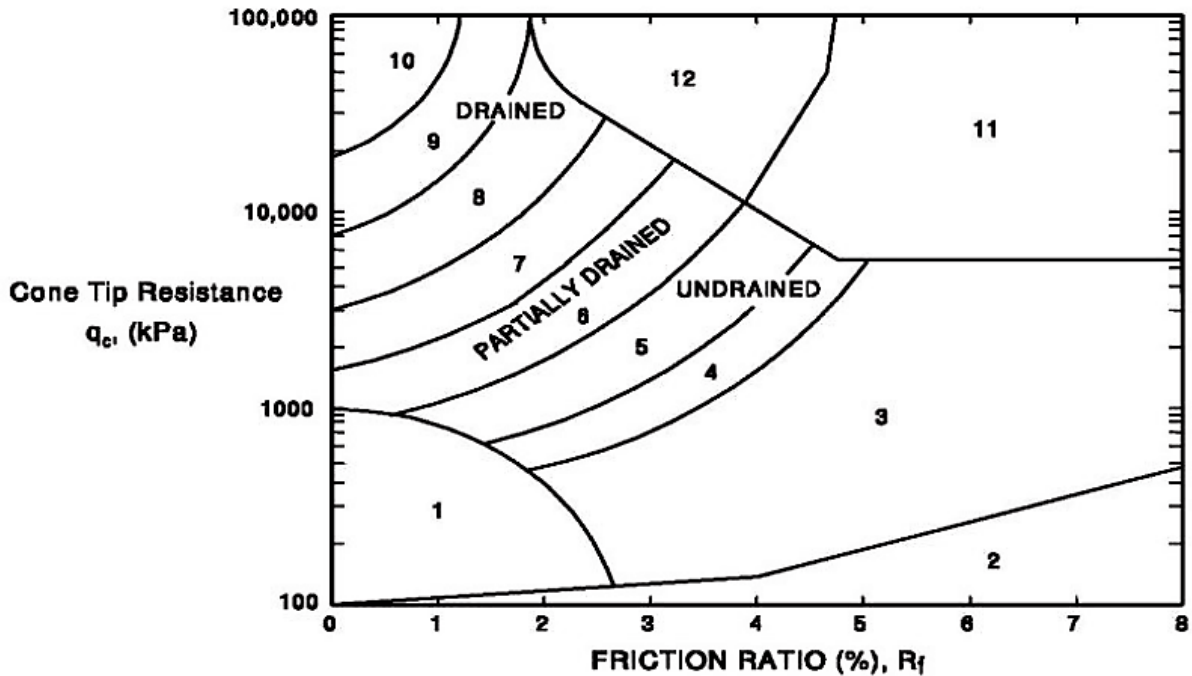


Figure B-1 Soil classification of Robertson et al. (Robertson and Campanella 1986)

Table B-3 Soil type classification used by GRLWEAP after Robertson et al. (Robertson and Campanella 1986)

Zone	Soil Description corresponding to	
	Hannigan et al. (2006)	SPT-N Value bases method (SA)
1	Sensitive fine grained	Poorly graded fine sand
2	Organic material	Peat
3	Clay	Clay
4	Silty clay to clay	Clay
5	Clayey silt to silty clay	Cohesive silt
6	Sandy silt to clayey silt	Split between 5 and 7
7	Silty sand to sandy silt	Cohesionless silt
8	Sand to silty sand	Sand
9	Sand	Sand
10	Gravely sand to sand	Well graded sand
11	Very stiff fine grained	Poorly graded fine sand
12	Sand to clayey sand	Sand

The resistance calculation is and distribution of friction and toe bearing is based on Schmertmann (Schmertmann 1978). An additional assumption is a uniform pile. This

simplification has been proposed by Schmertmann (Schmertmann 1978) and since unit resistance is the result of this calculation procedure and since the pile surface area will be as per user input, the error is considered immaterial. Additional inputs affecting the results include:

- Pile material: steel, concrete and timber
- Pile average diameter or width, B, for average depth D to B ratio
- Pile toe size is used to determine the averaging range for toe resistance calculation;
- Unit resistance limit based on a maximum q_c of 15 MPa.

Unit shaft resistance for cohesive soils

$$f_s = \alpha q_s$$

Where, α is the ratio of pile to sleeve friction in cohesive soil; a function of q_s and pile material (Schmertmann 1978).

q_s is the unit sleeve friction.

Unit shaft resistance for cohesionless soils

$$f_s = k_r K q_s$$

Where, K = Ratio of unit pile shaft resistance to unit cone sleeve friction (Schmertmann 1978) as a function of depth, Z , penetrometer type and pile material.

q_s = unit sleeve friction.

$k_r = Z/8B$ for $Z = 0$ to $8B$.

$k_r = 1$ for $Z \geq 8B$.

B = Pile width or diameter.

Note: In GRLWEAP's CPT routine, Schmertmann's curves for steel pipe piles are used for all steel piles and those for square concrete piles are used for all concrete piles.

$f_s \leq f_{s, \text{lim}}$ the unit shaft resistance limit entered by the user (default is 150 kPa)

Unit toe resistance for all soil types

$$q_t = \frac{1}{2} (q_{c1} + q_{c2})$$

Where, q_{c1} and q_{c2} are averages of unit cone tip resistance below and above pile toe (Schmertmann 1978).

$q_t \leq q_{t, \text{lim}}$ the unit toe resistance limit entered by user (default is 15 MPa).

iv. The API Method in GRLWEAP

The following calculation steps are taken from the background report (Pile Dynamics 2010) of the GRLWEAP program.

Unit Shaft Resistance for cohesive soils

$$f_s = \alpha c$$

Where, α is a dimensionless factor and it can be computed from:

$$\alpha = 0.5 \psi^{-0.5} \quad \text{for } \psi \leq 1.0$$

$$\alpha = 0.5 \psi^{-0.25} \quad \text{for } \psi > 1.0$$

$$\alpha \leq 1.0.$$

$$\psi = c/p_o'$$

p_o' = effective overburden pressure

c (S_u) = undrained shear strength of the soil, which is an input value

Unit shaft resistance for cohesionless soils

$$f_s = K p_o' \tan \delta$$

Where; K = dimensionless coefficient of lateral earth pressure (ratio of horizontal to vertical normal effective stress). $K = 0.8$ for unplugged. $K = 1.0$ for plugged (e.g. fully displacement piles).

δ = friction angle between the soil and pile wall.

$f_s \leq f_{s, \text{lim}}$ the unit shaft resistance limit.

Unit toe resistance for cohesive soil types

$$q_t = 9 c$$

Where, c (S_u) is the undrained shear strength.

Unit toe resistance for cohesionless soil types

$$q_t = p_o' N_q$$

Where, N_q is a bearing capacity factor, is taken from API (API 1993) Table B-4

$q_t \leq q_{t, \text{lim}}$ the unit toe resistance limit.

Table B-4 Design Parameter for Cohesionless Siliceous Soil* taken from API (API 1993)

Density	Soil Description	Soil-Pile Friction Angle (°)	Limiting Skin Friction Values (kPa)	N _q	Limiting Unit End Bearing Values (MPa)
Very Loose	Sand	15	47.8	8.0	1.9
Loose	Sand-Silt**				
Medium	Silt				
Loose	Sand	20	67.0	12	2.9
Medium	Sand-Silt**				
Dense	Silt				
Medium	Sand	25	81.3	20	4.8
Dense	Sand-Silt**				
Dense	Sand	30	95.7	40	9.6
Very Dense	Sand-Silt**				
Dense	Gravel	35	114.8	50	12.0
Very Dense	Sand				

Note: The parameters listed in this table are intended as guidelines only. Where detailed information such as in-situ cone tests, strength tests on high quality samples, model tests, or pile driving performance is available, other values may be justified.

**Sand-Silt includes those soils with significant fractions of both sand and silt. Strength values generally increase with increasing sand fractions and decrease with increasing silt fractions.

Appendix C Reference Tables and Formats

i. Recommended quake and damping values

Table C-1 Recommended Quake Values for Impact Driven Piles*. Source: (Pile Dynamics 2010)

	Soil Type	Pile Type or Size	Quake (mm)
Shaft Quake	All soil types	All Types	2.5
Toe Quake	All soil types, soft Rock	Non-displacement piles** i.e. driving unplugged	2.5
	Very dense or hard soils	Displacement Piles*** of diameter or width D	D/120 D/120
	Soils which are not very dense or hard	Displacement Piles*** of diameter or width D	D/60 D/60
	Hard Rock	All Types	1.0

*For vibratory driven piles in cohesive soils, quakes should be doubled.

** Non-displacement piles are sheet pile, H-Piles, or open-ended pipe piles which are not plugging during driving. Normally it can be assumed that pipe piles with diameters of 30 inches (900 mm) or more will not plug during driving while H-Piles and pipe piles of diameter 20 inches (500 mm) or less will plug during driving into a bearing layer. Between 20 and 30 inches (500 and 750 mm), pipe piles may or may not plug.

*** Displacement piles are closed-ended pipe piles, pipe piles, or H-Piles that are plugged during driving and solid concrete piles. Normally, we would analyze H-Piles and pipe piles with diameters 20 inches (500 mm) or less as displacement piles.

Table C-2 Recommended Damping Values for Impact Driven Piles*. Source: (Pile Dynamics 2010)

	Soil Type	Damping Factor (s/m)
Shaft Damping	Non-cohesive soils**	0.16
	Cohesive soils**	0.65
Toe damping	In all soil types	0.50

* For vibratory driven piles, use double values (Smith-viscous)

** For mixed soils, intermediate values may be appropriate; for example, a sandy silt or clayey sand may be modeled with 0.10 s/ft (0.33 s/m), a cohesive silt or a sandy clay with 0.15 s/ft (0.50 s/m).

ii. Recommended setup factors

Table C-3 Suggestions for shaft setup factors, f_s , for Impact pile driving. Source: (Rausche et al. 1997)

Soil Along Shaft	$f_s = \text{LTSR} / \text{SRD}^*$	Remarks
Clay	2.0	Range of 1 to 10 possible for impact hammers
Silt - Clay	1.0	Often > 1, e.g. 1.5, but occasionally less than 1 (relaxation)
Silt	1.5	Cohesionless silt may have lower setup factors
Sand - Clay	1.2	Sometimes sand clay mixtures have an f_s as high as 2
Sand	1.2	
Sand - Gravel	1.0	

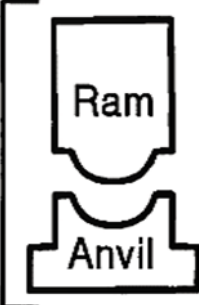

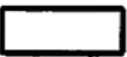
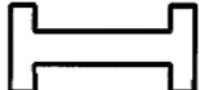
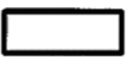

*LTSR - Long Term Static Resistance, e.g. from Static Load Test or from restrike test after a sufficiently long waiting time.

*SRD – Static Resistance to Driving; typically expected for EOD (End of Driving).

iii. Pile and driving equipment data form

Form 1: Pile and Driving Equipment Data Form

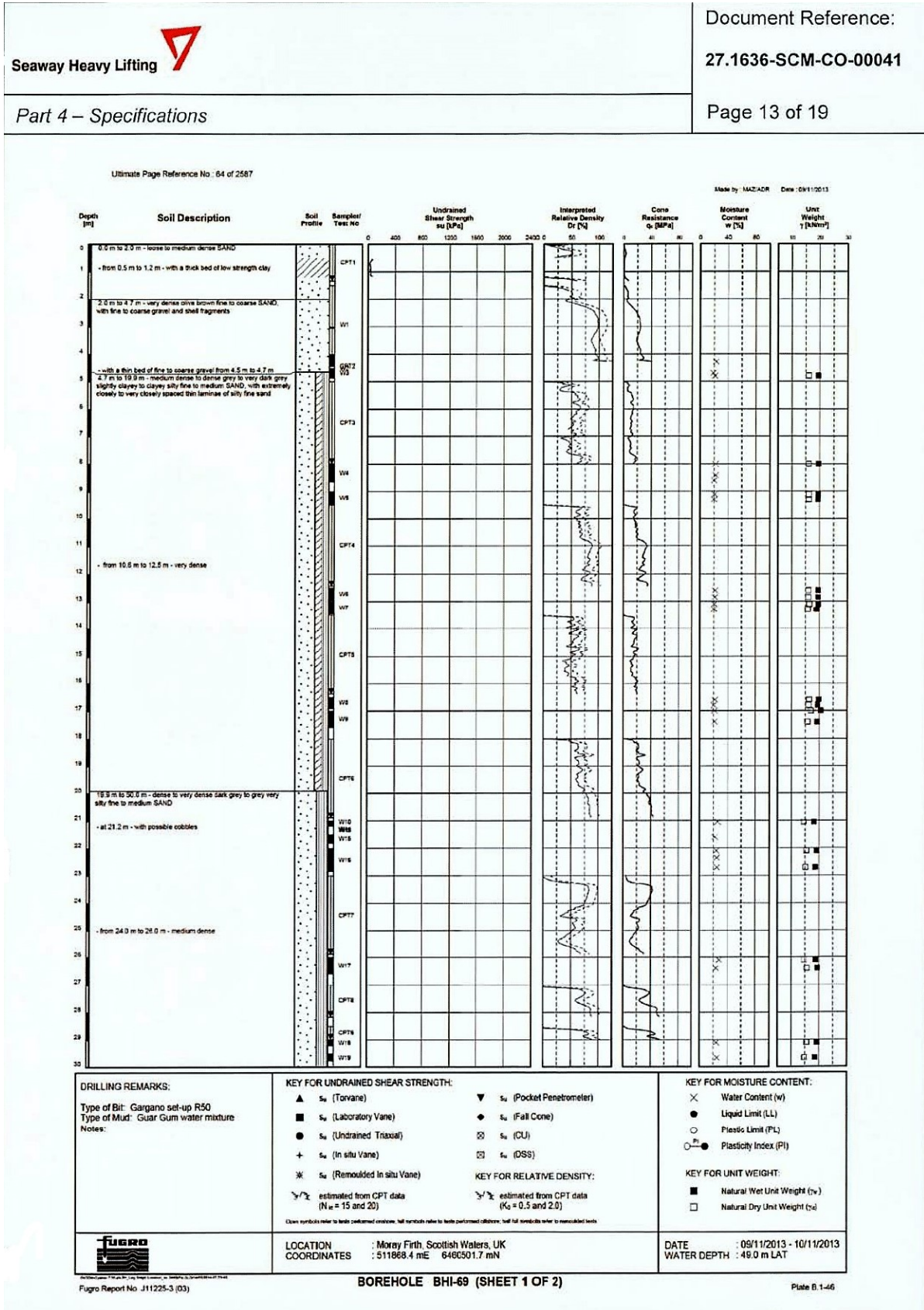
Contract No.: _____ Structure Name and/or No.: _____
 Project: _____ Pile Driving Contractor or Subcontractor: _____
 County: _____ (Piles driven by)

Hammer Components 	Hammer	Manufacturer: _____ Model No.: _____ Hammer Type: _____ Serial No.: _____ Manufacturers Maximum Rated Energy: _____ (Joules) Stroke at Maximum Rated Energy: _____ (meters) Range in Operating Energy: _____ to _____ (Joules) Range in Operating Stroke: _____ to _____ (meters) Ram Weight: _____ (kg) Modifications: _____ _____ _____
	Striker Plate	Weight: _____ (N) Diameter: _____ (mm) Thickness: _____ (mm) Material #1 _____ Material #2 _____ (for Composite Cushion) Name: _____ Name: _____ Area: _____ (cm ²) Area: _____ (cm ²) Thickness/Plate: _____ (mm) Thickness/Plate: _____ (mm) No. of Plates: _____ No. of Plates: _____ Total Thickness of Hammer Cushion: _____
	Hammer Cushion	
	Helmet (Drive Head)	Weight: _____ (kN)
	Pile Cushion	Material: _____ Area: _____ (cm ²) Thickness/Sheet: _____ (mm) No. of Sheets: _____ Total Thickness of Pile Cushion: _____ (mm)
	Pile	Pile Type: _____ Wall Thickness: _____ (mm) Taper: _____ Cross Sectional Area: _____ (cm ²) Weight/Meter: _____ Ordered Length: _____ (m) Design Load: _____ (kN) Ultimate Pile Capacity: _____ (kN) Description of Splice: _____ _____ Driving Shoe/Closure Plate Description: _____ _____ Submitted By: _____ Date: _____ Telephone No.: _____ Fax No.: _____

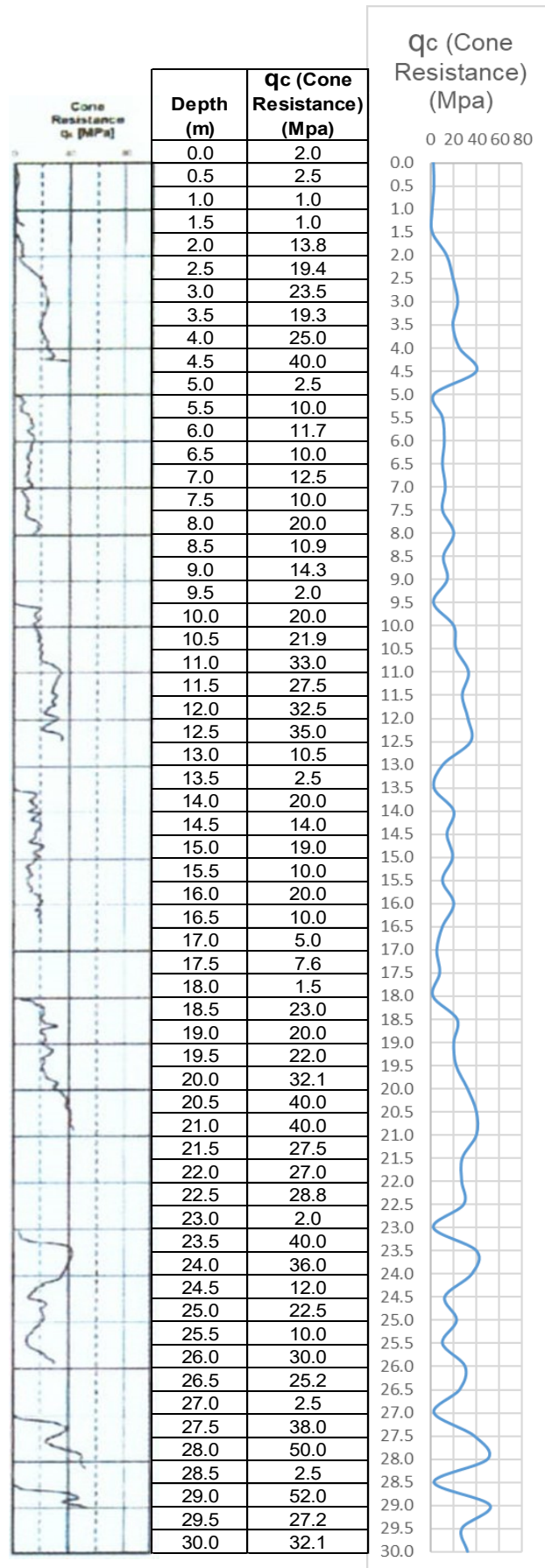
Source: (Pile Dynamics 2010)

Appendix D Raw and Correlation Data

i. BHI-69 - Original soil investigation bore log report



ii. Cone resistance approximation



iii. Pile driving monitoring data with plots

Paal
Hamer
Lengte
Diameter ø
Wanddikte
Schoor
Zelf penetratie
Datum

	L9_Pile2_R00
	S-2500
[m]	39.00
[mm]	2200
[mm]	60
	0°
[m]	1.80
	30-07-2017

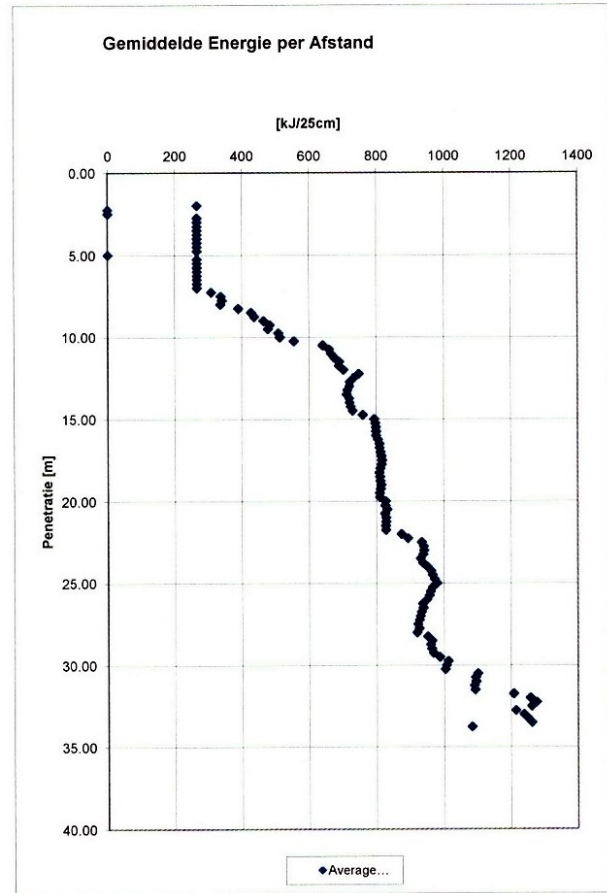
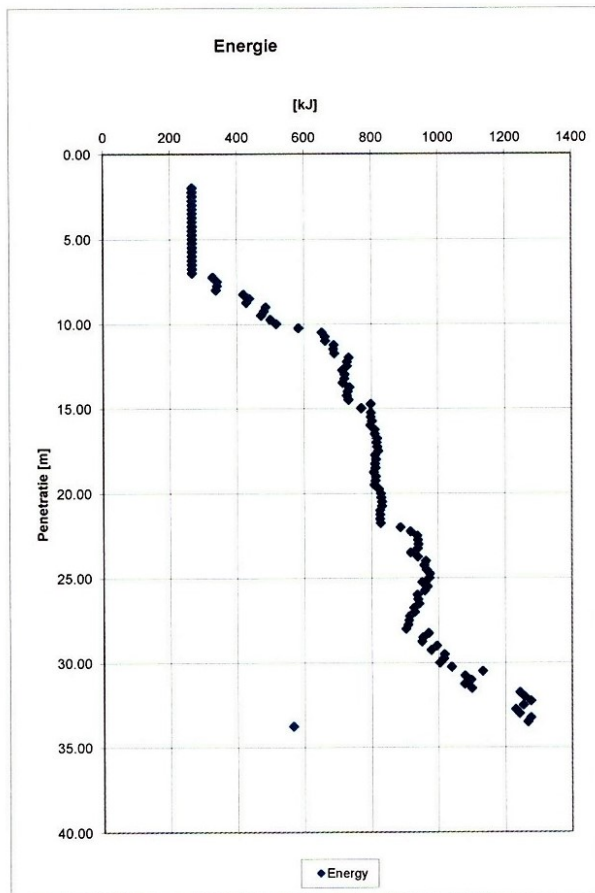
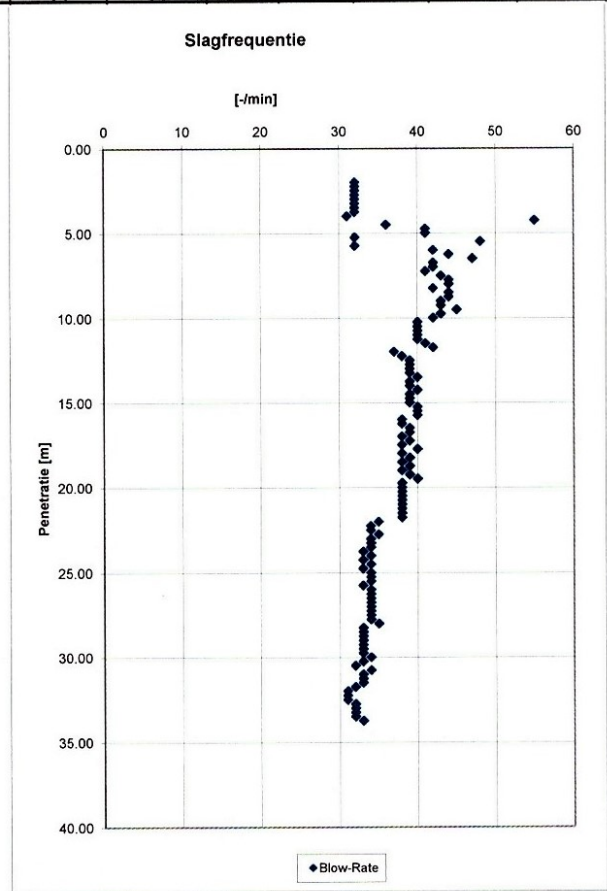
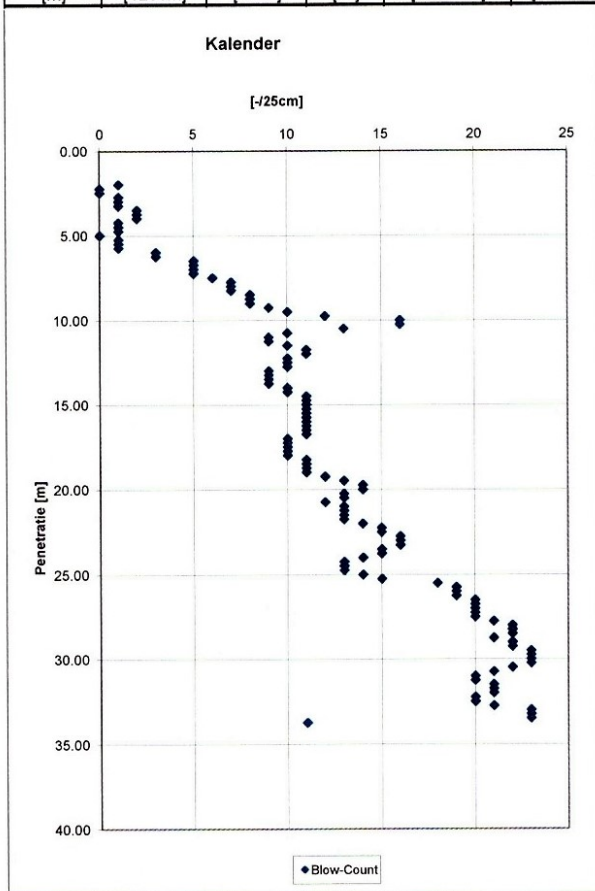
Neto tijd
Totaal tijd
Eind penetratie
Totaal slagen
Totaal energie

	00:46:14
	00:57:55
[m]	33.75
	1572
[kJ]	1388462

Penetratie [m]	Blow-Count [-/25cm]	Blow-Rate [-/min]	Energy [kJ]	Average Energy [kJ/25cm]	Total Energy [kJ/25cm]	Inclinomete [°]	Inclinomete [°]	Kap Dru [bar]	Kap Dru [bar]	Kap Dru [bar]	Hamer Die [m]	Hamer Die [m]
2.00	1	32	266	266	266	-0.7	0.0	0	0	30.576	0.0	0.0
2.25	0	32	266	0	266	-0.6	0.0	0	0	30.546	0.0	0.0
2.50	0	32	266	0	266	-0.1	0.0	0	0	30.733	0.0	0.0
2.75	1	32	266	266	266	-0.8	0.0	0	0	31.576	0.0	0.0
3.00	1	32	266	266	266	0.2	0.0	0	0	31.137	0.0	0.0
3.25	1	32	266	266	266	0.1	0.0	0	0	30.775	0.0	0.0
3.50	2	32	266	266	532	0.2	0.0	0	0	30.679	0.0	0.0
3.75	2	32	266	266	532	-0.3	0.0	0	0	31.538	0.0	0.0
4.00	2	31	266	266	532	0.1	0.0	0	0	31.141	0.0	0.0
4.25	1	55	266	266	266	0.5	0.0	0	0	30.595	0.0	0.0
4.50	1	36	266	266	266	-0.1	0.0	0	0	30.695	0.0	0.0
4.75	1	41	266	266	266	0.2	0.0	0	0	31.477	0.0	0.0
5.00	0	41	266	0	266	-1.0	0.0	0	0	30.992	0.0	0.0
5.25	1	32	266	266	266	0.3	0.0	0	0	30.626	0.0	0.0
5.50	1	48	266	266	266	0.3	0.0	0	0	30.912	0.0	0.0
5.75	1	32	266	266	266	0.0	0.0	0	0	30.546	0.0	0.0
6.00	3	42	266	266	798	0.4	0.0	0	0	48.38	0.0	0.0
6.25	3	44	266	266	798	-1.3	0.0	0	0	31.046	0.0	0.0
6.50	5	47	266	266	1330	0.0	0.0	0	0	47.567	0.0	0.0
6.75	5	42	266	266	1330	-0.1	0.0	0	0	30.122	0.0	0.0
7.00	5	42	266	266	1330	0.1	0.0	0	0	30.08	0.0	0.0
7.25	5	41	327	308.8	1544	-0.4	0.0	0	0	30.122	0.0	0.0
7.50	6	43	340	337.5	2025	-0.2	0.0	0	0	30.889	0.0	0.0
7.75	7	44	340	340.8571429	2386	-0.2	0.0	0	0	30.779	0.0	0.0
8.00	7	44	337	336.4285714	2355	-0.1	0.0	0	0	30.626	0.0	0.0
8.25	7	42	418	389	2723	0.1	0.0	0	0	30.077	0.0	0.0
8.50	8	44	436	427.375	3419	-0.1	0.0	0	0	30.595	0.0	0.0
8.75	8	44	427	436.625	3493	-0.4	0.0	0	0	30.122	0.0	0.0
9.00	8	43	485	464.125	3713	-0.2	0.0	0	0	29.996	0.0	0.0
9.25	9	43	480	482.7777778	4345	0.0	0.0	0	0	30.115	0.0	0.0
9.50	10	45	471	477.6	4776	0.2	0.0	0	0	29.993	0.0	0.0
9.75	12	43	499	508.1666667	6098	0.5	0.0	0	0	30.794	0.0	0.0
10.00	16	42	517	512.625	8202	-0.1	0.0	0	0	31.084	0.0	0.0
10.25	16	40	583	553.9375	8863	0.5	0.0	0	0	31.858	0.0	0.0
10.50	13	40	652	639.8461538	8318	0.3	0.0	0	0	42.905	0.0	0.0
10.75	10	40	661	658.9	6589	0.3	0.0	0	0	31.019	0.0	0.0
11.00	9	40	662	664.2222222	5978	0.3	0.0	0	0	32.068	0.0	0.0
11.25	9	40	687	674.2222222	6068	0.4	0.0	0	0	31.591	0.0	0.0
11.50	10	41	686	688.2	6882	0.4	0.0	0	0	32.064	0.0	0.0
11.75	11	42	689	687.6363636	7564	-0.5	0.0	0	0	30.836	0.0	0.0
12.00	11	37	732	701.3636364	7715	0.5	0.0	0	0	33.468	0.0	0.0
12.25	10	38	727	747.7	7477	0.4	0.0	0	0	32.873	0.0	0.0
12.50	10	39	727	732.5	7325	-0.2	0.0	0	0	31.717	0.0	0.0
12.75	10	39	713	720	7200	0.3	0.0	0	0	32.774	0.0	0.0
13.00	9	39	720	718.3333333	6465	-0.3	0.0	0	0	31.423	0.0	0.0
13.25	9	39	719	712.8888889	6416	0.1	0.0	0	0	32.564	0.0	0.0
13.50	9	40	714	710.8888889	6398	0.0	0.0	0	0	31.602	0.0	0.0
13.75	9	39	734	718.5555556	6467	-0.5	0.0	0	0	31.355	0.0	0.0
14.00	10	39	729	719.8	7198	0.2	0.0	0	0	32.465	0.0	0.0
14.25	10	40	726	723.1	7231	-0.6	0.0	0	0	31.885	0.0	0.0
14.50	11	39	731	729	8019	0.1	0.0	0	0	32.941	0.0	0.0
14.75	11	39	797	758.8181818	8347	0.3	0.0	0	0	31.74	0.0	0.0
15.00	11	39	769	792.8181818	8721	-0.6	0.0	0	0	31.767	0.0	0.0
15.25	11	40	798	795.6363636	8752	-0.4	0.0	0	0	31.862	0.0	0.0
15.50	11	40	797	797.6363636	8774	-0.1	0.0	0	0	31.961	0.0	0.0
15.75	11	40	801	798.0909091	8779	-0.3	0.0	0	0	31.736	0.0	0.0
16.00	11	38	796	798.4545455	8783	0.1	0.0	0	0	33.052	0.0	0.0
16.25	11	38	809	804	8844	0.2	0.0	0	0	32.972	0.0	0.0
16.50	11	39	809	808.4545455	8893	0.0	0.0	0	0	32.919	0.0	0.0
16.75	11	39	816	808.8181818	8897	-0.4	0.0	0	0	31.793	0.0	0.0
17.00	10	38	815	811.8	8118	0.1	0.0	0	0	31.587	0.0	0.0
17.25	10	39	817	813.8	8138	-0.3	0.0	0	0	32.892	0.0	0.0
17.50	10	38	819	815.9	8159	-0.2	0.0	0	0	31.74	0.0	0.0
17.75	10	40	810	815	8150	-0.2	0.0	0	0	31.591	0.0	0.0
18.00	10	38	813	811	8110	-0.2	0.0	0	0	31.713	0.0	0.0
18.25	11	39	810	808.3636364	8892	0.0	0.0	0	0	33.041	0.0	0.0
18.50	11	38	811	809.4545455	8904	-0.1	0.0	0	0	33.334	0.0	0.0
18.75	11	39	806	811	8921	0.0	0.0	0	0	32.289	0.0	0.0
19.00	11	38	812	813.2727273	8946	-0.4	0.0	0	0	32.625	0.0	0.0
19.25	12	39	811	811.6666667	9740	-0.2	0.0	0	0	33.235	0.0	0.0
19.50	13	40	808	809.3076923	10521	0.0	0.0	0	0	48.242	0.0	0.0
19.75	14	38	821	809.5714286	11334	-0.3	0.0	0	0	33.361	0.0	0.0

Penetratie [m]	Blow-Count [-/25cm]	Blow-Rate [-/min]	Energy [kJ]	Average Energy [kJ/25cm]	Total Energy [kJ/25cm]	Inclinomete [°]	Inclinomete [°]	Kap Dru [bar]	Kap Dru [bar]	Kap Dru [bar]	Hamer Die [m]	Hamer Die [m]
20.00	14	38	827	825.8571429	11562	0.1	0.0	0	0	33.456	0.0	0.0
20.25	13	38	828	825.3076923	10729	0.1	0.0	0	0	33.453	0.0	0.0
20.50	13	38	830	830.7692308	10800	0.2	0.0	0	0	50.855	0.0	0.0
20.75	12	38	830	825.0833333	9901	-0.1	0.0	0	0	32.384	0.0	0.0
21.00	13	38	824	827.8461538	10762	-0.2	0.0	0	0	32.438	0.0	0.0
21.25	13	38	825	827.7692308	10761	-0.3	0.0	0	0	46.495	0.0	0.0
21.50	13	38	824	826.5384615	10745	-0.4	0.0	0	0	32.922	0.0	0.0
21.75	13	38	826	827.1538462	10753	0.2	0.0	0	0	32.812	0.0	0.0
22.00	14	35	885	872.8571429	12220	-0.7	0.0	0	0	32.915	0.0	0.0
22.25	15	34	916	892.8666667	13393	-0.7	0.0	0	0	34.021	0.0	0.0
22.50	15	34	936	933.4	14001	-0.7	0.0	0	0	34.032	0.0	0.0
22.75	16	35	938	939	15024	-0.7	0.0	0	0	34.021	0.0	0.0
23.00	16	34	940	940.375	15046	-0.1	0.0	0	0	32.819	0.0	0.0
23.25	16	34	938	937.4375	14999	-0.4	0.0	0	0	33.788	0.0	0.0
23.50	15	34	917	929.6666667	13945	-0.4	0.0	0	0	32.77	0.0	0.0
23.75	15	33	938	935.6666667	14035	0.3	0.0	0	0	34.349	0.0	0.0
24.00	14	34	962	949.8571429	13298	-0.7	0.0	0	0	32.949	0.0	0.0
24.25	13	33	957	960.7692308	12490	0.2	0.0	0	0	33.876	0.0	0.0
24.50	13	34	964	965.3846154	12550	-0.5	0.0	0	0	33.151	0.0	0.0
24.75	13	33	974	971.3846154	12628	0.2	0.0	0	0	32.713	0.0	0.0
25.00	14	34	973	978.7142857	13702	-0.1	0.0	0	0	33.575	0.0	0.0
25.25	15	34	951	965.6666667	14485	0.0	0.0	0	0	32.789	0.0	0.0
25.50	18	34	967	958.9444444	17261	0.1	0.0	0	0	33.945	0.0	0.0
25.75	19	33	959	956.3157895	18170	-0.2	0.0	0	0	33.521	0.0	0.0
26.00	19	34	937	948.6842105	18025	-0.2	0.0	0	0	33.022	0.0	0.0
26.25	19	34	939	936.6315789	17796	-0.3	0.0	0	0	32.728	0.0	0.0
26.50	20	34	942	937.65	18753	0.1	0.0	0	0	32.968	0.0	0.0
26.75	20	34	927	932.6	18652	0.0	0.0	0	0	32.812	0.0	0.0
27.00	20	34	929	929.7	18594	0.0	0.0	0	0	33.289	0.0	0.0
27.25	20	34	913	926.7	18534	-0.2	0.0	0	0	32.636	0.0	0.0
27.50	20	34	911	922.4	18448	-0.2	0.0	0	0	32.655	0.0	0.0
27.75	21	34	909	925.6190476	19438	-0.3	0.0	0	0	32.751	0.0	0.0
28.00	22	35	902	919.4090909	20227	-0.3	0.0	0	0	32.655	0.0	0.0
28.25	22	33	970	951.3636364	20930	-0.1	0.0	0	0	33.392	0.0	0.0
28.50	22	33	954	963.3181818	21193	0.2	0.0	0	0	32.583	0.0	0.0
28.75	21	33	950	959.6666667	20153	-0.2	0.0	0	0	32.743	0.0	0.0
29.00	22	33	995	962.8181818	21182	-0.3	0.0	0	0	34.28	0.0	0.0
29.25	22	33	978	968.1363636	21299	0.1	0.0	0	0	33.846	0.0	0.0
29.50	23	33	1018	986.7391304	22695	0.0	0.0	0	0	32.693	0.0	0.0
29.75	23	33	1016	1012.173913	23280	-0.6	0.0	0	0	32.888	0.0	0.0
30.00	23	34	1004	1006.913043	23159	-0.4	0.0	0	0	32.922	0.0	0.0
30.25	23	33	1039	1003.304348	23076	-0.5	0.0	0	0	33.285	0.0	0.0
30.50	22	32	1132	1099.590909	24191	0.2	0.0	0	0	33.853	0.0	0.0
30.75	21	34	1079	1092.952381	22952	0.3	0.0	0	0	34.635	0.0	0.0
31.00	20	33	1097	1093.95	21879	-0.1	0.0	0	0	34.437	0.0	0.0
31.25	20	33	1078	1089.85	21797	-0.2	0.0	0	0	33.529	0.0	0.0
31.50	21	33	1099	1091.809524	22928	-0.2	0.0	0	0	33.418	0.0	0.0
31.75	21	32	1243	1207.190476	25351	-0.3	0.0	0	0	33.243	0.0	0.0
32.00	21	31	1257	1257.714286	26412	-0.1	0.0	0	0	33.51	0.0	0.0
32.25	20	31	1276	1276.4	25528	-0.1	0.0	0	0	33.769	0.0	0.0
32.50	20	31	1253	1261.7	25234	-0.2	0.0	0	0	33.449	0.0	0.0
32.75	21	32	1230	1214.285714	25500	0.1	0.0	0	0	35.055	0.0	0.0
33.00	23	32	1242	1238.565217	28487	-0.1	0.0	0	0	33.228	0.0	0.0
33.25	23	32	1276	1250.434783	28760	0.1	0.0	0	0	33.441	0.0	0.0
33.50	23	32	1267	1262.173913	29030	0.1	0.0	0	0	33.132	0.0	0.0
33.75	11	33	565	1082	11902	-0.2	0.0	0	0	32.766	0.0	0.0

Penetratie [m]	Blow-Count [-/25cm]	Blow-Rate [-/min]	Energy [kJ]	Average Energ [kJ/25cm]	Total Energy [kJ/25cm]	Inclinomete [°]	Inclinomete [°]	Kap Dru [bar]	Kap Dru [bar]	Kap Dru [bar]	Hamer Die [m]	Hamer Die [m]
----------------	---------------------	-------------------	-------------	-------------------------	------------------------	-----------------	-----------------	---------------	---------------	---------------	---------------	---------------



Penetratie [m]	Blow-Count [-/25cm]	Blow-Rate [-/min]	Energy [kJ]	Average Energ [kJ/25cm]	Total Energy [kJ/25cm]	Inclinomete [°]	Inclinomete [°]	Kap Dru [bar]	Kap Dru [bar]	Kap Dru [bar]	Hamer Die [m]	Hamer Die [m]
----------------	---------------------	-------------------	-------------	-------------------------	------------------------	-----------------	-----------------	---------------	---------------	---------------	---------------	---------------

